

In presenting this thesis in partial fulfillment of the requirements for an advanced degree at Idaho State University, I agree that the Library shall make it freely available for inspection. I further state that permission to download and/or print my thesis for scholarly purposes may be granted by the Dean of the Graduate School, Dean of my academic division, or by the University Librarian. It is understood that any copying or publication of this thesis for financial gain shall not be allowed without my written permission.

Signature _____

Date _____

Research and Development of a Wave Impact
Simulation Device for the Idaho State University
Component Flooding Evaluation Laboratory

by

Gregory David Roberts

A thesis

submitted in partial fulfillment

of the requirements for the degree of

Master of Science in Civil Engineering

Idaho State University

Spring 2017

To the Graduate Faculty:

The members of the committee appointed to examine the thesis of Greg Roberts find it satisfactory and recommend that it be accepted.

Dr. Bruce Savage,
Major Advisor

Dr. Chad Pope,
Committee Member

Dr. Jay Kunze,
Graduate Faculty Representative

To my parents Shawn and Mary, and my sister Katherine, for their love and support.

Acknowledgements

I would like to thank Dr. Chad Pope for the opportunity to be a part of the Component Flooding Evaluation Laboratory team. I would also like to thank my advisor Dr. Bruce Savage for his insight and guidance on my thesis.

Vita

Greg Roberts was born on November 11, 1992 in Pocatello, Idaho. In 2015, he received his undergraduate degree in Civil Engineering from Idaho State University (ISU). He was then accepted into the Civil Engineering master's program at ISU. Upon completion of his master's degree, he plans to pursue his professional engineering license.

Table of Contents

List of Figures	vii
List of Tables	x
List of Equations	xi
List of Abbreviations	xii
Abstract	xiii
Introduction.....	1
Literature Review.....	3
Wave Theory.....	4
Wave Breaking.....	6
Inundation	7
Tsunami Waves.....	9
Wave Impacts.....	11
Artificial Wave Generation.....	14
Computational Fluid Dynamics	18
Governing Equations	19
Numerical Methods.....	20
Computational Mesh.....	20
Solid Geometry	20
Fluid Surface	21
Boundary Conditions	21

General Moving Objects	22
Tsunami Wave Simulation Methodology	23
Tsunami Wave Simulation.....	23
Tsunami Wave Impact Studies	26
Tsunami Wave Simulation Results.....	33
WISD Methodology.....	35
Horizontal Piston WISD Design.....	38
Design A	43
Design B.....	44
Design C.....	45
Design D	46
Design E.....	49
Design E with Gates.....	54
Design F	58
Vertical Piston WISD Design.....	62
Design G	62
Design H	66
Air Pressure WISD Design.....	69
Design I.....	69
Grid Convergence Test for Air Pressure WISD Design	75
Design J.....	77
WISD Results.....	80
Conclusions and Future Work	81

References.....	83
Appendix A: Artificial Wave Generation References	88
Appendix B: Design E Calculations	93
Appendix C: Design F Calculations	94
Appendix D: Design I Calculations	95
Appendix E: Design F Flow-3D Input Text File	96
Appendix F: Design J Flow-3D Input Text File	110

List of Figures

Figure 1: Established Wave Theory Validity Regions	4
Figure 2: Large Wave Flume at Oregon State University	15
Figure 3: Directional Wave Basin at Oregon State University	16
Figure 4: Deltares Delta Flume.....	17
Figure 5: 20 Foot Solitary Wave Flow 3D Simulation Geometry (X-dimension in feet)	25
Figure 6: Impact Capture Comparison - Baffle Impact Condition – Isometric View	27
Figure 7: Impact Capture Comparison - Block Impact Condition – Isometric View	27
Figure 8. 20 Foot Solitary Wave Flow-3D Simulation (X-Z Plane).....	31
Figure 9. Initial Condition Pressure Distribution of 20 Foot Solitary Wave Simulation .	31
Figure 10. Pressure Distribution of a Solitary Wave Advancing Forward on a Beach	31
Figure 11. Velocity Distribution of a Solitary Wave Advancing Forward on a Beach	32
Figure 12. Isometric View of Wave Pressures at Imminent Baffle Impact	32
Figure 13: 20 Foot Solitary Wave Maximum Impact Force Summary	34
Figure 14. Design A: WISD Sections and Components	37
Figure 15. Fluid Tongue at Solitary Wave Base.....	39
Figure 16. Test Pit with Fluid Basin: Plan View (X-Y Plane).....	40
Figure 17. Test Pit with Fluid Basin: Side Elevation (X-Z Plane)	40
Figure 18. Design A-C: Side Elevation (X-Z Plane)	41
Figure 19. Design A-C: Front Elevation (Y-Z Plane).....	42
Figure 20. Design A-C Isometric View	42
Figure 21. Design A Isometric View: Wave Section Profile.....	43
Figure 22. Design B Isometric View: Wave Section Profile	44

Figure 23. Design C: Wave Section Profile.....	45
Figure 24. Design D Side Elevation (X-Z Plane)	47
Figure 25. Design D Front Elevation (Y-Z Plane).....	47
Figure 26. Design D Isometric View	48
Figure 27. Design D Isometric View: Wave Section Profile.....	48
Figure 28. Design E Elevation View (X-Z Plane)	50
Figure 29. Design E Front Elevation (Y-Z Plane)	50
Figure 30. Test Pit - No Fluid Basin Plan View (X-Y Plane).....	51
Figure 31. Test Pit - No Fluid Basin Side Elevation (X-Z Plane)	51
Figure 32. Design E: Displacement Plate Velocity Table	52
Figure 33. Design E Isometric View.....	53
Figure 34. Design E Isometric View: Wave Section Profile	53
Figure 35. Design E with Gate System: Isometric View	54
Figure 36. Design E with Gates: Gate Velocity Table.....	55
Figure 37. Design E with Gates Side Elevation (X-Z Plane)	56
Figure 38. Design E with Gates Front Elevation (Y-Z Plane).....	56
Figure 39. Design E with Gates Isometric View: Wave Section Profile	57
Figure 40. Design E with Gates Isometric View: Gates Opening	57
Figure 41. Design E with Gates Isometric View: Wave Section Profile	58
Figure 42. Design F Side Elevation (X-Z Plane).....	59
Figure 43. Design F Front Elevation (X-Z Plane)	59
Figure 44. Design F: Displacement Plate Velocity Table.....	60
Figure 45. Design F Isometric View.....	61

Figure 46. Design F Isometric View: Wave Section Profile	61
Figure 47. Design G Isometric View	62
Figure 48. Design G Side Elevation (X-Z Plane)	63
Figure 49. Design G Front Elevation (Y-Z Plane).....	64
Figure 50. Design G Modified Test Pit Plan View (X-Y Plane)	64
Figure 51. Design G Modified Test Pit Elevation View (X-Z Plane)	65
Figure 52. Design G Isometric View: Wave Section Profile.....	66
Figure 53. Design H Elevation View (X-Z Plane).....	67
Figure 54. Design H Isometric View	68
Figure 55. Design H Isometric View: Wave Section Profile.....	68
Figure 56. Design I: Gate Velocity Table	70
Figure 57. Design I Side Elevation (X-Z Plane).....	70
Figure 58. Design I Front Elevation (Y-Z Plane)	71
Figure 59. Design I: Pressure Boundary Table	72
Figure 60. Design I: History Probe	73
Figure 61. Design I Isometric View.....	74
Figure 62. Design I Isometric View: Gates Opening.....	74
Figure 63. Design I isometric View: Wave Section Profile.....	75
Figure 64. Modified Design I Grid Convergence: History Probe.....	76
Figure 65. Design J: Pressure Boundary Table.....	78
Figure 66. Design J Elevation View (X-Z Plane).....	79
Figure 67. Design J Isometric View	79
Figure 68. Design J Isometric View: Wave Section	80

List of Tables

Table 1: 20 Foot Solitary Wave Simulation Solid Component Limiters.....	25
Table 2: 20 Foot Solitary Wave Simulation Fluid Region Limiters.....	25
Table 3: Baffle Impact Force vs Block Impact Force Comparison: X =160 ft, z = 25-26 ft	28
Table 4. 20 Foot Solitary Wave Impact Simulation: Grid Convergence.....	29
Table 5: 20 Foot Solitary Wave Simulation: Variable Mesh in the X-direction	30
Table 6: 20 Foot Solitary Wave Maximum Impact Force Summary	33
Table 7: WISD Iterations and Key Design Elements	37
Table 8. WISD Design Drawings: Hatch Legend.....	38
Table 9. History Probe Coordinates in Design I Simulation	73
Table 10. History Probe Coordinates in Modified Design I Simulation.....	76
Table 11. Modified Design I Grid Convergence: Maximum Velocity Values.....	77
Table 12. Modified Design I Grid Convergence: Fluid Velocity Percent Difference at Fluid Pointer.....	77

List of Equations

Equation 1: Idealized Wave Celerity	5
Equation 2: Shallow Water Wave Celerity	6
Equation 3: Morison Equation	12
Equation 4: General Continuity Equation	19
Equation 5: General Momentum Equation	19
Equation 6: Flowrate Continuity Equation	52
Equation 7: Bernoulli Equation	71
Equation 8: Simplified Bernoulli Equation	72

List of Abbreviations

CFEL	Component Flooding Evaluation Laboratory
CFD	Computational Fluid Dynamics
FAVOR	Fractional Area/Volume Obstacle Representation
FEMA	Federal Emergency Management Agency
GMO	General Moving Objects
RANS	Reynolds-averaged Navier-Stokes
VOF	Volume of Fluid
WISD	Wave Impact Simulation Device

Abstract

Flooding events pose a risk to nuclear reactor facilities, as evidenced by the recent Fukushima Daiichi nuclear power plant failure and other potential flood scenarios at nuclear facilities. To improve probabilistic risk modeling of these circumstances, water rise, spray, and wave impact testing capabilities are being developed for the Component Flooding Evaluation Laboratory (CFEL) at Idaho State University. The wave impact portion of CFEL is the topic of this paper.

Research into creating extreme wave impacts for CFEL testing is conducted, with the assumption of tsunami waves representing a worst case scenario. The design process of a device capable of simulating the impact of tsunami wave heights up to 20 feet is presented. Wave Impact Simulation Device (WISD) designs using a horizontal piston, a vertical piston, or an air pressure system as methods of fluid displacement are explored.

Design F, using a horizontal piston system, and Design J, using an air pressure system, are deemed viable for further study. These WISD designs are selected because the near-vertical wave section they produce meets the testing conditions desired for CFEL experiments.

Introduction

In the field of nuclear energy, the reliability and safety of nuclear reactor facilities is of utmost importance. Recent events such as the damage at the Fukushima Daiichi nuclear power plant show the need for risk assessment of flooding scenarios at nuclear plants and facilities. To generate probabilistic data and models for non-containment nuclear power plant components under various flooding scenarios, the Component Flooding Evaluation Laboratory (CFEL) is under development at Idaho State University. The laboratory will provide water rise, spray, and wave impact testing capabilities. The information collected from testing will be applied to risk modeling studies of nuclear power plant components and facilities. Wave impact research and preliminary Wave Impact Simulation Device (WISD) designs are presented in this paper.

A literature review of tsunami and ocean wave research is conducted, with an emphasis on wave impact studies. The research includes wave theory and idealized wave behavior, representative waveforms of natural waves, wave impact studies, artificial wave generation systems, and software wave simulation methods. It was found that wave research has generally targeted idealized wave behavior, methods of simulating waveforms numerically, and artificial wave generation. Wave impact studies often consider a structure of interest, such as a sea wall or pier, under specific wave impact conditions, and empirical methods are used to provide a method of predicting wave impact forces. To generate artificial waves, wave flumes and basins are the most common methods. These facilities use wave paddles and other displacement techniques to produce artificial waves. Numerous numerical techniques have been applied to model wave behavior, and the computational fluid dynamics (CFD) approach is applied to this project.

In an effort to simulate full scale wave impacts on prototype components and structures, the CFD code Flow-3D is used to model large tsunami wave impacts. Natural wave behavior is influenced by parameters such as fluid depth, ocean floor and coastline topography, and wavelength. The complex interaction of these parameters produces a vast range of wave conditions. Tsunami wave impacts are investigated to represent a worst case scenario, and constant approach geometry is used in Flow-3D simulations. In the simulations, solitary waves are used to represent a tsunami wave. Solitary wave assumptions are taken from previous research and established wave theory.

Flow-3D is also used to design a device capable of simulating these impacts. To design a WISD to be used in CFEL wave impact tests, two goals have been specified. The velocity and momentum of a tsunami wave with a maximum height of 20 feet must be matched, and a near vertical ten foot by ten foot section of water must be generated for impact tests. Achieving both goals will allow large components or structures to be subjected to impact forces equivalent to a full scale wave of varying height and velocity. Tsunami wave celerity is approximated using shallow water wave equations.

A key restriction in the design process is the limited lab space and funding available for the WISD. As a result, wave generation systems such as wave basins and flumes are not viable solutions. Instead of generating an artificial wave for impact testing, a high velocity jet is proposed as an alternate means of simulating a high velocity wave impact. By producing a fluid jet with a near vertical profile exiting the ten foot wide by ten foot high conduit, a ten foot wide section of a ten foot high wave can be imitated. For wave heights greater than ten feet, the wave section will represent the base of the wave with the corresponding wave speed.

The research presented is limited by assumptions concerning wave speed and tsunami wave behavior. The wave characteristic guiding the design process is wave celerity, which is tied directly to fluid depth based on shallow wave equations. Only non-breaking waves are governed by idealized wave equations. Other factors, such as variable coastline topography, influence the behavior of breaking waves and inundation flows.

The design approach of matching a maximum wave speed provides flexibility in simulating a variety of wave impact conditions. The proposed method of using a variable speed fluid jet to simulate tsunami wave impacts may also be applied to other impact conditions. If wave celerity can be specified, an approximate wave impact can be produced. This provides extensive future work to investigate different impact conditions based on one or more parameters such as different wave types, approach geometries of interest, and inundation flows.

Literature Review

Ocean wave research encompasses all aspects of waves. Topics investigated for this research project were wave theory and idealized behavior, wave breaking, inundation flows, and wave impacts. For the specialized case of tsunami waves, established assumptions and previous studies were investigated. Methods of studying waves physically with artificial wave generation are presented, and software modeling of fluid motion was explored.

Wave Theory

The identification of natural waveforms and the description of their behavior is the foundation of ocean research. By observing natural waves, wave theories have been developed that describe wave behavior. The wave type which best represents natural conditions is identified, and an equation is used to describe wave characteristics such as height and wavelength. By comparing wave height and wavelength to fluid depth, regions of application for different wave theories have been developed for use in wave research. Figure 1 displays these regions (Apelt & Piorewicz, 1987).

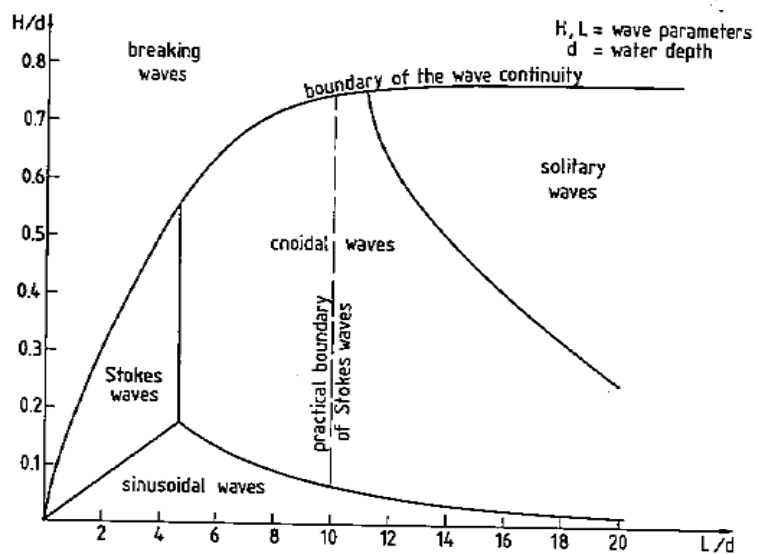


Fig. 2. Areas of wave theory validity (after Druet, 1968).

Figure 1: Established Wave Theory Validity Regions

Depending on the wave of interest, the appropriate waveform can be identified to serve as a model for study, but the sinusoidal waveform is often used to describe wave behavior beyond the area of application due to its simplicity (Apelt & Piorewicz, 1987). As an example, tsunami waves are often modeled by solitary waves (Malek mohammadi,

2009; Malek mohammadi & Testik, 2010; Goseberg & Schlurmann, 2013). The fluid motion follows a sinusoidal pattern as the wave travels, and the fluid rotation transfers the energy along the wave path. Equation 1 defines idealized wave velocity, which is dependent on wavelength and fluid depth (Mayo, 1997).

$$c = \sqrt{\frac{g\lambda}{2\pi} \tanh\left(2\pi \frac{d}{\lambda}\right)}$$

Equation 1: Idealized Wave Celerity

where c is the wave celerity, λ is the wavelength, d is the fluid depth including the wave height, and g is the gravitational acceleration on earth.

Equation 1 can be modified at the boundary conditions of the hyperbolic tangent term by comparing the wavelength to the fluid depth. If the fluid depth is greater than half of the wavelength, the celerity is controlled by the wavelength only, and is described as a deep water wave. Wind driven waves are the most common type seen in nature, and are classified as deep water waves.

When the wavelength is greater than the fluid depth by a factor of 20 or more, the equation is governed solely by fluid depth (Mayo, 1997). This flow regime is deemed shallow water wave behavior. The maximum velocity of a shallow water wave is limited by critical flow, which is defined by a Froude number equal to one. The Froude number is the ratio of inertial and gravitational forces in a fluid depth (Akan, 2006). Non-breaking tsunami wave celerity is described by shallow water theory (Mayo, 1997). Equation 2 shows the simplified wave celerity equation for shallow water waves.

$$c = \sqrt{gd}$$

Equation 2: Shallow Water Wave Celerity

where c is the wave celerity, g is the gravitational acceleration on earth, and d is the fluid depth including the wave height.

Wave Breaking

Wave breaking or cresting describes the process of a waveform losing stability before reaching shore or as it reaches land. Once a wave breaks, the resulting flow is described as a bore as it travels onshore (Yeh, 2006). Wave theory assumptions do not describe fluid behavior once the waveform is lost, and as seen in Figure 1, the breaking wave boundary has been estimated as a ratio of wave height to fluid depth. No theory exists that describes this phenomenon for all scenarios (Apelt & Piorewicz, 1987).

Baldock, Cox, Maddux, Killian, and Fayler performed laboratory tests to study the kinematics of breaking tsunami wave fronts. A large data set was collected and made accessible for use in further research. The Directional Wave Basin at Oregon State University, formally known as the Tsunami Wave Basin, was the facility where the tests were performed. Ten different solitary wave conditions were studied, with non-breaking and breaking wave conditions being included. Key parameters in the tsunami impact study included offshore conditions, flow depths and fluid accelerations, and time dependent flow behaviors (Baldock et al., 2009).

Breaking waves are often studied for the impacts they cause on coastal structures. Broken, slightly breaking, high-aeration, and low-aeration wave impacts on vertical or

steep walls were investigated by Bullock, Obhrai, Peregrine, and Bredmose. High variability was found in recorded impact forces, and the results predict wave impact conditions for a small number of impact situations (Bullock et al., 2007).

Breaking waves and their impact on vertical and inclined columns were investigated by Wienkea and Oumeracib. Tests were performed in the large wave flume at the large wave flume of Forschungszentrum Küste in Hanover, Germany. The breaking wave impact force was determined experimentally, and empirical terms were developed that brought the theoretical results into good agreement with the experimental results (Wienkea & Oumeracib, 2005)

In the referenced papers, breaking wave behavior is extremely variable, even for a narrow scope of experiment conditions. The bathymetry and topography of the location of interest greatly influence this behavior. Wave breaking will be a topic of interest for CFEL, but in order to investigate this wave condition, a specific scenario must be identified to narrow the scope of the study.

Inundation

Inundation flow, or the run-up on land from wave action, is turbulent, and is not described by idealized wave theory. The flow regimes and flow patterns resulting from wave inundation are heavily dependent on coastline topography and wave conditions. As a result, this behavior, like wave breaking, is studied in simplified scenarios or in site specific studies.

Matsutomi, Okamoto, and Harada attempted to match field data such as tsunami-trace waterlines and inundation heights from the 2009 Samoa earthquake tsunami with

scaled, steady state flow experiments. A model building was placed in a rectangular wave flume, and steady state flows were generated. A drag force equation was developed from the wave flume test results. Correlations between the scaled experiments and tsunami field data were used to create judgment criteria for building damage, and the results were compared to an established tsunami fragility curve for Japanese wooden buildings (Matsutomi et al., 2010). The results agreed well with the Japanese wood building fragility data gathered from the 2011 Great East Japan tsunami event (Leelawat et al., 2015).

Yeh (2006) used nonlinear shallow-water theory to estimate tsunami runup velocity on a uniformly sloping beach, and the momentum flux of the fluid was determined. The momentum flux was equivalent to the inundation depth multiplied by the squared fluid velocity, and impact forces were found to be proportional to the momentum flux. The results were used to provide a convenient method of estimating impact forces on objects if appropriate assumptions are used concerning the wave conditions and inundation depths (Yeh, 2006).

When the Flores Island tsunami (1992) and the Okushiri tsunami (1993) produced run up heights on islands that exceeded expectations, Choi, Kim, Pelinovsky, and Woo (2007) performed physical and numerical model studies to understand why. For the physical model, a large wave basin at the Coastal and Hydraulics Laboratory of the US Army Corps of Engineers was used to generate solitary waves to impact a small conical island representative of small islands impacted by the Flores Island and Okushiri tsunamis. For the numerical model, a 2D and a 3D model of the laboratory experiment were prepared using the CFD code Flow-3D. The physical and numerical model results

were found to agree well, and provided a better understanding of the tsunami inundation for the location of interest (Choi et al., 2007).

In all cases, the inundation results presented are only valid for a simplified scenario or for a site-specific study. If the inundation zone topography is altered, so will the flow patterns. Inundation flows are often treated as bores in modeling and analysis. It is likely that these turbulent flows will be a topic of interest for CFEL and will need to be simulated with the WISD. At that point in time, inundation flows for a chosen scenario can be researched further.

Tsunami Waves

As the goal of this research was to simulate an extreme wave impact, tsunami waves were chosen to represent a worst case scenario due to potential for large wave heights and high wave celerity. To understand the wave impact conditions to be simulated in laboratory tests, tsunami behavior and existing research was investigated. Topics included tsunami formation, established assumptions describing tsunami behavior, and previous tsunami research.

Tsunami waves are formed when a large volume of water is rapidly displaced. Earthquakes, submarine landslides, and underwater volcanic eruptions can cause these displacements. The energy released from the sudden displacement becomes a shockwave that travels through the entire fluid depth. A wave with a small wave height and enormous wavelength propagates from the displacement epicenter. Tsunami waves are modeled using shallow wave assumptions due to the ratio of enormous wavelengths to relatively shallow fluid depths. The wave speed of shallow waves is directly dependent

on the depth of water the wave travels through, which explains how tsunami waves can travel hundreds of miles an hour in deep water (Bascom, 1964).

The complex near-shore behavior of tsunami waves is influenced by the same parameters as wind-driven ocean waves, and is also affected by a process called by shoaling. Shoaling is the compression of the tsunami wavelength as the wave nears shore, resulting in an increase in wave amplitude as the wavelength decreases (Shoaling, 2011). The breaking and inundation behavior of tsunami waves, like wind driven waves, is difficult to predict without extensive, site specific studies and modeling due to the dependence on local bathymetry and topography data.

To model tsunami waves in laboratory settings or with numerical models, solitary waves have been used as a representative waveform in studies. Unlike wind-driven waves, a solitary wave has no trailing or preceding waves associated with it, and has a very long wavelength. Methods of producing solitary waves in a laboratory setting have been improved over time, but solitary waves have remained the most common method of long wave and tsunami wave simulation (Malek mohammadi, 2009; Malek mohammadi & Testik, 2010; Goseberg & Schlurmann, 2013).

Tsunami waves and their impact on coastal areas have been studied in detail at specific locations. Park, Cox, Lynett, Wiebe, and Shin performed physical experiments by constructing a 1:50 scale representation of the city of Seaside, Oregon in the Directional Wave Basin at the Oregon State University O.H. Hinsdale Wave Research Laboratory. Idealized bathymetry, topography, and surface roughness values of the coastal area were constructed for the scaled experiment. A design wave height corresponding to the a full scale wave height of ten meters was generated in the

Directional Wave Basin, and parameters such as free surface elevation and fluid velocity were recorded as the wave inundates into the scale model of Seaside. The physical results were compared to a numerical model using a Boussinesq set of equations. A comparison of the numerical and physical model indicated that the numerical model is sensitive to the input data, such as friction factors or the imported topography and bathymetry information. The importance of validating tsunami inundation velocities calculated using numerical models was emphasized (Park et al., 2013).

Like wind-driven waves, tsunami wave behavior is described by idealized equations. Laboratory studies of tsunami waves are performed using solitary waves as a representative wave form. Once the idealized waveform is lost, tsunami waves must be studied under specific scenarios to accurately account for the effects of bathymetry, topography, and other factors to describe breaking and inundation behavior.

Wave Impacts

As ocean waves approach deep sea structures or shorelines, wave impacts on shoreline structures become an important topic. Typical structures of interest include deep sea piers, seawalls, dikes, and buildings. Due to the complex behavior of ocean waves, wave impact studies generally investigate the effect of one variable on the chosen scenario while holding the other variables constant. Simplified coastline geometries are often chosen, along with a specific wave type.

The Morison equation estimates impact forces on deep sea piers empirically by considering momentum and drag terms. These empirical terms are dependent on the Reynolds number and the geometry of the object impacted, and are determined with extensive testing. Equation 3 displays the semi-empirical Morison equation.

$$F = \frac{1}{2}\rho C_D D u |u| + \rho \pi \frac{D^2}{4} C_I \dot{u}$$

Equation 3: Morison Equation

where ρ is the fluid density, C_D is the drag coefficient, D is the pier diameter, C_I is the inertia coefficient, u is wave velocity, and \dot{u} is the wave acceleration (Apelt & Piorewicz, 1987). By using both terms of the Morison equation, non-steady effects can be considered in determining the impact force.

Apelt and Piorewicz used the Morison equation in a study of wave impact conditions on piers. In wave flumes, scaled down piers were subjected to a range of scaled wave impact conditions. Horizontal fluid velocities and accelerations were used to predict wave impact forces on structures, and the empirical coefficients were determined for the object being impacted using data from previous wave impact studies. It was found that wave impact forces could be approximated by the Morison equation, but the unique empirical coefficients had to be developed for test conditions, such as the Reynold's number regime and specific cylinder drag coefficients (Apelt & Piorewicz, 1987).

Wienkea and Oumeracib also used the Morison equation in their study concerning breaking wave impacts on inclined and vertical slender piles. The Morison equation was used to determine the quasi-static impact forces, and dynamic forces are determined experimentally. The impact force was found to depend on the distance between where the wave breaking occurred and cylinder location. The maximum impact force on the cylinder occurred when the wave broke immediately in front of the cylinder. Under this

condition the fluid velocity was equal to the generated wave celerity (Wienkea & Oumeracib, 2015).

Ko, Cox, Riggs and Naito investigated the impacts caused by tsunami driven debris such as cargo ship containers. At the Large Wave Flume at Oregon State University, scaled experiments were conducted modeling solitary waves. Waves were generated by the flume to represent tsunami inundation conditions. An aluminum 1:5 scale model of a shipping container was placed in the wave impact zone, and was driven by wave action into a load cell placed on a fixed column inside the flume. The load cell recorded the impact force of the aluminum model on the column. Experiments were run at various locations under various wave conditions, and the collected data provided impact force peaks and impact durations that were used to evaluate established peak impact load calculations from Federal Emergency Management Agency (FEMA) guidelines. The impact duration is significant in determining the impact force in FEMA calculations, and it was found that the values predicted by the FEMA calculations tend to be conservative. Values from 0.1 to 1.0 seconds are recommended for FEMA calculations, while recorded impact durations were less than seven milliseconds. Shorter impact durations tended to correlate with a higher fluid velocity and a higher impact force (Ko et al., 2015).

Fluid velocity is found to be a controlling parameter in all wave impact force studies. The idealized wave equation calculates non-breaking wave velocities. More complex flow patterns, such as breaking waves and inundation flows, require detailed site information to accurately model a specific scenario, or are studied under a simplified scenario.

Artificial Wave Generation

Traditional wave generation facilities, such as wave flumes and basins, are used to generate waves for study and to create scaled wave impact conditions. Depths of water are contained in channels or basins of varying scale, and plates, paddles, or pistons are used to displace fluid in a prescribed motion, generating waves of varying amplitude and wavelength (Malek mohammadi, 2009; Malek mohammadi & Testik, 2010; Goseberg & Schlurmann, 2013).

The waves produced by these facilities inherently have wave height restrictions because wave speed in open channel flow cannot exceed a Froude number of one. The Large Wave Flume at the Oregon State University O.H. Hinsdale Wave Research Laboratory is the largest of its kind in North America, and can generate solitary waves at a maximum wave height of 1.7 meters (5.6 feet). Figure 2 is a photo of the Large Wave flume facility. A data sheet for the Large Wave Flume facility can be found in Appendix A (Large Wave Flume, 2017).

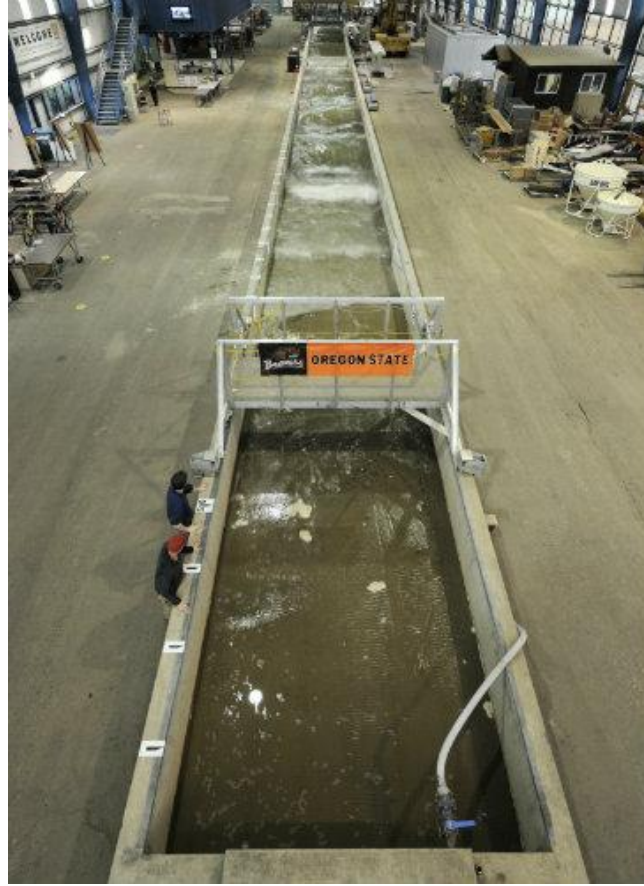


Figure 2: Large Wave Flume at Oregon State University

Another facility at the O.H. Hinsdale Wave Research Laboratory is the Directional Wave Basin, shown in Figure 3. The facility is used for tsunami research and coastal engineering studies, and can produce waves up to 0.75 meters (2.5 feet) high. A data sheet for the Directional Wave Basin facility can be found in Appendix A (Directional Wave Basin, 2017).



Figure 3: Directional Wave Basin at Oregon State University

The largest wave flume in the world, the Deltares Delta Flume in the Netherlands, can produce solitary wave heights of up to 4.5 meters (14.8 feet). Figure 4 is a view of a section of the facility. An article discussing the Delta Flume can be found in Appendix A (van Gent, 2015)



Figure 4: Deltares Delta Flume

In summary, waves are produced in wave flumes and basins for studies investigating behavior, impacts, inundation flows, and other aspects of wave research. It was found that even the largest facilities in the world cannot produce wave heights of 20 feet, which is the desired capability for use in future CFEL wave impact tests. Further information on laboratory wave generation, and on solitary wave generation using wave flumes, can be found in the referenced papers by Malek Mohammadi (2009, 2010) and the paper by Goseberg, Wurpts, and Schlurmann (2013).

Computational Fluid Dynamics

To efficiently model and predict the complex nature of fluid under various conditions, computer software is often used in research. Numerous approaches have been applied in previous research, such as Boussinesq, particle finite element, and smoothed particle hydrodynamics methods. Further information on these methods can be found in referenced papers (Chen et al., 2000; Birknes & Pedersen, 2006; Altomare et al., 2015). The computational fluid dynamics (CFD) method is used in all wave impact and WISD design simulations. The CFD code Flow-3D is used for this project. Flow-3D is a commercially available software, and has a reputation for modeling free surface flows, which encompasses ocean wave behavior and wave impact scenarios.

In the CFD approach, the domain of interest is discretized into a grid of cells. The cells can be body-fitted or in a fixed rectangular grid. Boundary conditions add a layer of fictitious cells on the perimeter of the simulation to represent a condition of interest. Fluid flow parameters, such as velocities and pressures, are computed at the cell nodes as a function of time. The fluid flow behavior is calculated by solving numerically the Reynolds-averaged Navier-Stokes (RANS) equations and the continuity equation from cell to cell. The time step used to evaluate fluid behavior is a function of cell size and fluid velocity. The time step must be small enough to ensure fluid does not skip cells from one time step to the next, and is dynamically computed by Flow-3D. Fluid and solid surfaces are approximated using 3D planes within the computational cells. More detailed descriptions of CFD methods can be found in referenced literature (FLOW-3D user manual, 2017).

Governing Equations

To describe the behavior of fluids, the RANS equations and the continuity equation govern the simulation. Cartesian coordinates are used to describe location in the simulation domain. Equations 4 and 5 list the continuity and momentum equations governing incompressible flow, respectively. Incompressible flow is used to describe the behavior of water, a nearly incompressible fluid.

$$\frac{\partial}{\partial x}(uA_x) + \frac{\partial}{\partial y}(vA_y) + \frac{\partial}{\partial z}(wA_z) = 0$$

Equation 4: General Continuity Equation

$$\frac{\partial U_i}{\partial t} + \frac{1}{V_F} \left(U_j A_j \frac{\partial U_i}{\partial x_j} \right) = - \frac{1}{\rho} \frac{\partial P'}{\partial x_i} + g_i + f_i$$

Equation 5: General Momentum Equation

where u , v , and w are the velocities in the x , y , and z directions, V_F is the fractional volume of fluid in a cell, A_x , A_y , and A_z are fraction areas open to flow in the each direction, ρ is the fluid density, P' is pressure, g_i is the gravitational force in the subscript direction, and f_i is Reynolds stresses provided by the chosen turbulence model (Johnson & Savage, 2001).

Numerical Methods

Flow-3D describes fluid motion using non-linear, transient, second-order differential equations. The RANS equations and the continuity equation are solved with finite-volume approximations for user defined time intervals. Averaged values of fluid parameters such as pressure, velocity, and temperature are evaluated as a function of time at cell nodes. The finite volume method ensures continuity is maintained in the computational cells. Cell size and spacing are specified by a user defined mesh (FLOW-3D user manual, 2017).

Computational Mesh

The program solves the fluid equations of motion at cell nodes specified by a user defined mesh. The mesh discretizes the simulation into rectangular cells, and each cell has multiple nodes where averaged values of parameters such as pressure, velocity, and temperature are evaluated. To accurately model fluid behavior, a sufficiently fine mesh must be specified, but as the mesh becomes more refined, the simulation becomes more computationally intensive. Available computational time and computing power forces the use of an optimized mesh to achieve an acceptable level of accuracy within computational capabilities (FLOW-3D user manual, 2017).

Solid Geometry

The solid surfaces in Flow-3D simulations are described by the Fractional Area/Volume Obstacle Representation (FAVOR) method, which describes a solid interface using a 3D plane in a computational cell. This surface is found using a first

order approximation. A porosity of zero is assigned to solid regions and a porosity of one is assigned to nonsolid regions. If a cell has solid and nonsolid regions, a value between one and zero is assigned based the percentage of the cell defined as solid. Curved or irregular surfaces are approximated by the 3D planes (Johnson & Savage, 2001).

Fluid Surface

Similarly to the FAVOR method, the Volume of Fluid (VOF) method assigns a value of zero to regions without fluid, and a value of one to cells filled entirely with fluid. A value between zero and one is assigned to cells based on the percentage of the cell filled by fluid. A 3D plane is used to describe a fluid free surface. The VOF method determines the free surface with respect to time and space, allowing the planes to adjust as the fluid conditions change (Johnson & Savage, 2001).

Boundary Conditions

Boundary conditions are important in numerical simulations. To get realistic results, appropriate boundary conditions must be used. Flow-3D adds a layer of fictitious cells on the perimeter of a simulation domain to provide a means of specifying a boundary condition. The boundary conditions important to the wave research and WISD design process are presented.

A wall boundary condition is a rigid surface that forces any normal fluid velocities at the boundary to a value of zero. The surface can be assigned as a free-slip condition for a scenario with no wall shear stresses. A no-slip condition describing a rigid wall with shear stresses can also be assigned.

Symmetry boundary conditions are a free-slip condition that does not alter the fluid velocities at the boundary. If the flow effects are insignificant in a coordinate direction, symmetry boundaries can reduce the size of a simulation by creating a sectional model.

The outflow boundary condition ensures smooth continuative flows move through the boundary, and then dampens fluid velocity terms outside of the simulation domain. This is done to prevent upstream effects from altering simulation results.

A pressure boundary condition can be defined as stagnant or static. A stagnant boundary forces velocities outside the boundary to zero, and a static boundary assigns a fairly continuous pressure to the boundary and does not force the velocity terms to zero. The stagnation pressure boundary is considered more realistic for most scenarios.

The solitary wave boundary is based on McCowan's theory, and assumes a solitary wave enters the simulation domain from a flat bottom reservoir of constant depth. By specifying a fluid depth, wave height, and the distance away from the fluid boundary the wave is initiated, the nonlinear non-oscillatory wave is produced. This wave type is commonly used in tsunami wave simulations (FLOW-3D user manual, 2017).

General Moving Objects

To specify rigid body motion during the simulation runtime, the General Moving Objects (GMO) model is used. The motion of the rigid body is dynamically coupled with fluid flow or is user-prescribed. All six degrees of freedom can be manipulated, and time dependent motion can be assigned. If desired, it can be specified that a moving rigid

object overlaps instead of collides with another solid region in a simulation (FLOW-3D user manual, 2017).

Tsunami Wave Simulation Methodology

Initial simulation efforts were focused on simulating tsunami waves and tsunami wave impacts. To this end, the computational fluid dynamics (CFD) software Flow-3D was used to simulate tsunami waves with a height of 20 feet. The model provided flow data such as peak impact forces, pressures, and velocities from the simulations. This information was used to guide the design of the WISD. The commercial code Flow-3D by Flow Science is well known for its ability to track free surface flows, which includes ocean waves.

Tsunami Wave Simulation

Using Flow-3D, the 20 foot tsunami waves were simulated as solitary waves, and the impact forces caused by the waves were recorded for fixed approach geometry. In each simulation, a 20 foot high solitary wave traveled from left to right in a body of water with a constant 20 foot depth, and approached a ten degree slope leading to a horizontal beach. To reduce computational time, the simulations were designed as sectional models; a thin slice of an infinitely wide wave perpendicularly approaching a shoreline. This effectively creates a 2D model that is valid because the flow variations parallel with the beach are not significant. The impact force on a small baffle located on the beach at various locations provided insight into how the wave impacts structures and recorded the

effective force of the wave based on what section of the wave impacts the baffle. A run time of 10 seconds was used in all solitary wave simulations.

The Flow-3D simulation for the 20 foot solitary wave was setup as follows. Water at standard conditions was specified as an incompressible fluid with a free surface interface. The gravity and non-inertial reference frame physics model was used with the gravitational constant of 32.2 feet per second squared in the negative z-direction. The Renormalized Group model was used as the turbulence model to cover a wide range of turbulent flows.

The solitary wave simulation geometry is shown in Figure 5, and the mesh planes and simulation boundaries are outlined by the green lines. The x dimension was 200 feet, the y dimension was 3 feet, and the z dimension was 50 feet. Two frictionless nonmoving solid components were used to create the sloping beach shown in red, designated Shelf and Slope. The Slope component was rotated negative ten degrees about the y-axis and translated to rest flush against the Shelf component, creating the sloped approach. The coordinates of both solid components are listed in Table 1. The components were extended beyond the simulation boundaries to eliminate computational errors at solid interfaces. One fluid region was used to generate the static fluid in the simulation domain, and the maximum and minimum coordinates are listed in Table 2. The 0.125 foot fluid depth above the horizontal beach height was used to generate artificial friction as the wave advances on the beach since friction coefficients cannot be accurately applied to sectional models. This fluid depth was chosen to fill one layer of cells in an eight cell per foot mesh size. By doing this, the solution for flow behavior in this shallow depth was more stable. The chosen mesh size is justified later in impact force convergence tests.

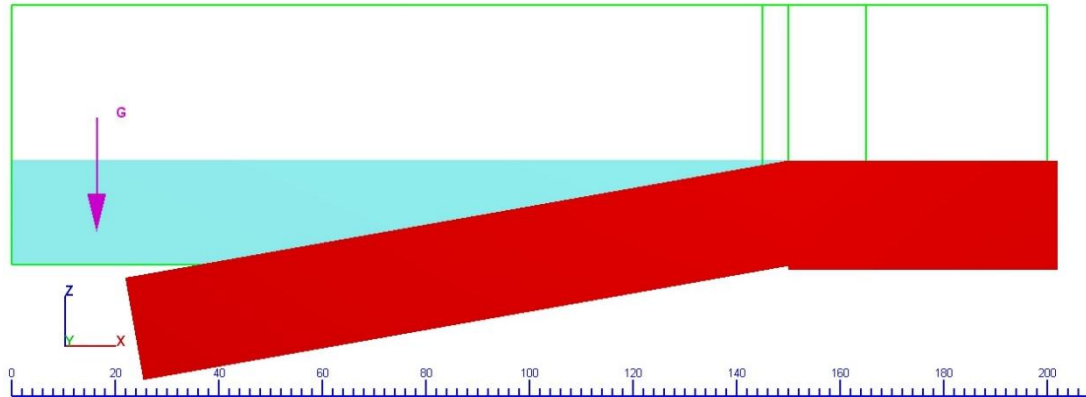


Figure 5: 20 Foot Solitary Wave Flow 3D Simulation Geometry (X-dimension in feet)

Table 1: 20 Foot Solitary Wave Simulation Solid Component Limiters

Component	X-Max	X-Min	Y-Max	Y-Min	Z-Max	Z-Min
Shelf	202.00	150.00	2.50	-1.50	20.00	-1.00
Slope	153.47	21.97	2.50	-1.50	20.00	-22.27

Table 2: 20 Foot Solitary Wave Simulation Fluid Region Limiters

Fluid Region	X-Max	X-Min	Y-Max	Y-Min	Z-Max	Z-Min
1	200.00	0.00	-1.00	2.00	20.125	0.00

The x-minimum boundary condition was specified as a solitary wave boundary. A mean fluid depth of 40 feet, a wave height of 20 feet, and a distance of 20 feet from the simulation boundary were specified for the initial wave conditions. It was noted that Flow-3D assumes the solitary wave approaches the simulation domain from a constant depth reservoir, and that Flow-3D automatically corrected the distance from the simulation boundary to half of the wavelength of the 20 foot wave (480.6 feet) when the simulation was run. A constant 20 foot fluid depth was specified at the wave boundary.

The x-maximum boundary was an outflow boundary that does not allow fluid inflow. Both the y minimum and maximum boundaries were set as symmetry boundaries to ensure no boundary conditions altered the behavior of the sectional model. The z-maximum boundary was set as a stagnation, zero pressure boundary with a fluid fraction of zero to represent atmospheric pressure. The z-minimum boundary was a free slip wall boundary, acting as the bottom of a flat reservoir.

Tsunami Wave Impact Studies

Two methods were investigated to capture impact force data: baffle output and component output. To determine the best option for impact force capture in Flow 3D, a comparison study was conducted. The main concern investigated was the comparison of edge effects as fluid accelerated around a baffle versus a block component. Since a baffle is an infinitely thin element, fluid may accelerate around the edge of the baffle differently than the edge of three dimensional object, influencing the recorded impact force. If edge effects were found to be negligible, a single baffle was the more efficient method to collect impact force data. If edge effects were not negligible, multiple baffles or blocks would have been used to account for edge effects.

Solitary wave simulations were run for both a block impact condition and a non-porous baffle impact condition at a fixed location. Figures 6 and 7 show the baffle and block configurations, respectively. The center baffle or block was 2 feet high by 3 feet wide, and the top and bottom baffles or blocks were 3 feet wide by 0.5 feet high. Impact forces were only recorded on the baffle or block face struck by the incoming wave.

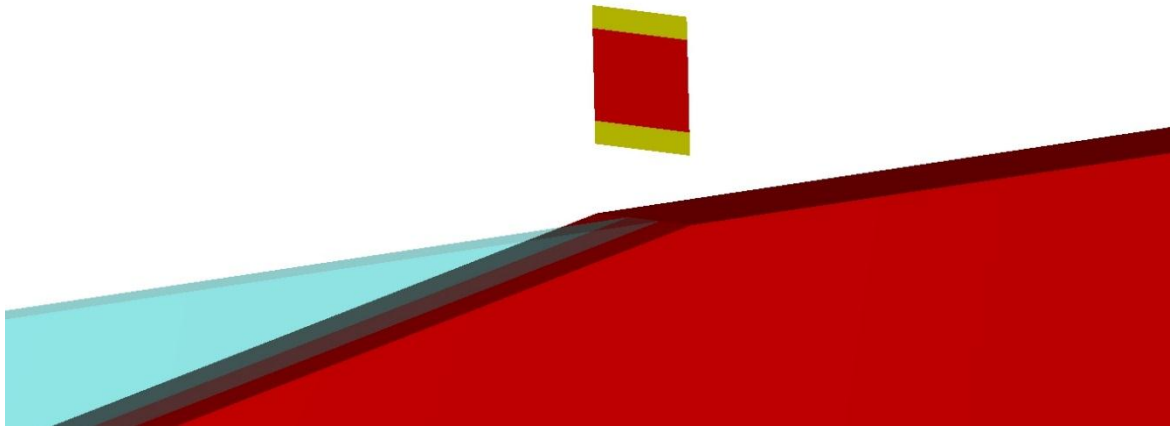


Figure 6: Impact Capture Comparison - Baffle Impact Condition – Isometric View

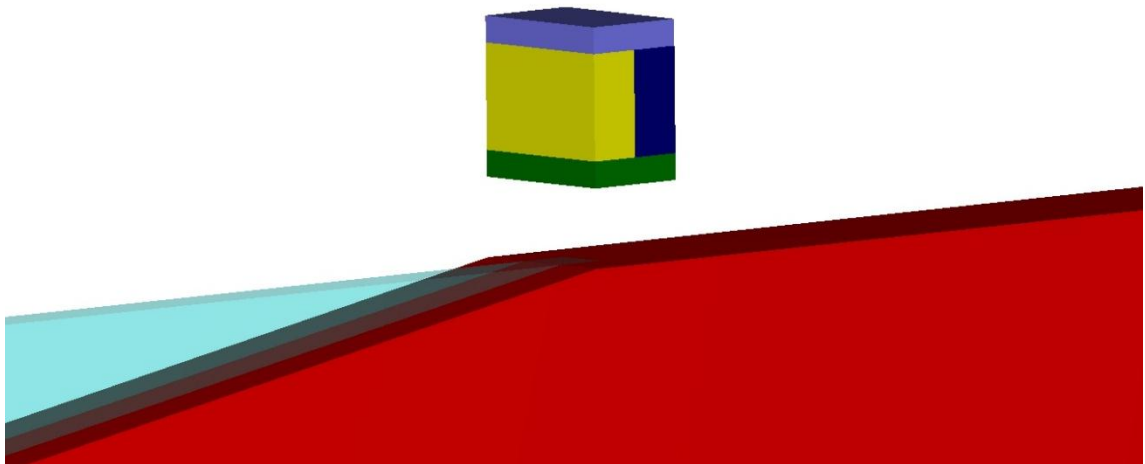


Figure 7: Impact Capture Comparison - Block Impact Condition – Isometric View

The impact force results recorded by Flow-3D are summarized in Table 3. It can be seen that between the corresponding blocks and baffles, very little difference was seen in the recorded values. This indicated that edge effects were negligible when recording an impact force. As a result, baffles were selected as the method of recording impact forces

in the wave impact zone, and a single baffle replaced the three discrete baffles to streamline the simulation.

Table 3: Baffle Impact Force vs Block Impact Force Comparison: X = 160 ft, z = 25-26 ft

<u>Component</u>	<u>Time (sec)</u>	<u>Force Magnitude (lbs)</u>	<u>Percent Difference (%)</u>
Top Block	8.48	1306.30	-
Top Baffle	8.48	1320.28	-
			1.05
Center Block	8.48	4680.71	-
Center Baffle	8.48	4693.46	-
			0.27
Bottom Block	8.45	832.33	-
Bottom Baffle	8.45	822.38	-
			-1.2

To identify the optimum mesh size to use in the described wave simulation, a grid convergence study was performed. The mesh size, measured in cells per foot, was kept constant in all directions in each simulation run. The impact forces on a one foot by one foot baffle recorded at a constant location served as the convergence criteria. The baffle was located at an x coordinate of 160 feet and from 25 to 26 feet in in the z coordinate. As shown in Table 4, the percent difference of the impact forces indicated that a mesh

size of eight cells per foot was the optimum option to minimize simulation runtime without compromising results.

Table 4. 20 Foot Solitary Wave Impact Simulation: Grid Convergence

Mesh	Time of Impact (sec)	Force (lbs)	Percent Difference (%) from Previous Mesh
2 cells/ft	8.9988	1178.12	-
4 cells/ft	9.0997	1321.90	10.87
6 cells/ft	9.0999	1363.65	3.06
8 cells/ft	8.8999	1388.85	1.81
10 cells/ft	8.9001	1429.41	2.84

The optimized mesh size was applied to the 2D sectional model. The mesh in the x direction was modified to utilize a variable grid. This was done to refine the mesh near the impact location, and to use a coarse mesh away from the impact zone to reduce computation time. A mesh plane was placed at a location of 145 feet to initiate mesh refinement approaching the impact zone of the beach. Another mesh plane was placed at the impact location to ensure the eight cells per foot mesh spacing occurred at the location of interest. The final mesh plane was placed outside of the impact zone at 165 feet to produce a more coarse mesh beyond the impact zone. Table 5 defines the variable mesh used in the x-direction for a baffle located at 150 feet along the x -axis. The mesh in the y-direction was kept constant at 4 cells per foot because edge effects were negligible in the sectional model. A constant 8 cells per foot mesh was used in the z-direction.

Table 5: 20 Foot Solitary Wave Simulation: Variable Mesh in the X-direction

<u>Mesh Plane</u>	<u>X-axis Location</u>	<u>Cell Size</u>	<u>Cell Count</u>
1	0	Variable	-
2	145	8 cells/foot	40
3	150	8 cells/foot	120
4	165	Variable	-
5	200	-	-
<u>Total Cell Count</u>			1100

Impact forces at various locations and elevations were recorded in the impact zone, which extended from 150 feet to 160 feet in the x direction. The solitary wave simulation with x-coordinates is shown in Figure 8. Figure 9 shows the initial velocity conditions of the tsunami wave simulation at time zero, and Figures 10 and 11 display the pressure and velocity patterns of the wave as it travels from left to right towards the horizontal beach. Figure 11 illustrates how the wave front moves forward with an atmospheric pressure. This aspect of wave behavior must be recreated by the WISD to produce realistic wave impact test conditions. A baffle about to be struck by the solitary wave is shown in Figure 12.

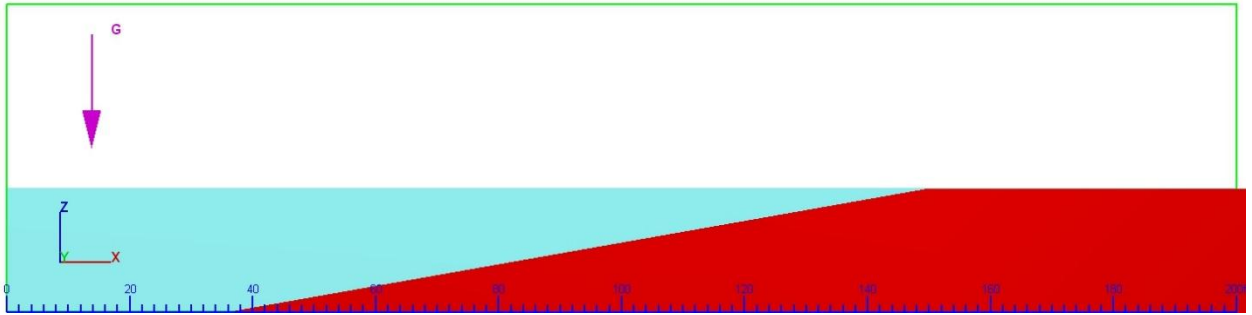


Figure 8. 20 Foot Solitary Wave Flow-3D Simulation (X-Z Plane)

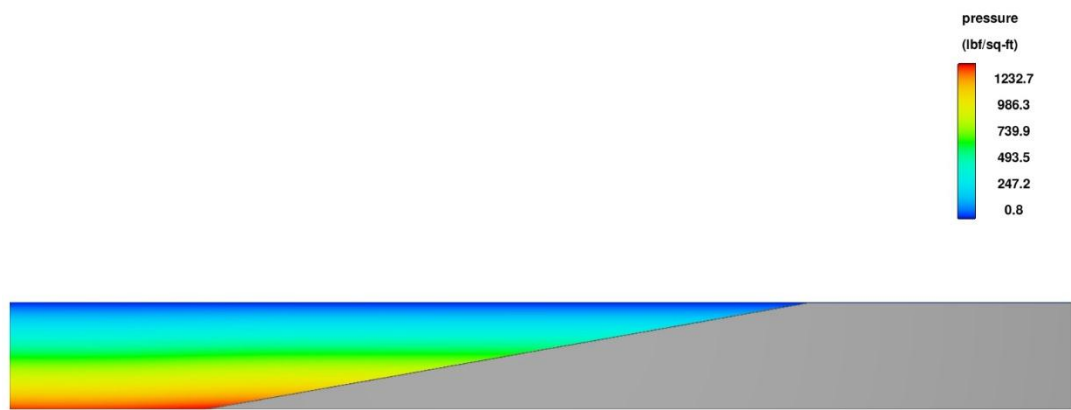


Figure 9. Initial Condition Pressure Distribution of 20 Foot Solitary Wave Simulation

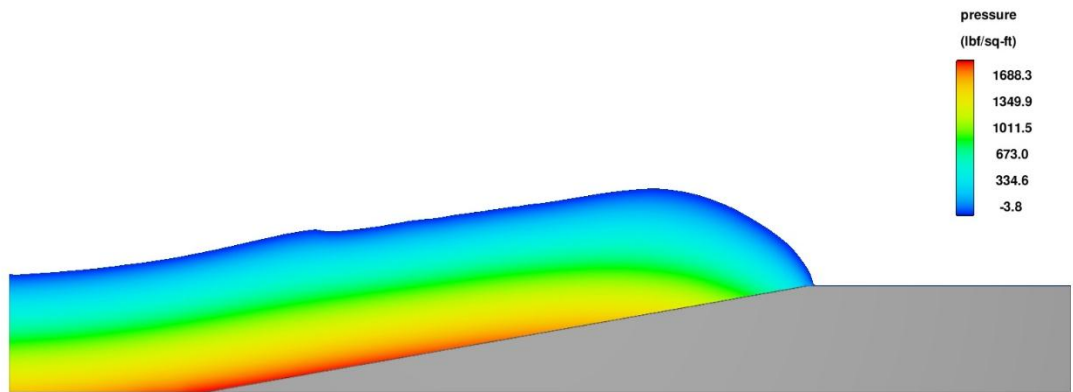


Figure 10. Pressure Distribution of a Solitary Wave Advancing Forward on a Beach

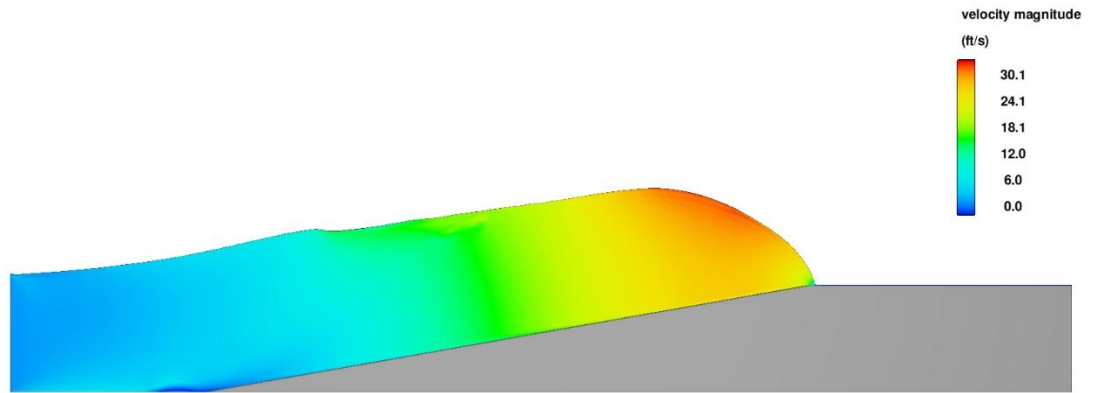


Figure 11. Velocity Distribution of a Solitary Wave Advancing Forward on a Beach

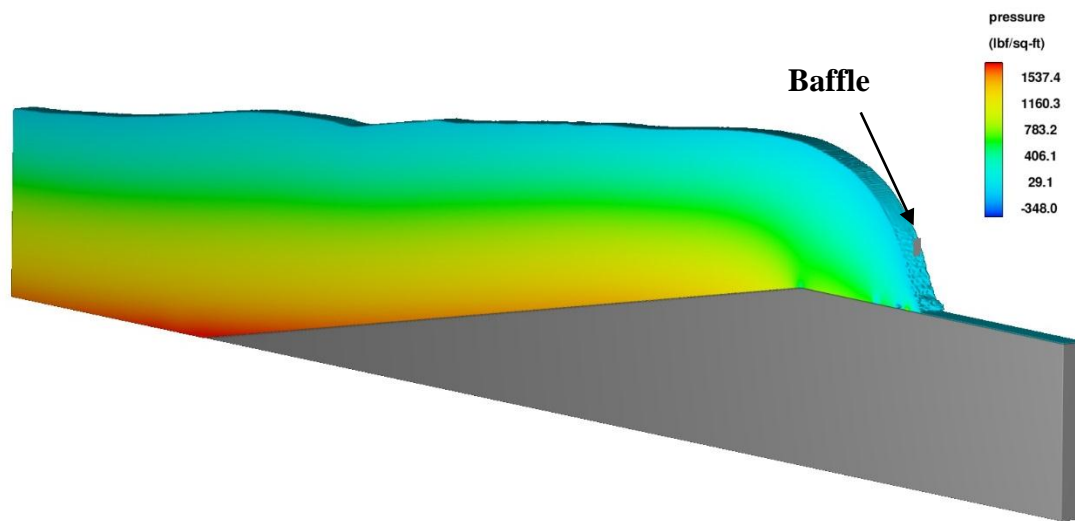


Figure 12. Isometric View of Wave Pressures at Imminent Baffle Impact

Tsunami Wave Simulation Results

The impact forces recorded by nonporous baffles in the Flow-3D solitary wave simulations are presented in Table 6 and shown visually in Figure 13. The baffles are two feet high in the z-direction and one foot wide in the y direction, and are centered along the centerline of the sectional model in the x-direction. The results were found to have high variability in the impact zone of interest, with the location of the baffle greatly influencing the results. It was observed that the variability in results occurs when the waveform loses stability and the flow becomes more turbulent. The impact zone is outlined by mesh planes at x coordinates of 150 feet and 160 feet in Figure 5.

Table 6: 20 Foot Solitary Wave Maximum Impact Force Summary

Data Point	Baffle Z Location (ft)	Force (lbs) at X = 150	Force (lbs) at X = 155 ft	Force (lbs) at X = 160 ft
1	20-22	2681.46	8600.11	5777.51
2	22-24	2518.07	4310.88	8515.18
3	24-26	2327.7	2674.78	5201.58
4	26-28	2203.89	2295.38	3268.38
5	28-30	2217.74	2589.22	3050.39
6	30-32	2296.12	2502.73	2778.18
7	32-34	2230.55	2378.2	2502.35
8	34-36	1974.33	1864.46	1127.53
9	36-38	0	0	0

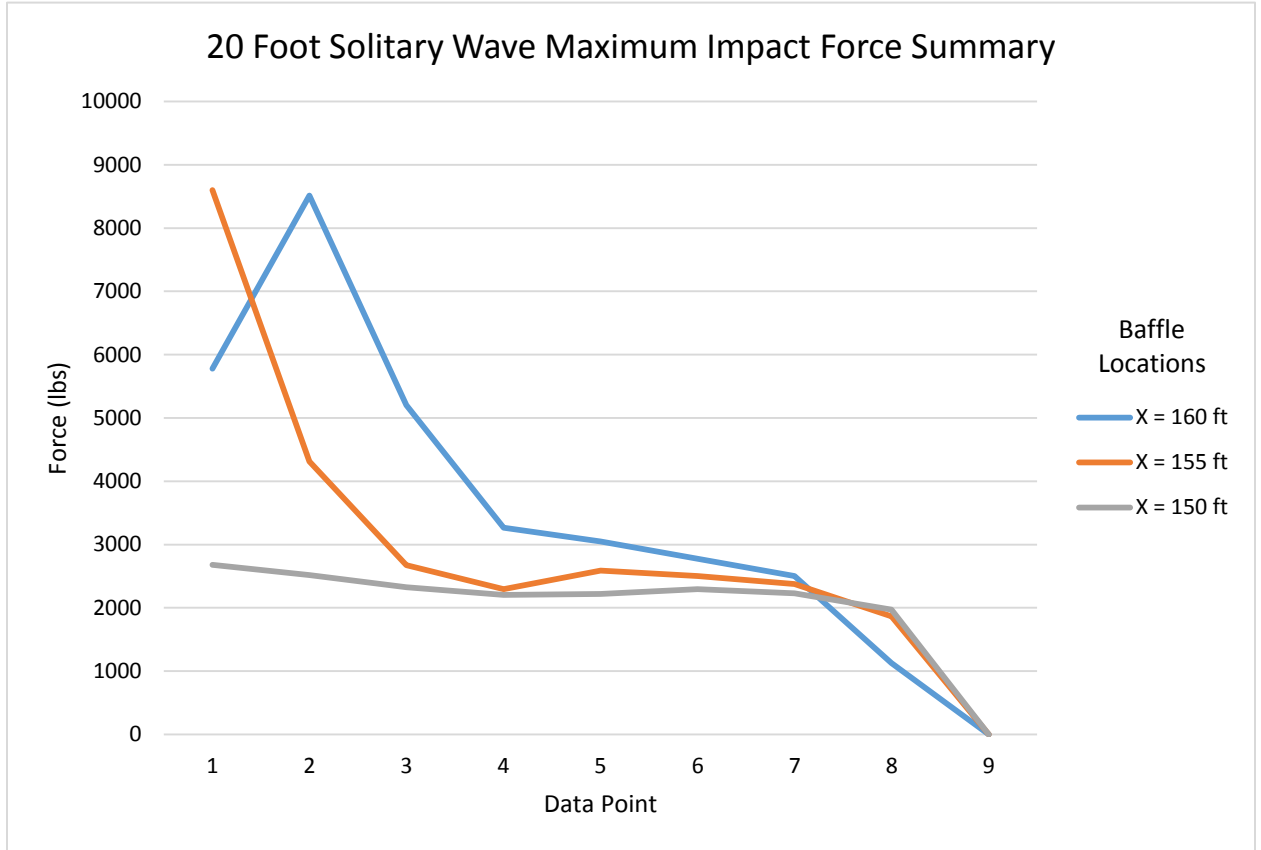


Figure 13: 20 Foot Solitary Wave Maximum Impact Force Summary

It was concluded that the approach of identifying the impact force caused by a wave for all possible impact locations was not practical, even if the simplified scenario used in the sectional solitary wave simulations was the only scenario studied. The results only applied to the simplified geometry used in the sectional wave simulation, and could not be used to accurately predict wave impact forces in different scenarios.

To provide a method of simulating wave impacts for CFEL, idealized wave behavior must be assumed to simplify the wave impact conditions. Only non-breaking wave velocities can be described by the idealized wave celerity equation. It was proposed

that the maximum horizontal fluid velocity for a specified wave shall be determined from the idealized wave equation for non-breaking wave conditions. By considering only non-breaking waves, horizontal fluid velocities control the impact force of the wave, and vertical velocity components can be deemed negligible. The WISD would then be designed to produce fluid velocities matching those of a specified wave. Equation 2 was used to establish the target velocities of shallow water waves in the pursuit of simulating tsunami wave impacts.

To simulate wave impacts for breaking waves and inundation flows, a scenario-specific study can be performed to identify a wave impact condition of interest. Flow 3D can be used to simulate a wave impact condition in a similar manner to the sectional model used in wave impact studies. Once a wave impact velocity is identified, the impact conditions can then be simulated using the WISD.

WISD Methodology

By defining a tsunami wave as a shallow water wave and applying Equation 2, a maximum horizontal fluid velocity of 25.4 feet per second for a wave height of 20 feet was obtained. This maximum velocity was used to determine the necessary capabilities of the WISD. To meet the goals for CFEL testing capability, a wave section 10 feet wide by 10 feet high with a controlled profile must be produced.

Following the review of traditional wave generation using wave flumes and basins, it was found that these methods are not feasible for this project due to inherent wave height restrictions in open channel flow. Open channel wave generation techniques do not provide a realistic solution to meet the CFEL project goal of simulating a 20 foot

solitary wave impact due to financial and logistical restrictions. As a result, alternative methods of wave impact simulation, such as closed conduit flow, had to be investigated to develop a WISD design. The advantage of using closed conduit flow is that no fluid depth restrictions limit fluid velocity. Effort was put towards matching an idealized wave celerity by using high velocity closed conduit flow, and different methods of producing a high velocity fluid flow were investigated. Another consideration was to reproduce the behavior of a wave front moving forward with an atmospheric pressure. This aspect of wave behavior must be recreated by the WISD to produce realistic wave impact test conditions.

A multitude of models were simulated in Flow-3D to determine an ideal design for a WISD capable of creating a near vertical wave section with the same velocity as a 20 foot tsunami wave. Flow 3D models exploring vertical and horizontal pistons displacement mechanisms are presented, as well as designs using an air pressure to displace fluid. The designs are presented in chronological order of development. Table 7 lists the designs presented and the key design element for each iteration.

Table 7: WISD Iterations and Key Design Elements

<u>WISD Design Iteration</u>	<u>Displacement Method</u>	<u>Key Design Element</u>
A	Horizontal Piston	Horizontal Piston System
B	Horizontal Piston	Fluid Entrainment
C	Horizontal Piston	Rotating Plate
D	Horizontal Piston	Fillet Contraction
E	Horizontal Piston	Horizontal Baffles
E with Gates	Horizontal Piston	Vertical Gate System
F	Horizontal Piston	Friction and Thin Plates
G	Vertical Piston	Vertical Piston on Fluid Free Surface
H	Vertical Piston	Compact Vertical Piston System
I	Air Pressure	Air Pressure System
J	Air Pressure	Air Pressure on Fluid Free Surface

The WISD design iterations are all composed of three main sections: the fluid reservoir, the exit conduit, and the test pit. Figure 14 displays a cross-sectional view of Design A, with each region labeled. Each design was drawn in AutoCAD, and then exported as an STL file into Flow 3D as a solid component. The hatch pattern definitions for the dimension drawings are given in Table 8.

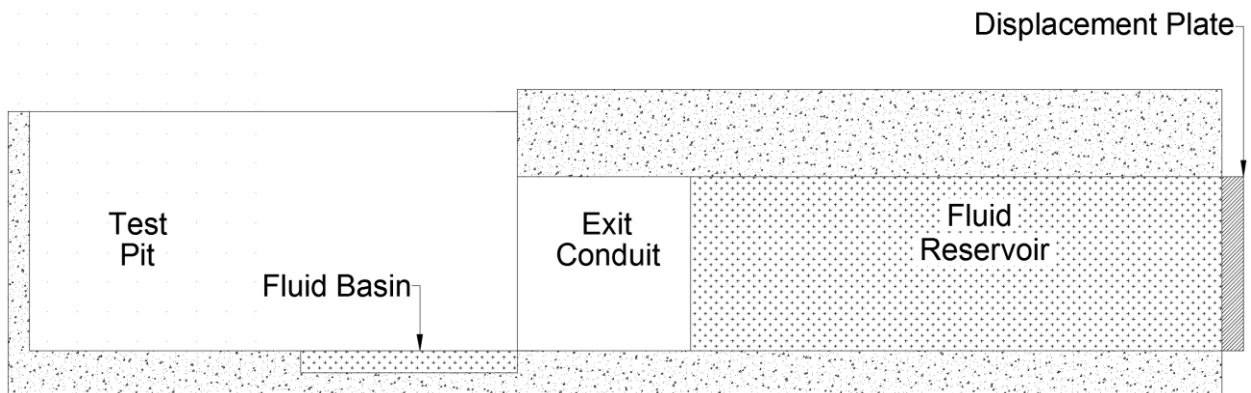


Figure 14. Design A: WISD Sections and Components

Table 8. WISD Design Drawings: Hatch Legend

<u>Hatch</u>	<u>Definition</u>
	Fluid Region
	Concrete Wall/Rigid Boundary
	Rigid Plate Or Gate

Each simulation used the eight cells per foot grid size established in the optimum mesh size study for the wave impact simulations. A zero pressure boundary was specified as the z-maximum boundary for all simulations. All other boundary conditions are wall boundaries unless otherwise specified.

Water at standard conditions was specified as an incompressible fluid with a free surface interface. The gravity and non-inertial reference frame physics model was used with the gravitational constant of 32.2 feet per second squared in the negative z-direction. The Renormalized Group model was used as the turbulence model to cover a wide range of turbulent flows.

Horizontal Piston WISD Design

A WISD design obstacle identified in the computer modeling of solitary waves was gravitational acceleration. Fluid was pulled towards the bottom of a wave profile as the waveform loses stability, creating an advanced fluid front at the base of the advancing wave section. This is illustrated by the orange fluid tongue shown in Figure 15. Although a small advance front or tongue is present in natural waves, the slope of the wave face produced by the WISD must be controlled to produce realistic wave sections for impact

testing. To counter this behavior, a shallow fluid basin was placed in the test pit directly in front of the exit conduit, with a depth of one foot, a width of 12 feet, and a length of ten feet. The intent was to slow the wave front by forcing the fluid tongue to entrain the still water and create a momentum transfer, slowing the advanced front to allow the wave section to catch up and entrain the fluid tongue. This feature is present in WISD designs A through D. Figures 16 and 17 show the standard test pit dimensions with the fluid basin.

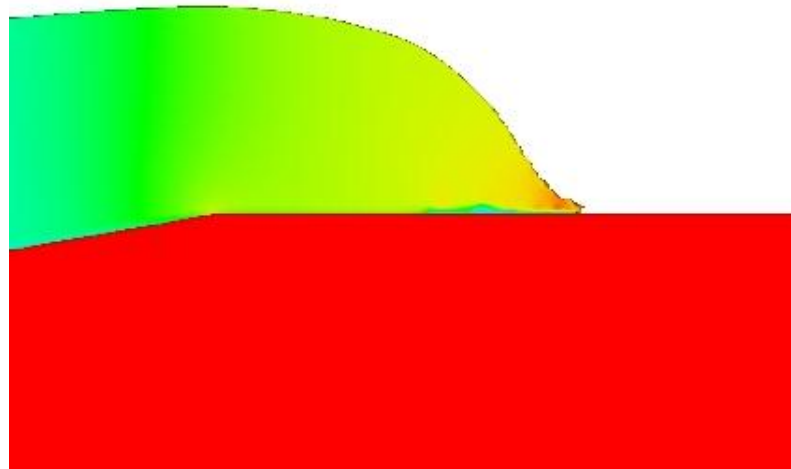


Figure 15. Fluid Tongue at Solitary Wave Base

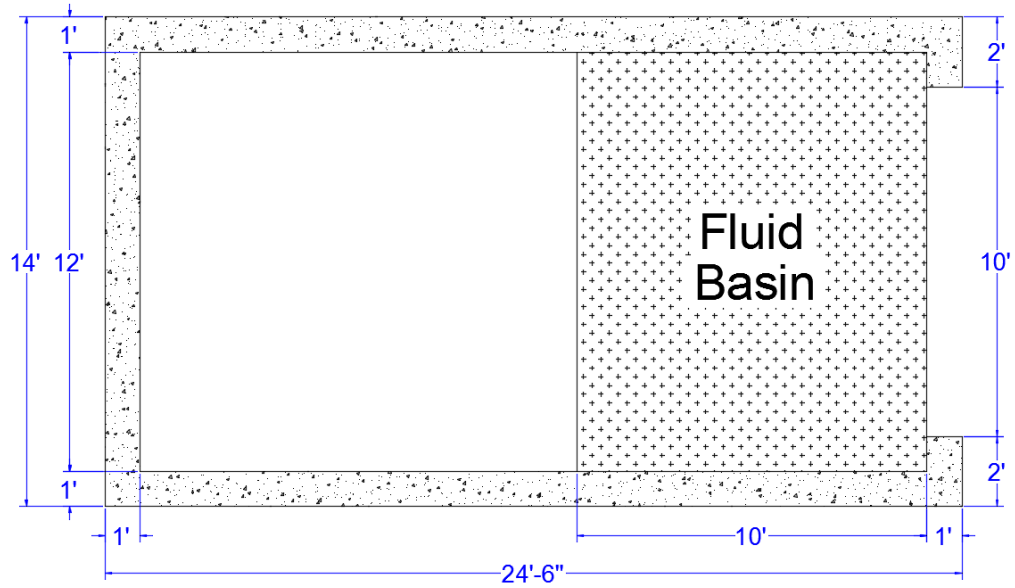


Figure 16. Test Pit with Fluid Basin: Plan View (X-Y Plane)

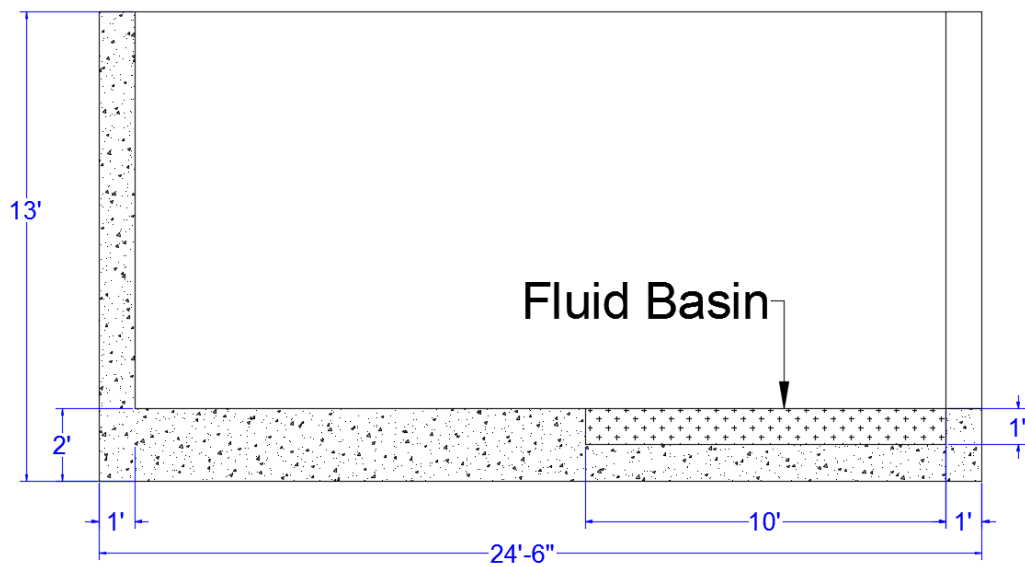


Figure 17. Test Pit with Fluid Basin: Side Elevation (X-Z Plane)

The WISD designs A, B, and C use a vertical plate, like a piston, to push fluid out of a constant geometry conduit into the test pit, and served as instructional models to guide an effective future design. The exit conduit and fluid reservoir dimensions are

shown in Figures 18 and 19. The plate was modeled as a rigid moving component that moved at a constant velocity of 25.4 feet per second in the negative x-direction for a distance of 15 feet to match the target velocity of a 20 foot solitary wave. All solid components and walls were frictionless boundaries. A simulation finish time of 1 second was used. Figure 20 displays an isometric view of the simulation before fluid motion is initiated.

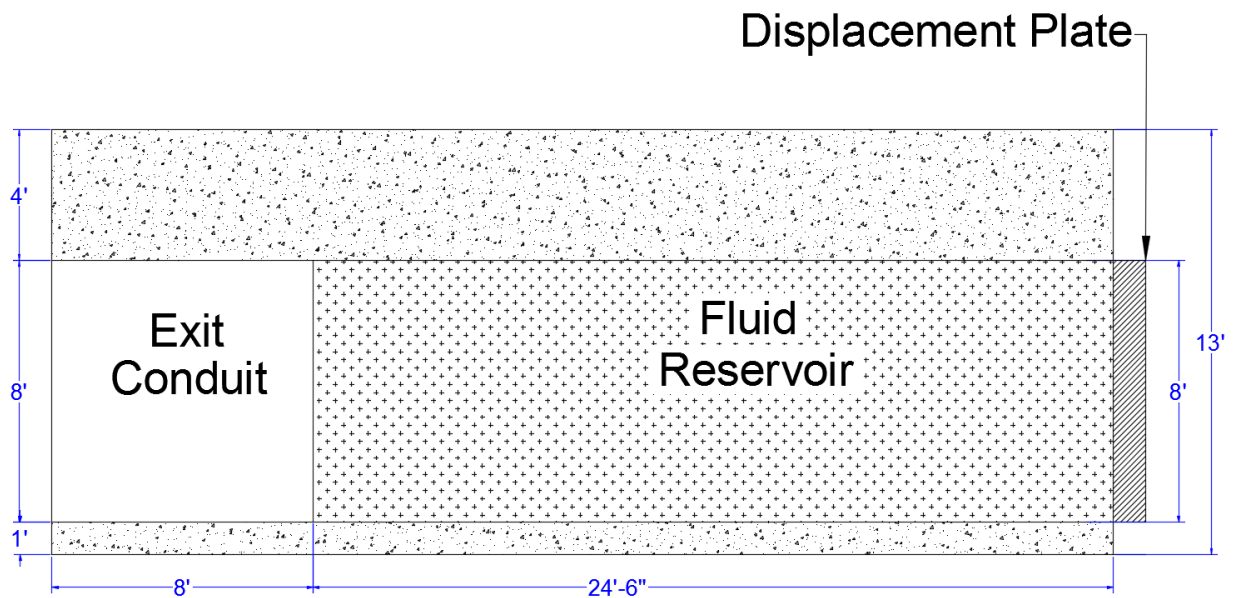


Figure 18. Design A-C: Side Elevation (X-Z Plane)

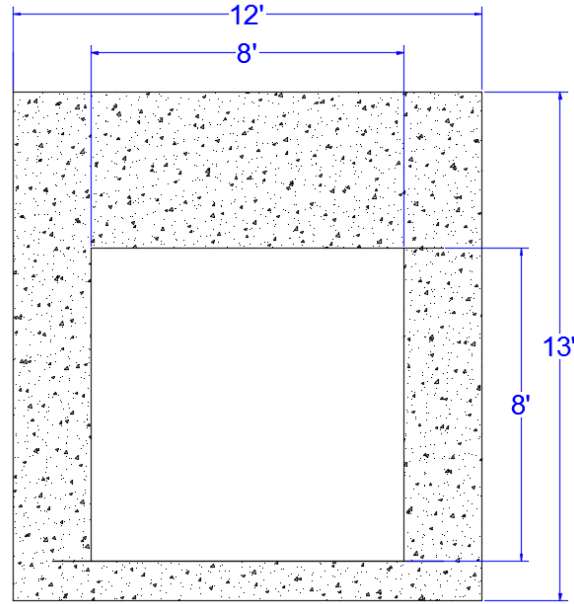


Figure 19. Design A-C: Front Elevation (Y-Z Plane)

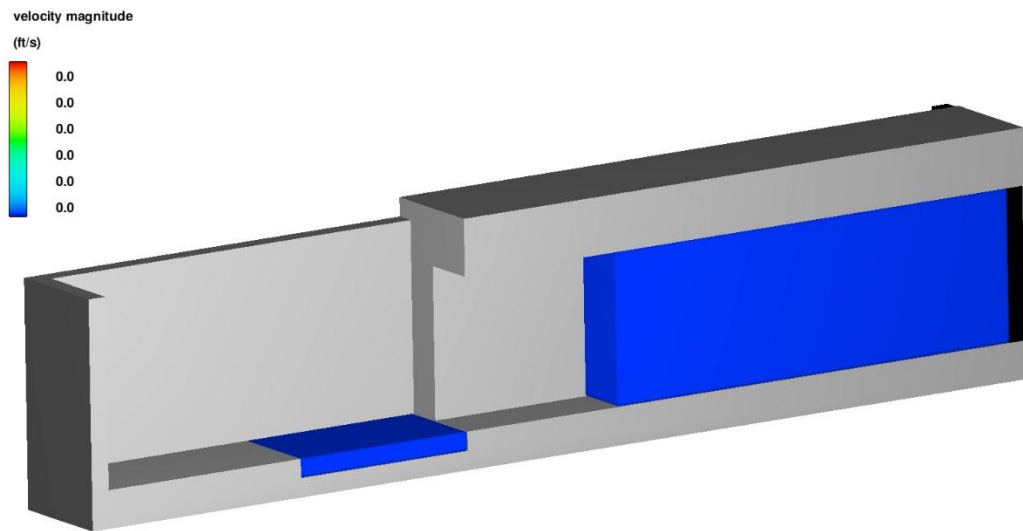


Figure 20. Design A-C Isometric View

Design A

As the vertical plate pushes the water from right to left into a test pit at a constant velocity of 25.4 feet per second, the effect of gravity was seen on the fluid profile. Figure 21 shows the advancing wave front just prior to reaching the basin of water. It was observed that the fluid rapidly loses the original vertical profile as the simulation was run. The fluid drops to the base of the conduit, and velocities up to 41.2 feet per second were produced at the base of the wave section. Because of this high velocity, the fluid basin cannot entrain the base of the sloped wave section, and the fluid skipped over the basin into the test pit.

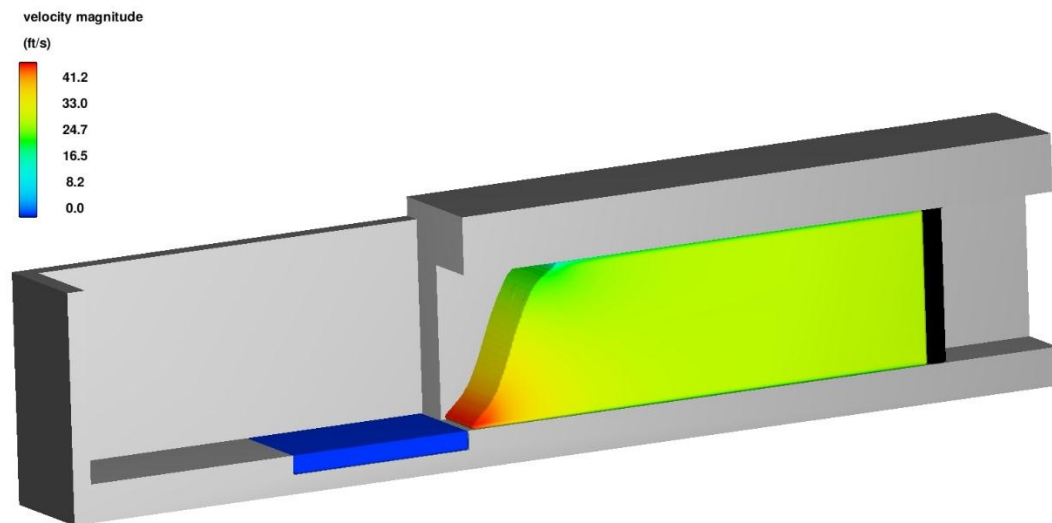


Figure 21. Design A Isometric View: Wave Section Profile

Design B

In an effort to combat the effects of gravity on the fluid profile, a one foot depth of water was placed inside the conduit and test pit to immediately impede the advancing flow at the base of the wave section. It was thought that by impeding the fluid inside of the conduit, the high velocities at the base of the conduit could be dampened over a longer distance by the static fluid. All other conditions were unchanged from Design A. As shown in Figure 22, the one foot fluid depth eliminates the fluid tongue in front of the wave section, but induces wave breaking behavior at the mid-height of the conduit. Similar to natural wave breaking, fluid velocity was redirected up to the mid-height of the conduit where there was less flow resistance, and the velocity of the fluid at the mid-height of the conduit exceeded the reduced velocity at the conduit base. Design B was deemed unsuitable for creating a near vertical wave section.

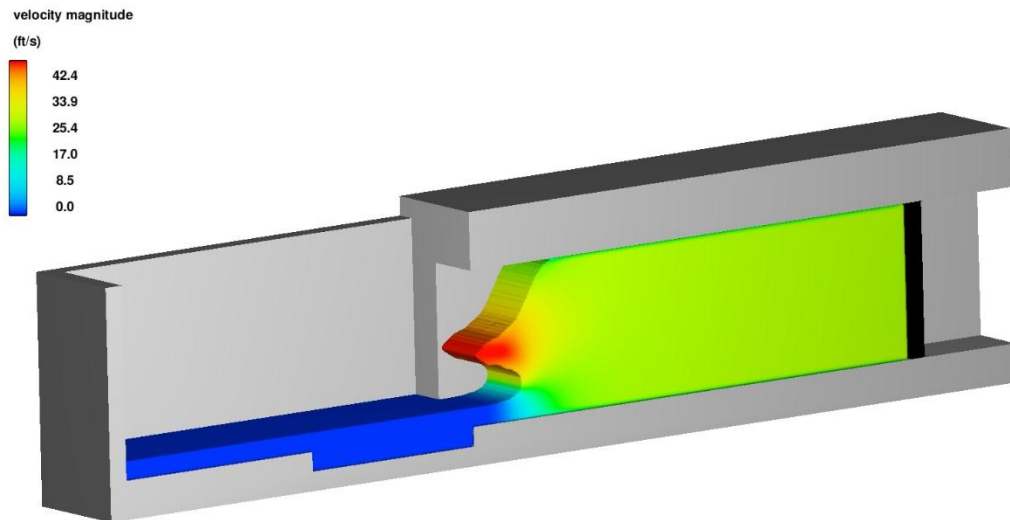


Figure 22. Design B Isometric View: Wave Section Profile

Design C

To create a more uniform wave section, fluid near the top of the conduit must be accelerated to match the fluid velocity at the bottom of the conduit. To achieve this, Design A was modified to introduce plate rotation, and was designated Design C. By rotating the plate counterclockwise while moving it horizontally, the fluid near the top of the conduit was accelerated in an attempt to match the fluid velocity at the base of the wave section. The constant velocity of 25.4 feet per second in the negative x-direction was maintained, and an angular rotation of negative one radian per second about the y axis was specified. As shown by Figure 23, the wave section has a more vertical profile using this approach. However, larger fluid velocities were still present at the base of the wave section. Also, designing a displacement mechanism capable of such complex motion would add an additional level of difficulty for this project.

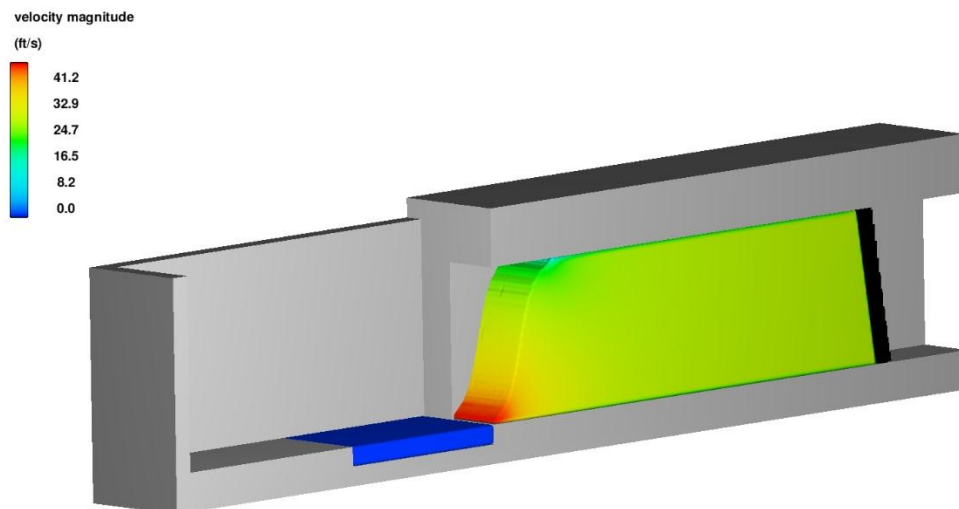


Figure 23. Design C: Wave Section Profile

Design D

An alternate method of accelerating fluid near the top of the conduit was explored for Design D. Design A was altered by adding a fillet at the top of the conduit to accelerate the fluid near the top via a conduit contraction, and the exit conduit was expanded to be ten feet wide and ten feet tall. The fillet had a radius of 2 feet, and Figures 24 and 25 display the exit conduit and fluid reservoir dimensions for Design D. The Test pit dimensions were unchanged. Figure 26 shows this simulation at time zero. As the vertical plate pushed fluid a velocity of 25.4 feet per second, a near vertical wave face formed in the exit conduit, as seen in Figure 27. The tongue at the base of the wave was reduced, and a promising fluid profile was produced by this design. It was noted that the wave section velocity was higher than the target 25.4 feet per second. The fluid basin did not retain the fluid at the base of the wave section due to the excessive velocity of the wave section, but was deemed unnecessary due to the reduced fluid tongue produced by Design D. As a result, the fluid basin was removed for future designs.

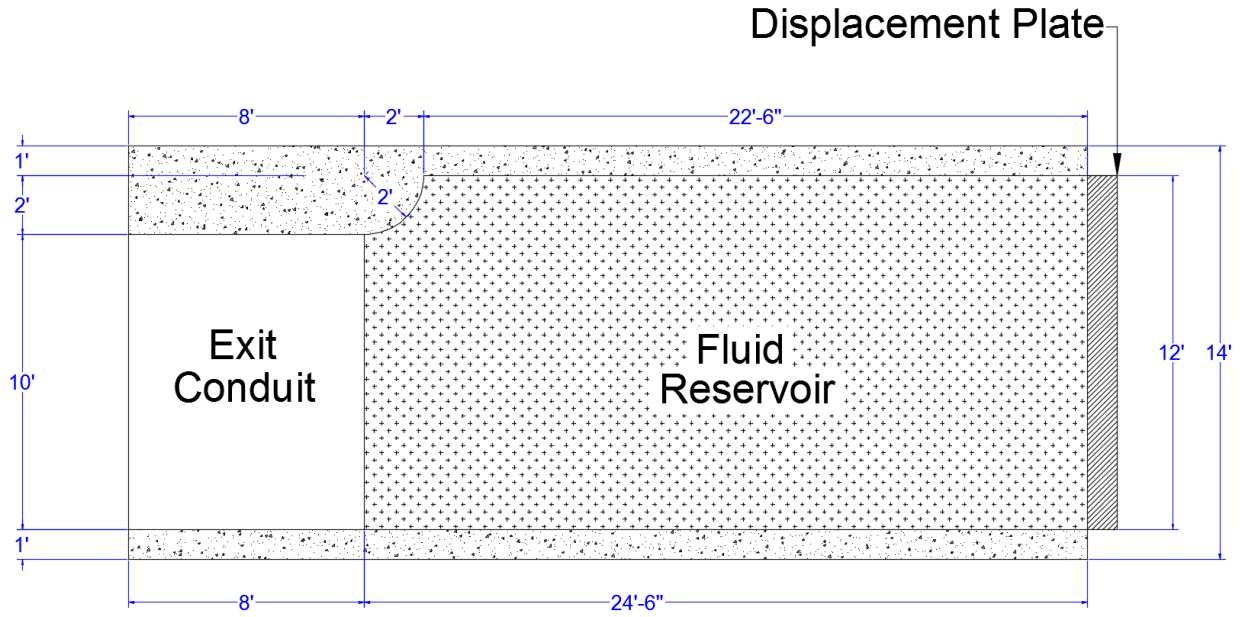


Figure 24. Design D Side Elevation (X-Z Plane)

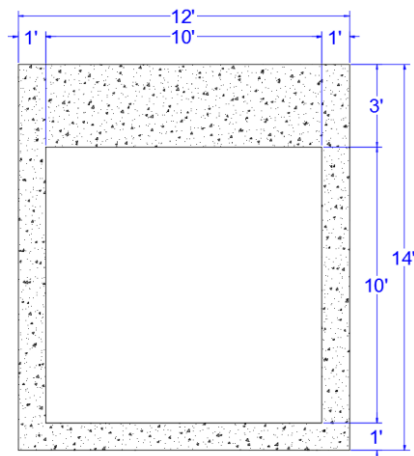


Figure 25. Design D Front Elevation (Y-Z Plane)

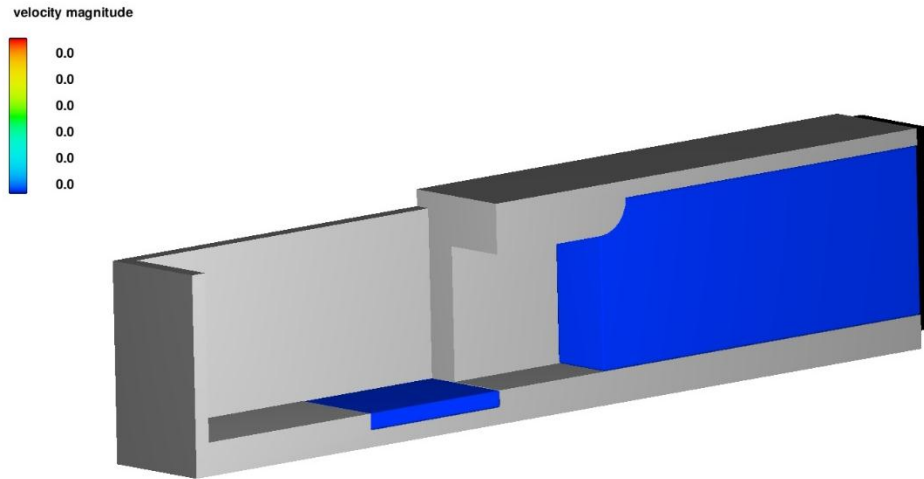


Figure 26. Design D Isometric View

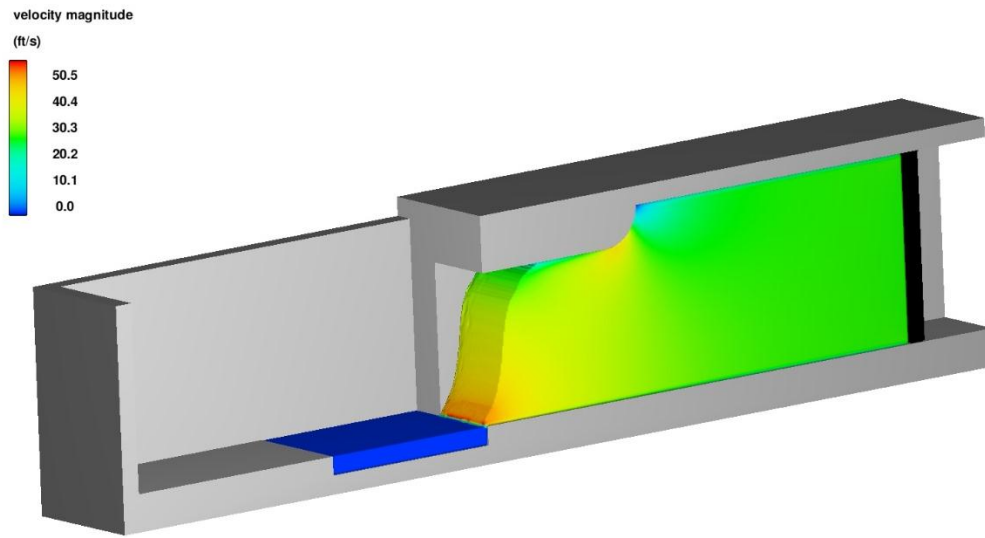


Figure 27. Design D Isometric View: Wave Section Profile

Design E

As a method of delaying the effect of gravity on the fluid profile, horizontal baffles were placed at one foot height intervals in the conduit exit in to modify Design D. The baffles were assigned zero porosity and are frictionless, acting as infinitely thin rigid and impermeable boundaries. Nine baffles, each ten feet wide and four feet long, were placed at one foot height intervals, dividing the ten foot high wave section into ten one foot sections. As a result, gravity could not pull water from the top of the conduit to the bottom inside the exit conduit. The baffles begin one foot away from the vertical fluid boundary at the fluid reservoir, and end one foot short of the conduit opening. This left space between the baffles and the fluid reservoir for a gate mechanism that was implemented in later designs, and provided a section where the separated flows rejoined and formed a cohesive wave section before entering the testing tank. Also, the fluid basin in the test pit was removed since the fluid tongue at the base of the wave section was reduced by Design D. Figures 28 and 29 display the baffle locations and dimensions in the conduit exit, and Figure 30 and 31 show the modified test pit dimensions.

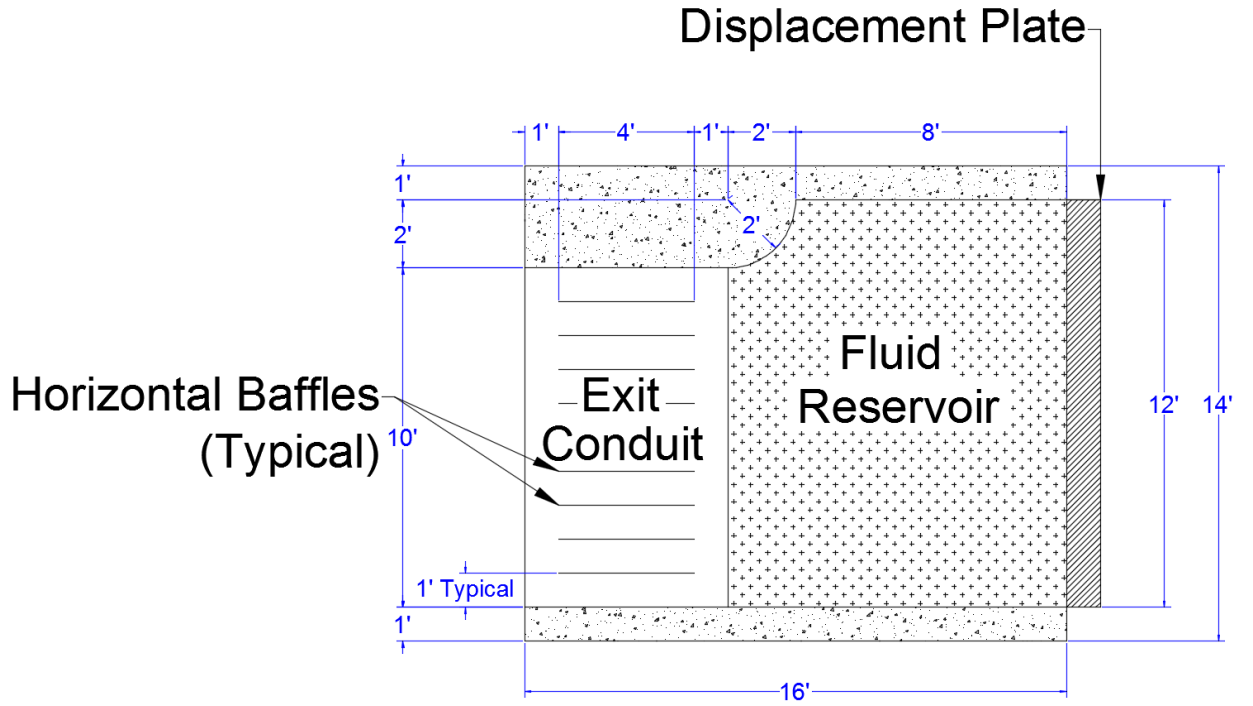


Figure 28. Design E Elevation View (X-Z Plane)

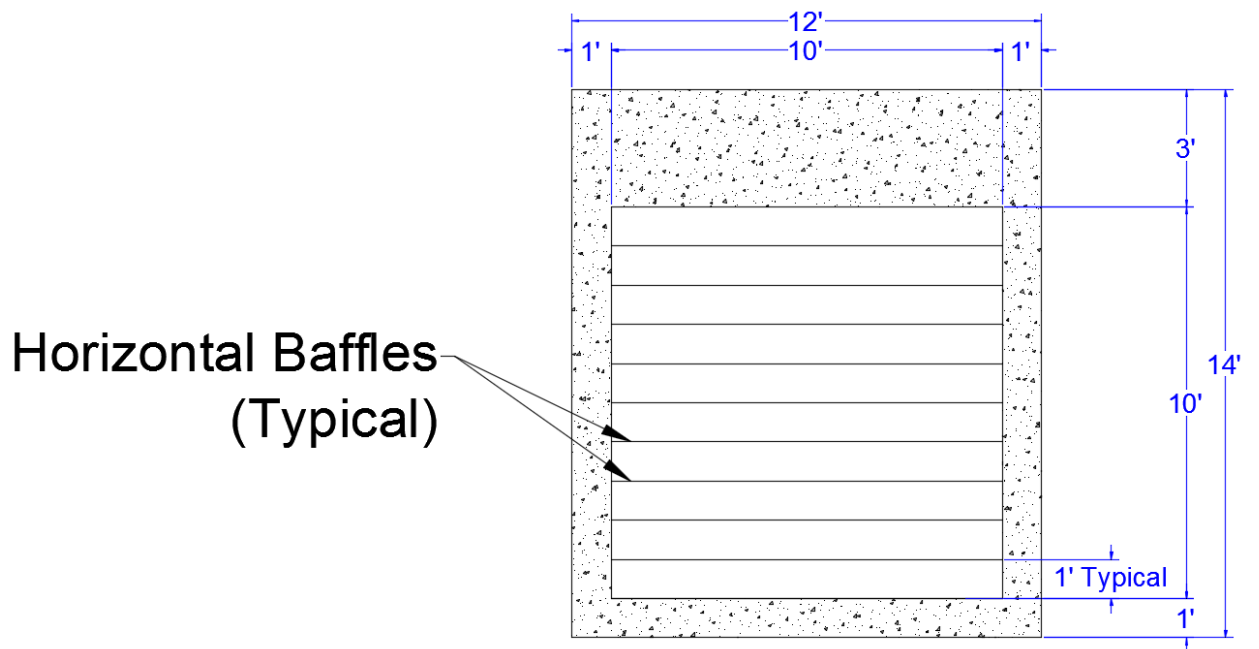


Figure 29. Design E Front Elevation (Y-Z Plane)

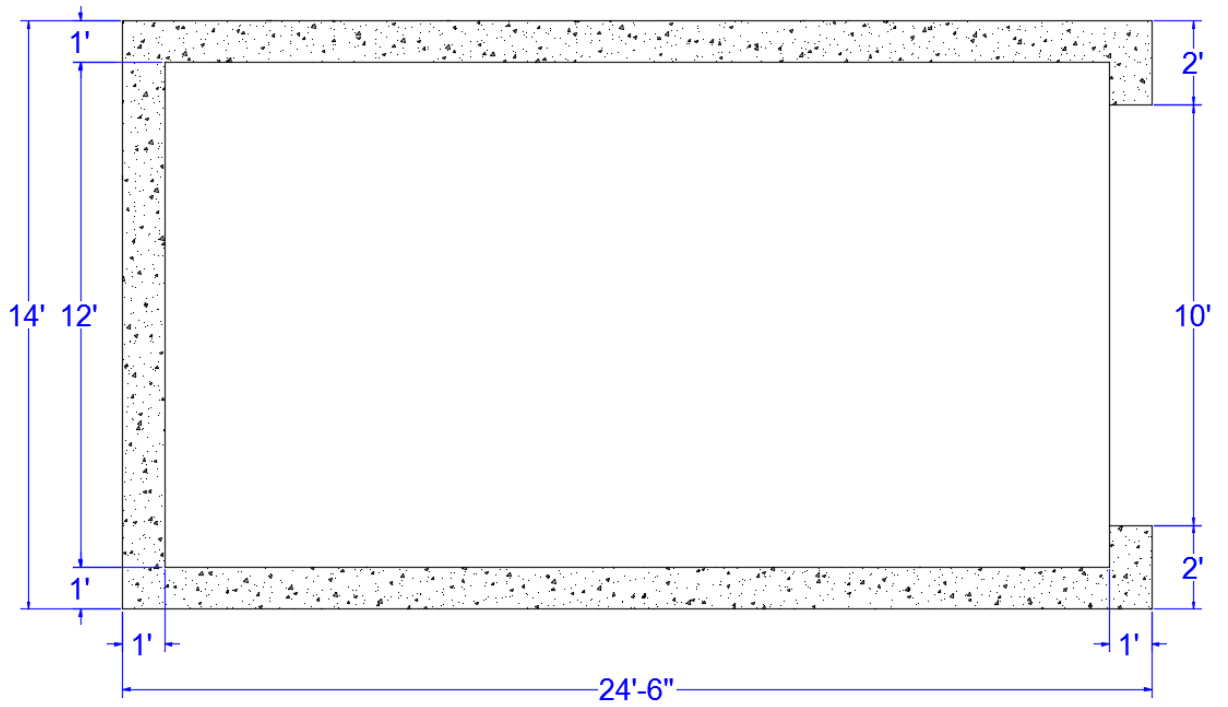


Figure 30. Test Pit - No Fluid Basin Plan View (X-Y Plane)

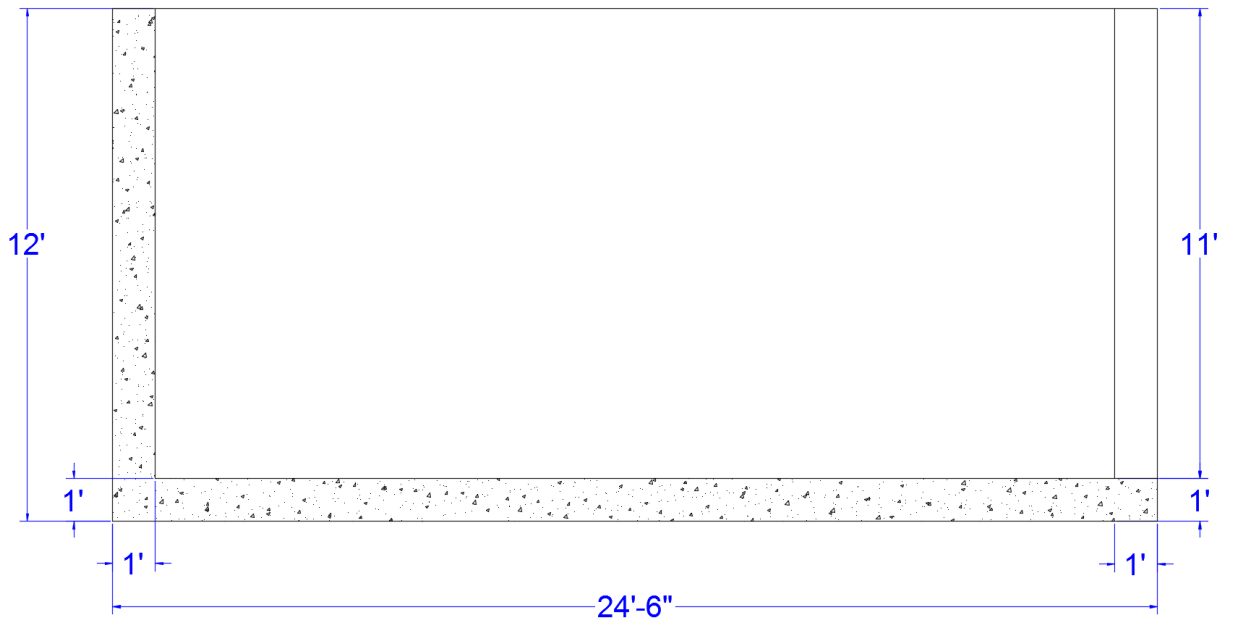


Figure 31. Test Pit - No Fluid Basin Side Elevation (X-Z Plane)

The displacement plate velocity was adjusted to ensure a velocity of 25.4 feet per second was produced using flowrate continuity for the new fluid reservoir dimensions. Equation 6 was used to calculate the target velocity of the plate in the fluid reservoir. The fluid reservoir flowrate was calculated to be 21.66 feet per second, and was rounded up to 22 feet per second to account for minor losses in the system. This velocity was assigned to the displacement plate in the negative x-direction. Figure 32 is a screen shot of the plate velocity in the x-direction over time. Appendix B can be referenced for velocity calculations. The simulation finish time was 0.5 seconds.

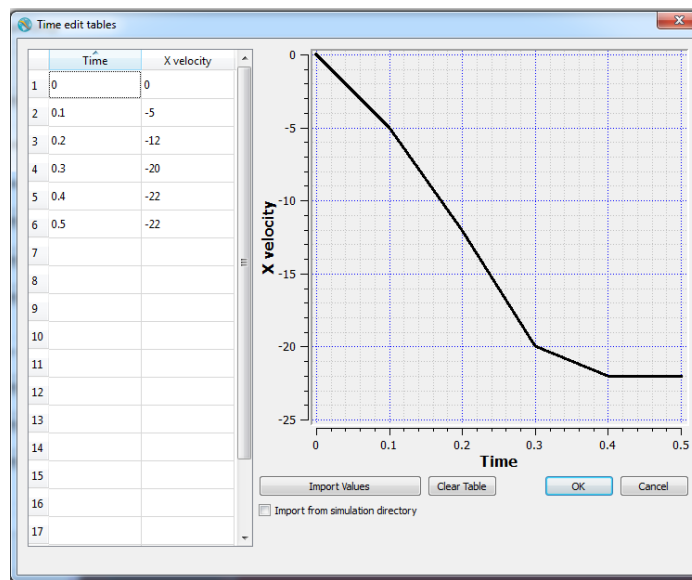


Figure 32. Design E: Displacement Plate Velocity Table

$$V_1 A_1 = V_2 A_2$$

Equation 6: Flowrate Continuity Equation

where V_i is a horizontal fluid velocity, and A_i is a flow area.

Figure 33 is an isometric view of Design E, and Figure 34 depicts the resulting wave section profile. It was noted a gate system must be implemented that supports the artificial vertical fluid boundary at time zero and opens rapidly to allow the fluid to enter the exit conduit.

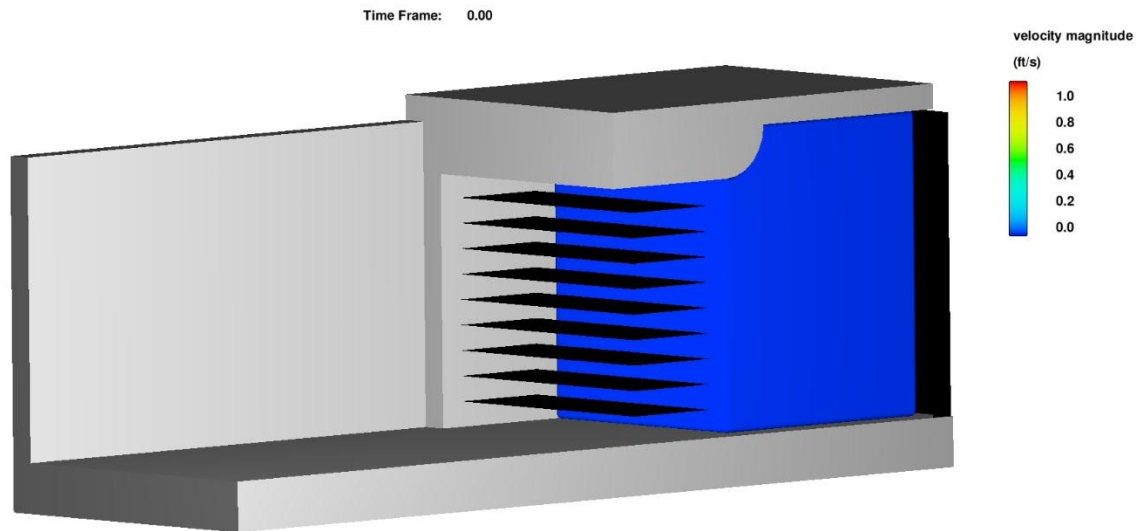


Figure 33. Design E Isometric View

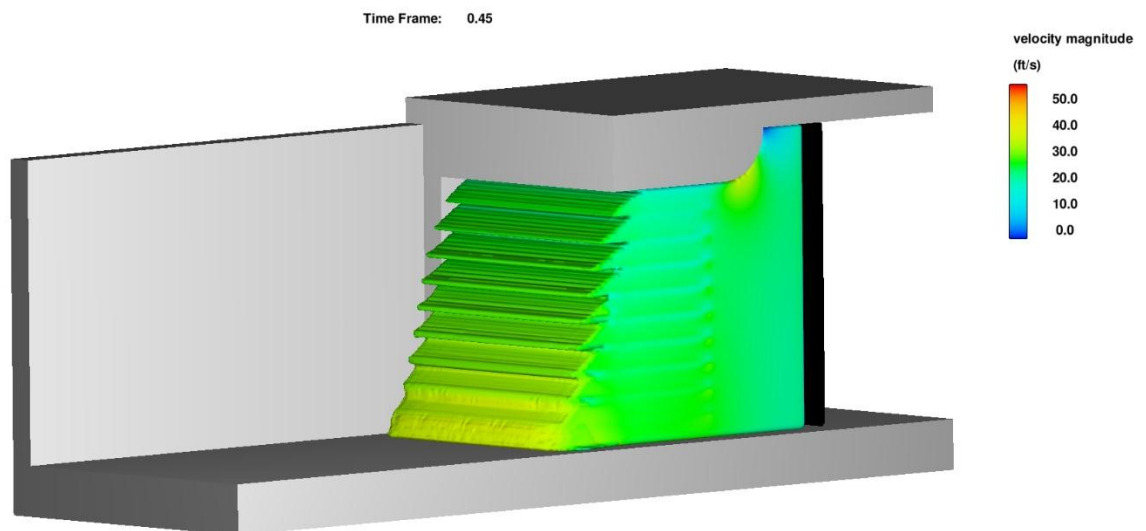


Figure 34. Design E Isometric View: Wave Section Profile

Design E with Gates

A gate system was implemented to further evaluate Design E. The gate system consisted of ten identical plates that were ten feet tall, one foot wide, and three inches thick. The gates were positioned immediately next to the vertical fluid boundary of the fluid reservoir. A rotation was assigned to each gate plate about the z axis through the plate centroid. Each gate rotated with an average velocity of ± 15.7 feet per second for a duration of 0.1 seconds, which resulted in a 90 degree rotation. All plates open away from the centerline of the conduit, as shown in Figure 35. Figure 36 displays the time table for the vertical gates. To allow time for the gates to open, the plate motion was delayed for 0.1 seconds, and the simulation finish time was extended to 1 second.

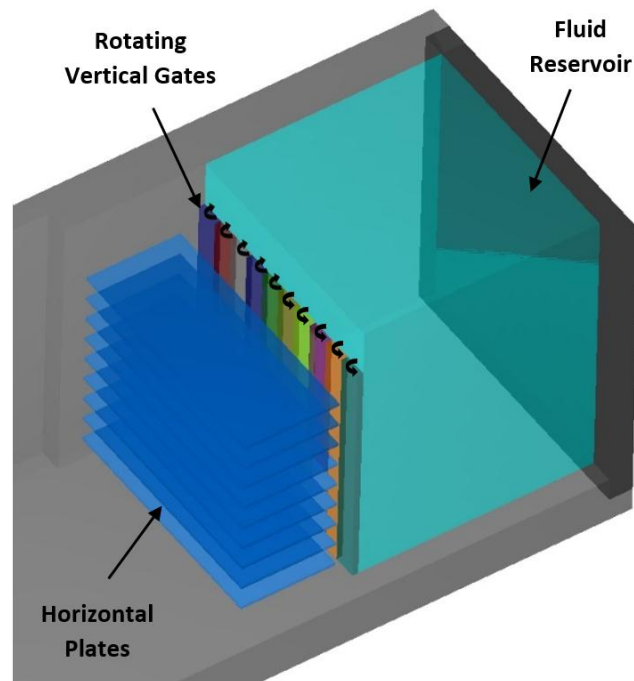


Figure 35. Design E with Gate System: Isometric View

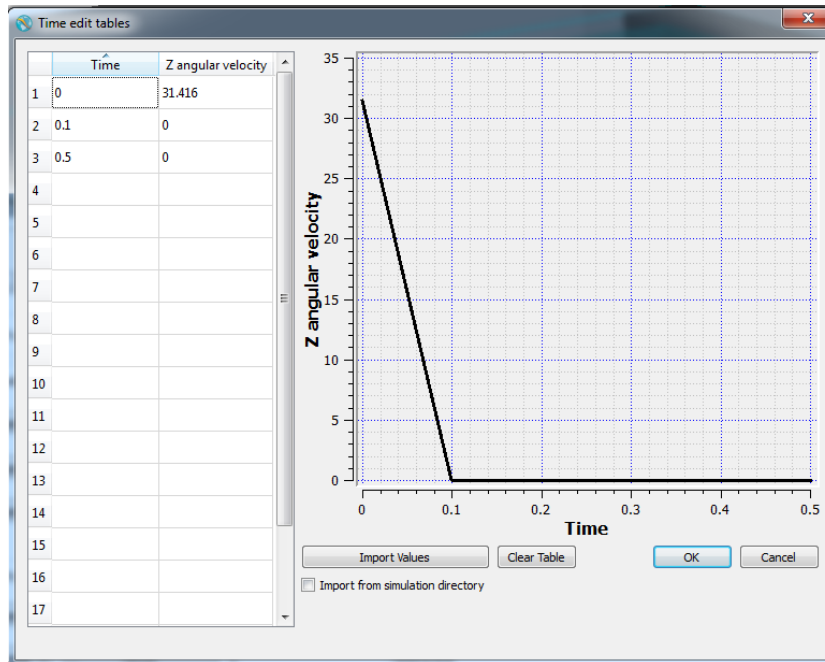


Figure 36. Design E with Gates: Gate Velocity Table

Figures 37 and 38 display the gates in the system. In Figure 39, the WISD is depicted at time zero, while in Figure 40 the gates are shown opening to allow fluid to exit the reservoir. Figure 41 shows the resulting wave section profile using this design. It was noted that friction effects must be added to the simulation to produce realistic results.

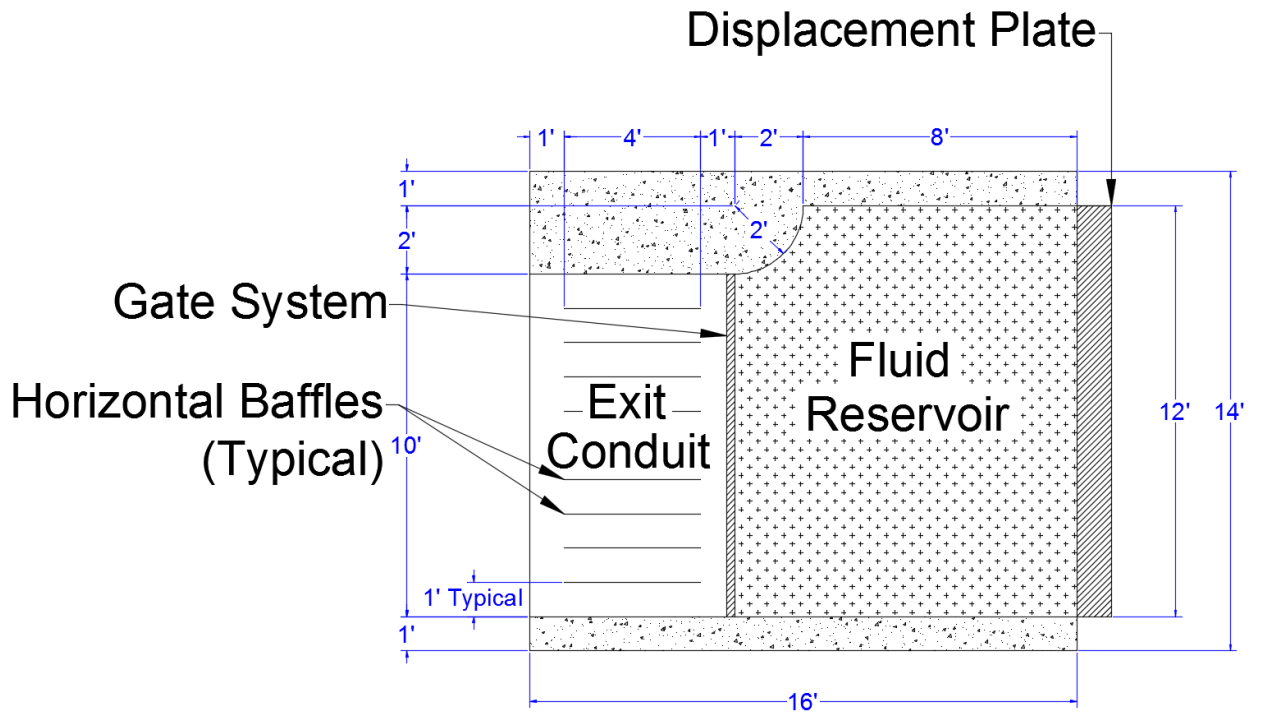


Figure 37. Design E with Gates Side Elevation (X-Z Plane)

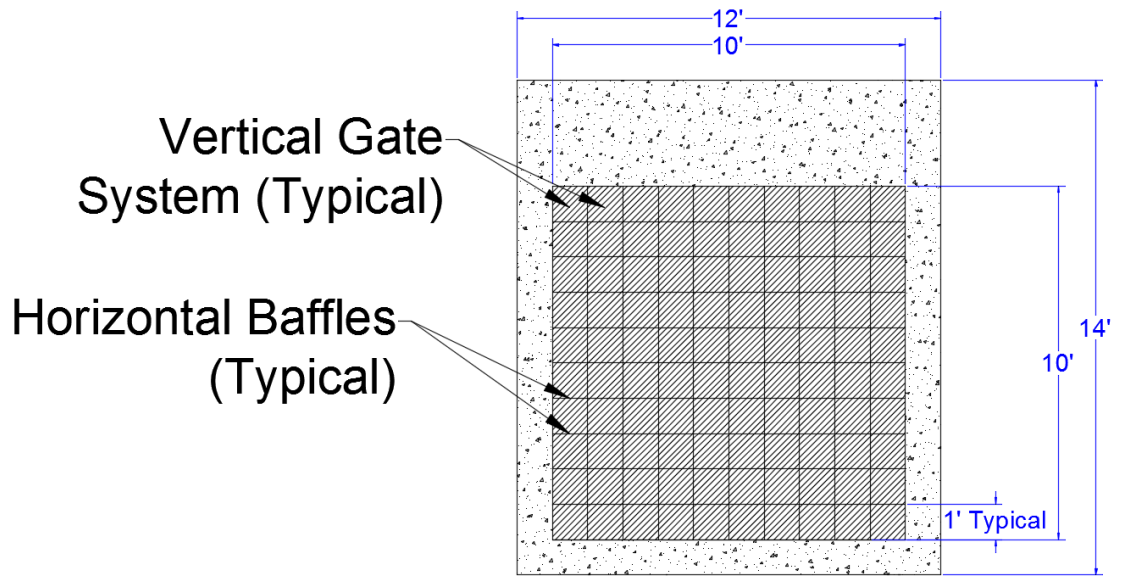


Figure 38. Design E with Gates Front Elevation (Y-Z Plane)

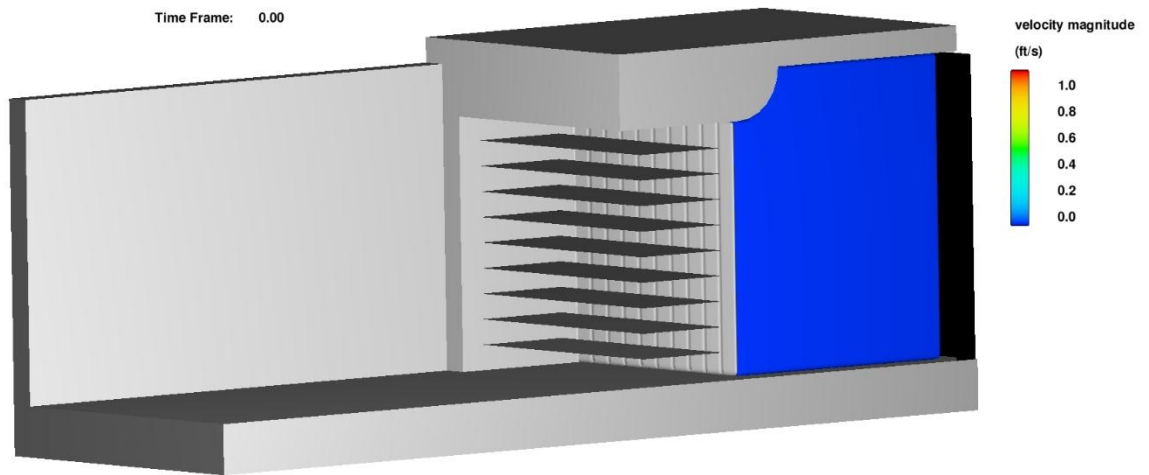


Figure 39. Design E with Gates Isometric View: Wave Section Profile

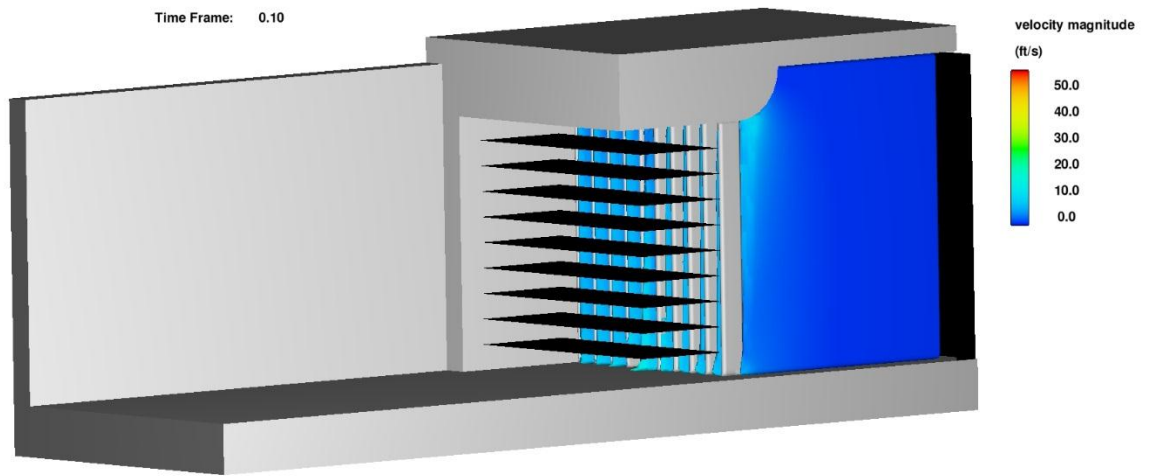


Figure 40. Design E with Gates Isometric View: Gates Opening

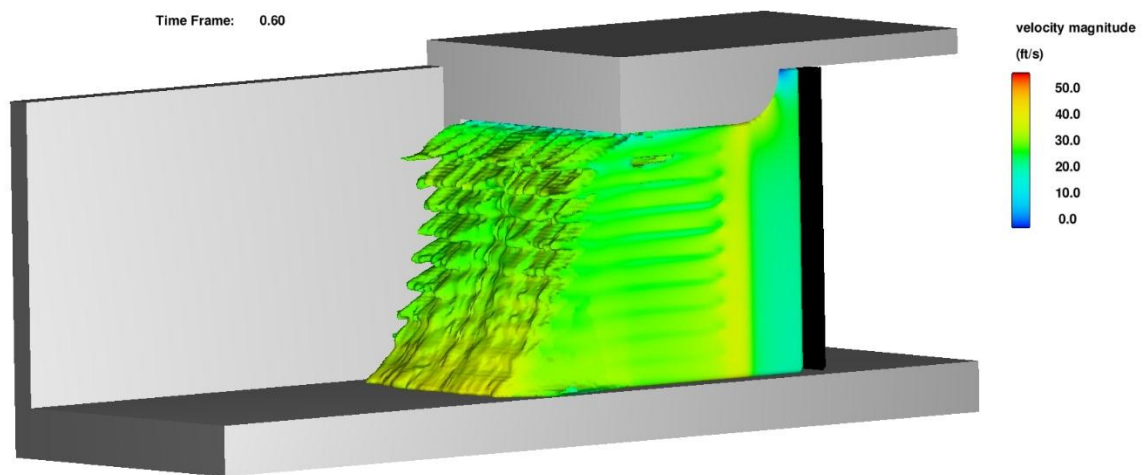


Figure 41. Design E with Gates Isometric View: Wave Section Profile

Design F

Design E was altered to add friction to simulation components. The baffles were replaced with components assigned a surface roughness coefficient, which was also be assigned to all other components in the simulation. Thin plates, each one 1.5 inches (0.125 feet) thick, ten feet wide and four feet long, replaced the thin baffles. A surface roughness coefficient equivalent to concrete (0.013) was assumed and assigned to all solid components (Akan, 2006). Figures 42 and 43 show the thin plates in the exit conduit and their dimensions.

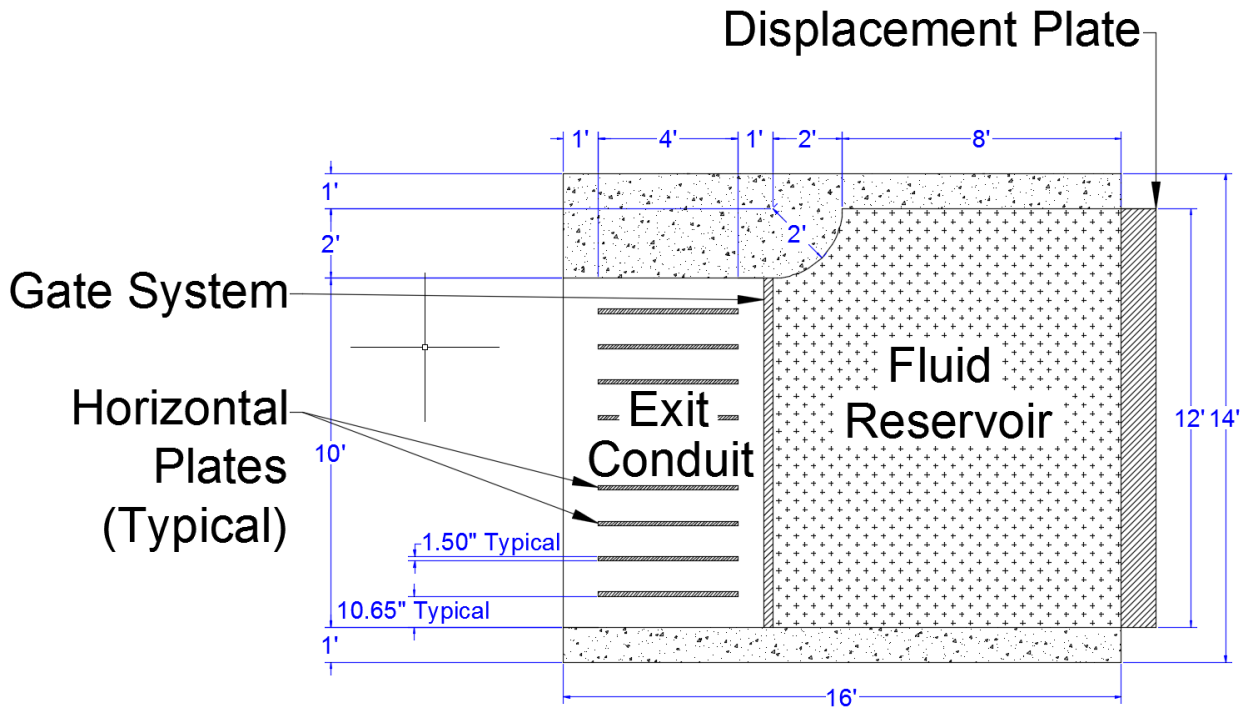


Figure 42. Design F Side Elevation (X-Z Plane)

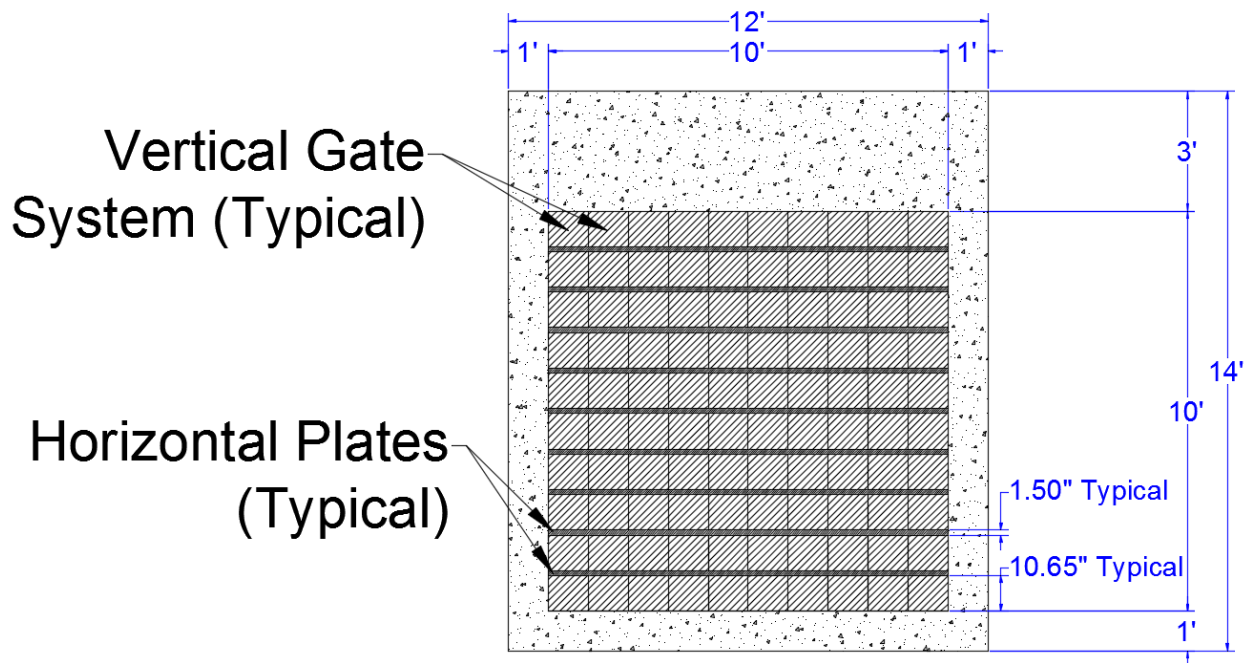


Figure 43. Design F Front Elevation (X-Z Plane)

By assigning a thickness to the horizontal plates, the flow area of the exit conduit was changed. To ensure flowrate continuity, the ten foot by twelve foot fluid reservoir velocity was adjusted. Equation 6 was used to calculate the target velocity of the displacement plate in the fluid reservoir. The required fluid reservoir flowrate was calculated to be 18.8 feet per second, and was rounded up to 20 feet per second to account for minor losses in the system and for simplicity. This velocity was assigned to the displacement plate in the negative x-direction. Appendix C can be referenced for velocity calculations, and a screen shot of the plate velocity in the x-direction over time is shown in Figure 44.

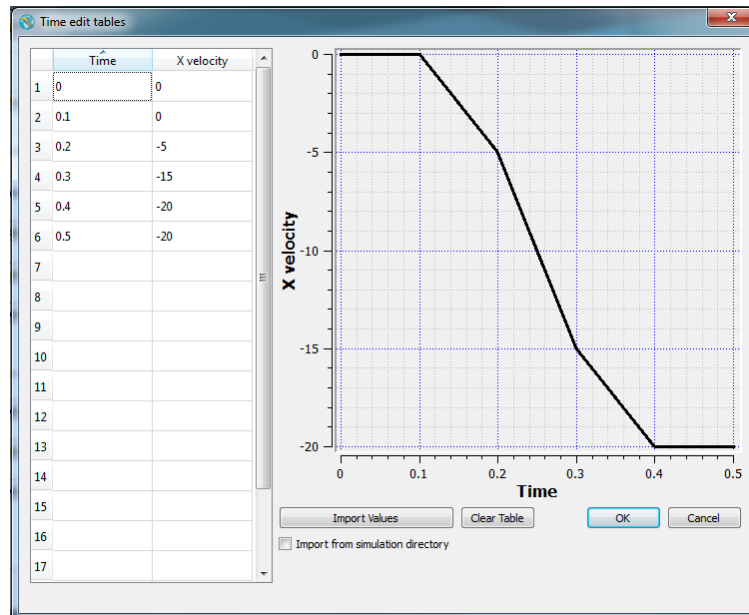


Figure 44. Design F: Displacement Plate Velocity Table

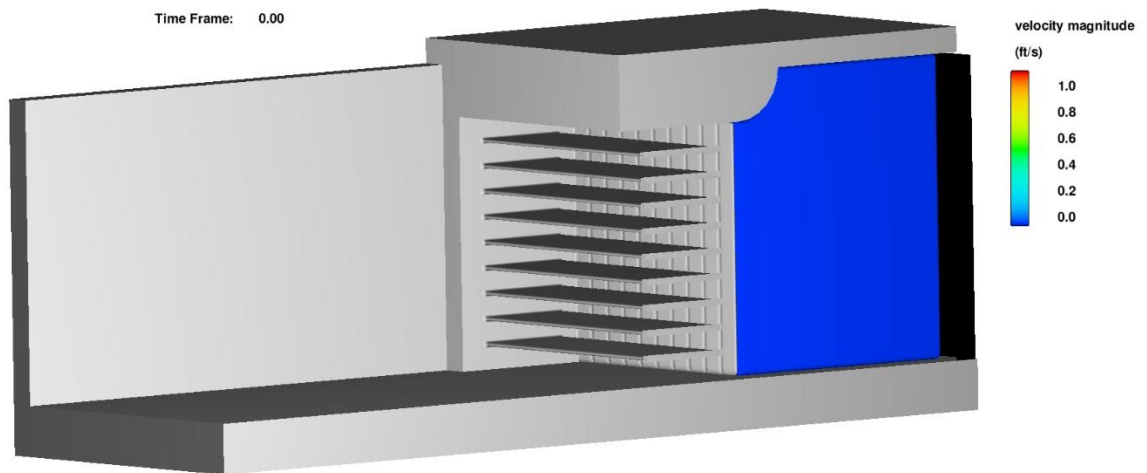


Figure 45. Design F Isometric View

The addition of friction dampened the fluid jets exiting the conduit seen in Figure 41, and Design F produced the more unified wave section seen in Figure 46. The wave section was nearly vertical, and had a velocity profile very close to the target velocity of 25.4 feet per second.

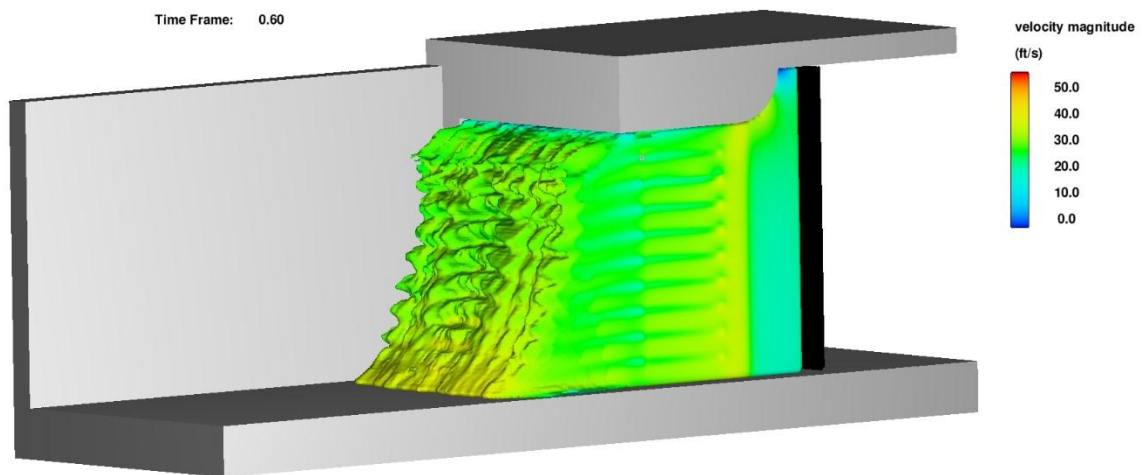


Figure 46. Design F Isometric View: Wave Section Profile

Vertical Piston WISD Design

The concepts developed in previous WISD designs were carried over to Designs G and H. The fluid reservoir regions of each design were modified to specify fluid displacement using vertical plate motion instead of horizontal motion.

Design G

Figure 47 depicts Design G, which used horizontal plate motion to displace fluid. The displacement plate pushed fluid down into a curving tube at a rate of 15 feet per second over a distance of 10 feet in the negative z-direction. By using vertical displacement, no static pressure acted on the plate due to fluid depth, making it easier to initialize plate motion. The vertical gate system and exit conduit design from the Design E were used, and the concrete roughness coefficient of 0.013 was assigned to all simulation components. A simulation finish time of 1 second was used.

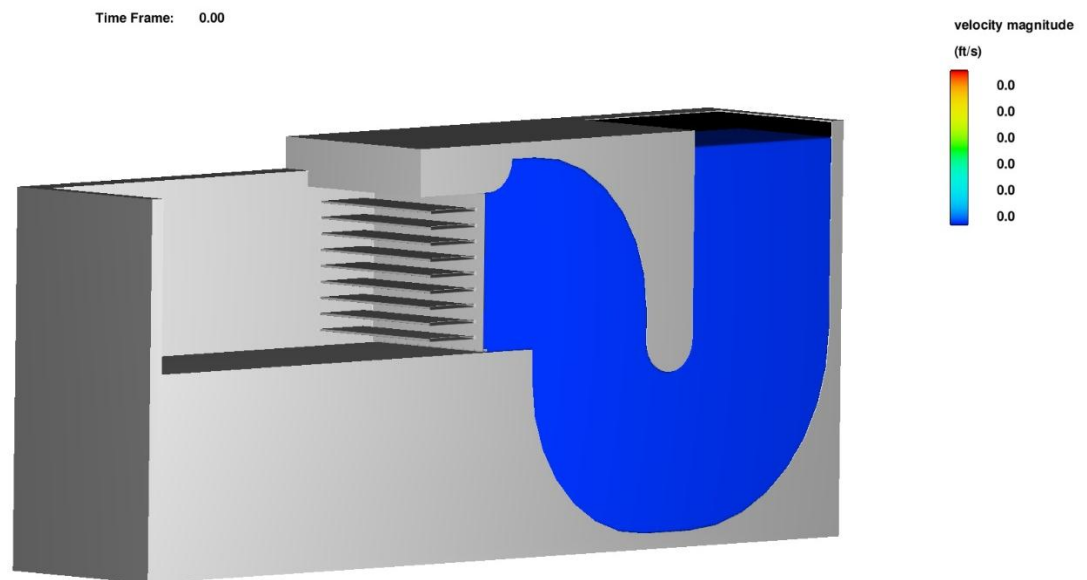


Figure 47. Design G Isometric View

Figures 48 and 49 show the dimensions of the fluid reservoir and exit conduit used in Design G. The modified test pit dimensions are shown in Figures 50 and 51.

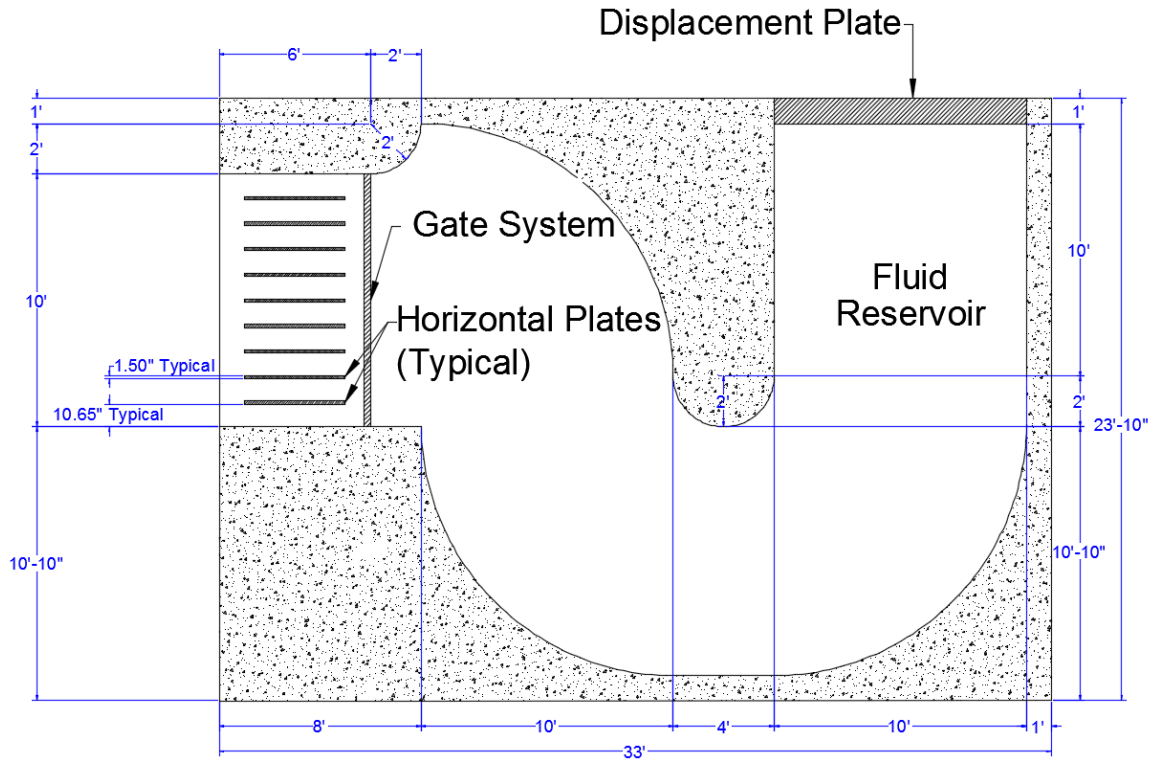


Figure 48. Design G Side Elevation (X-Z Plane)

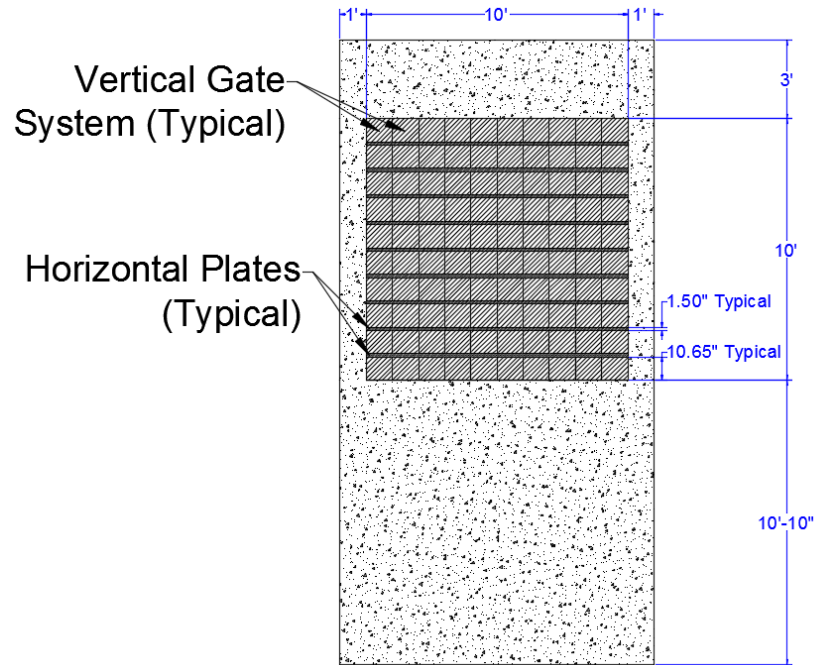


Figure 49. Design G Front Elevation (Y-Z Plane)

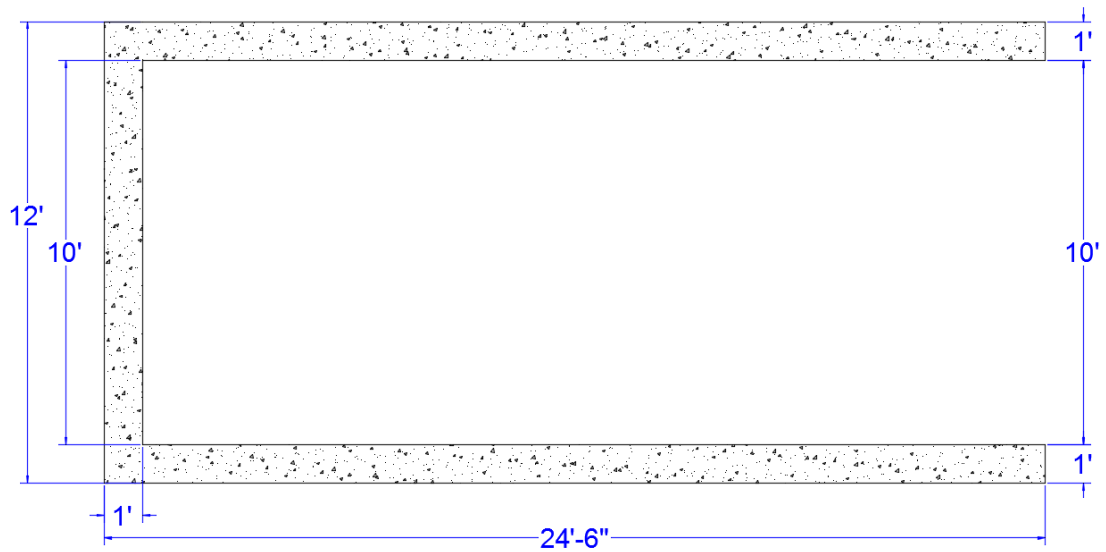


Figure 50. Design G Modified Test Pit Plan View (X-Y Plane)

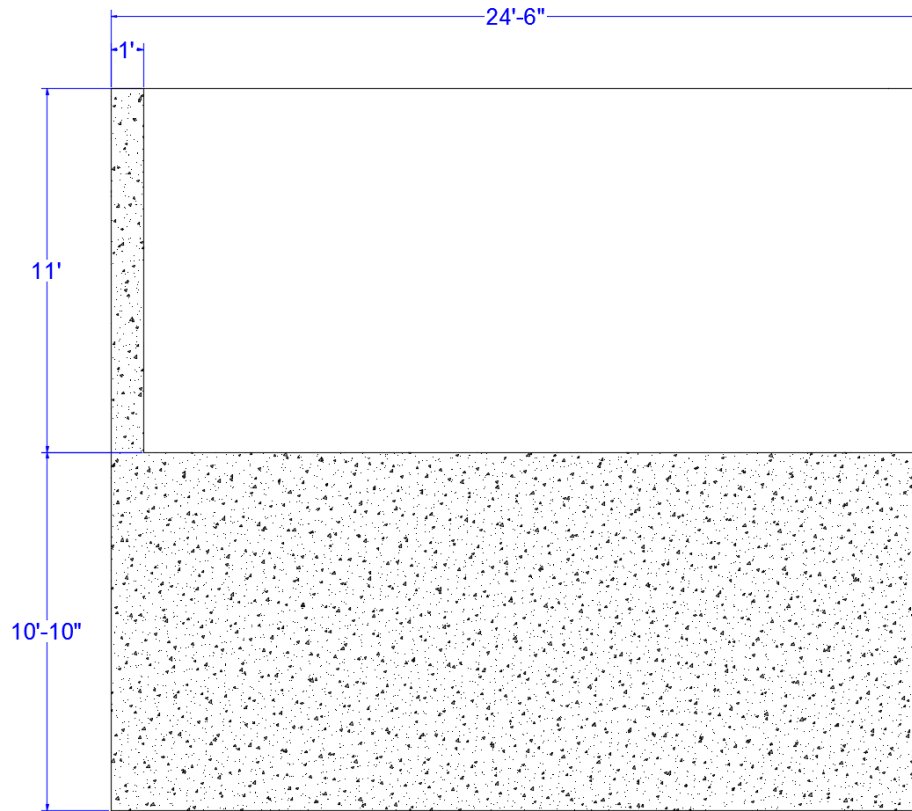


Figure 51. Design G Modified Test Pit Elevation View (X-Z Plane)

Figure 52 shows the resulting wave section and the velocity profile. It can be seen that the wave section became less vertical. This was due to pressure differences between the top and bottom of the fluid reservoir tube and fluid accelerations as the fluid was redirected through the reservoir. As the fluid was pushed out of the tube, pressure differences created additional fluid velocity at the bottom of the conduit as the fluid exited. This approach was not well suited to create the near vertical wave section due to the non-uniform velocity profile it creates.

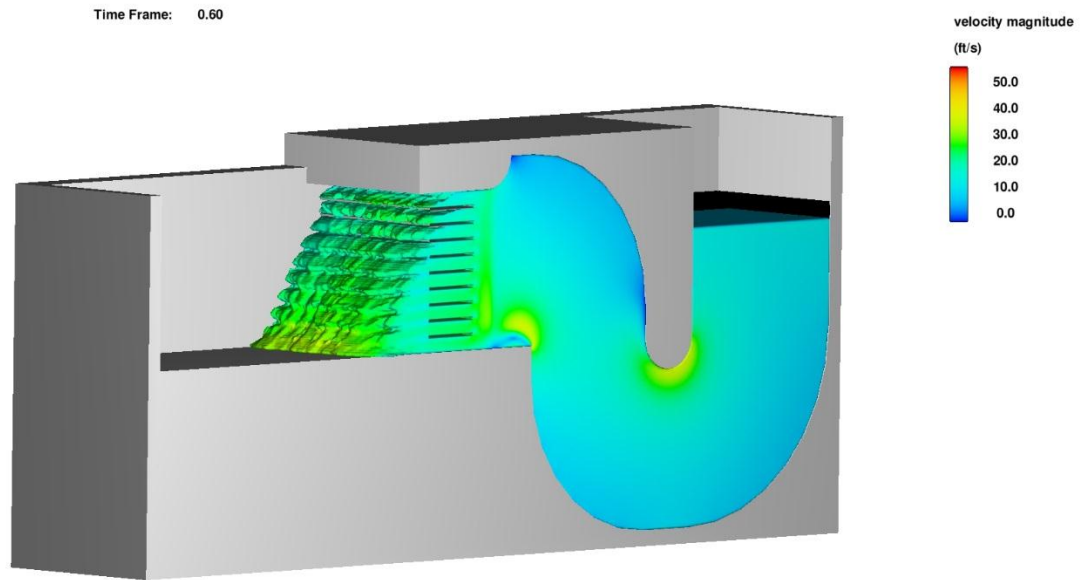


Figure 52. Design G Isometric View: Wave Section Profile

Design H

Next, a more compact vertical piston design was attempted to reduce flow redirections and to reduce the time for a non-uniform velocity profile to develop. The velocity constraints for the displacement plate used in Design I were applied to Design H. Figure 53 shows the dimensions of Design G. The same exit conduit design from Design F was used, and the test pit dimensions were not modified. A simulation finish time of 1 second was used.

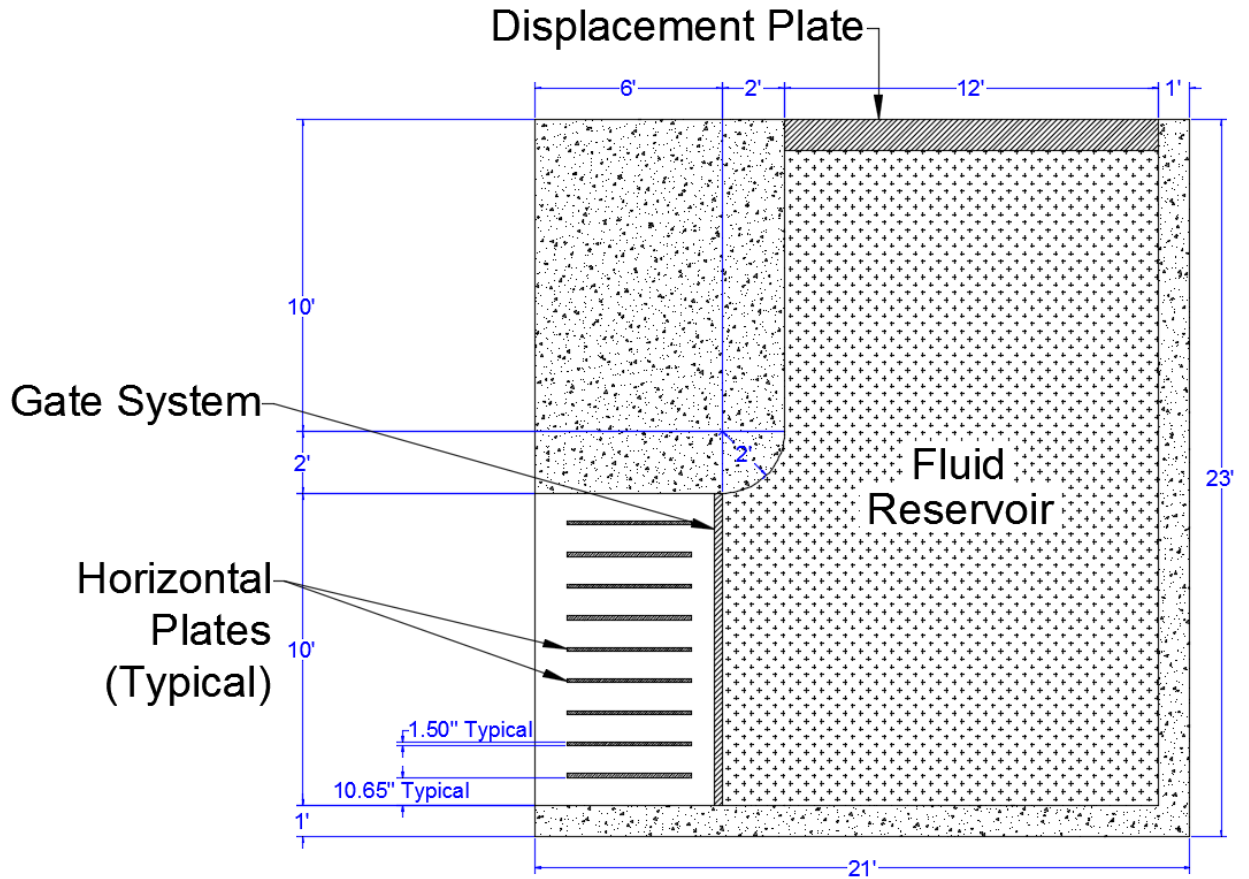


Figure 53. Design H Elevation View (X-Z Plane)

Figure 54 exhibits the plunger tank design at time equal to zero. Figure 55 shows the resulting wave section using the plunger tank design. It was determined that a more vertical wave section profile was obtained, but the flows did not form a unified wave section near the top of the conduit exit. The rapid redirection of fluid in the fluid reservoir created a non-uniform fluid velocity profile and a non-cohesive wave section. This approach did not achieve the design goals of the project.

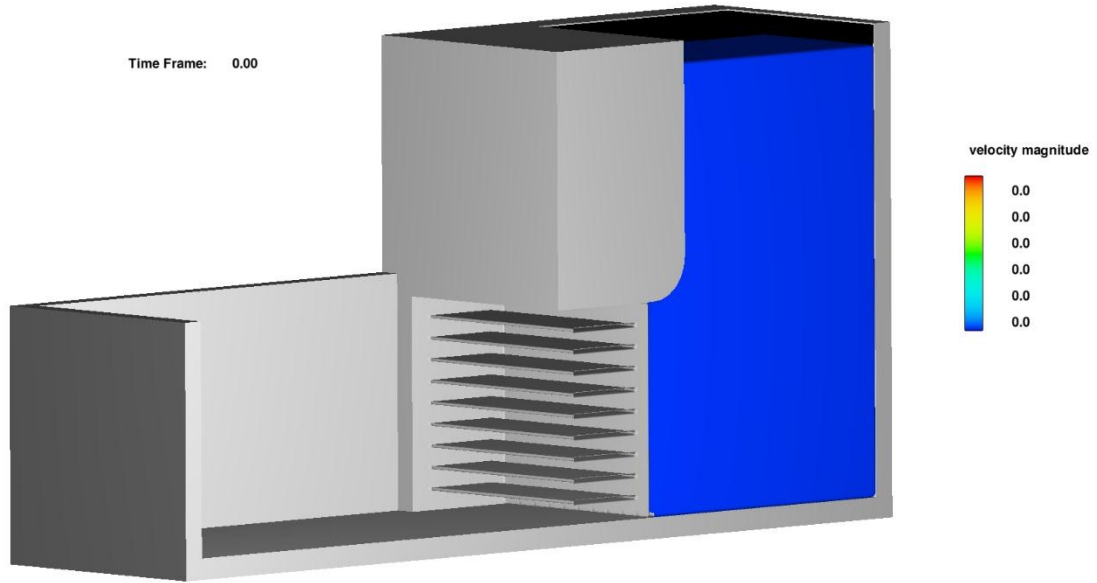


Figure 54. Design H Isometric View

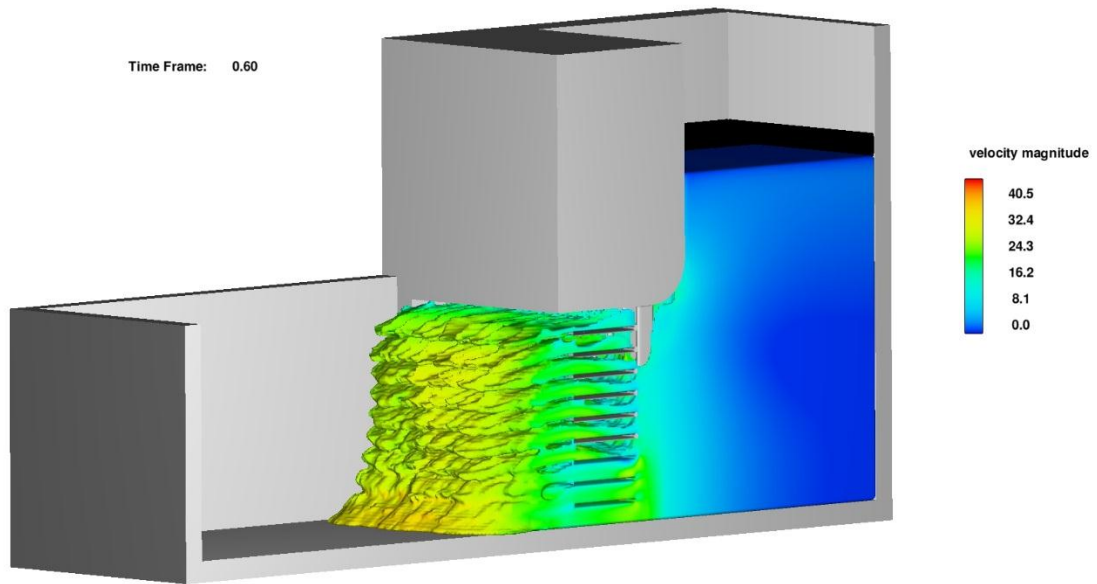


Figure 55. Design H Isometric View: Wave Section Profile

Air Pressure WISD Design

The concepts developed in previous WISD designs were adapted to specify fluid displacement using air pressure instead of plate motion for Designs I and J.

Design I

To investigate air pressure fluid displacement, the conduit geometry reverted to a constant rectangular profile, and the horizontal plates were extended to the back of the fluid reservoir, dividing the reservoir into ten discrete channels. Additionally, the 1.5 inch thick gate components were modified to rotate horizontally, with an independent gate for each flow channel. The plates were assigned a peak velocity of -15.7 feet per second over a duration of 0.2 seconds, resulting in a 90 degree rotation about the y-axis. The rotation reference point of each gate was about its own base at the centerline of the exit conduit. Figure 56 displays the time table for the horizontal gates. It was specified that the moving gates overlapped with the solid plates to create a smooth, continuous channel boundary. Figures 57 and 58 show the dimensions of Design I with the new horizontal gate system.

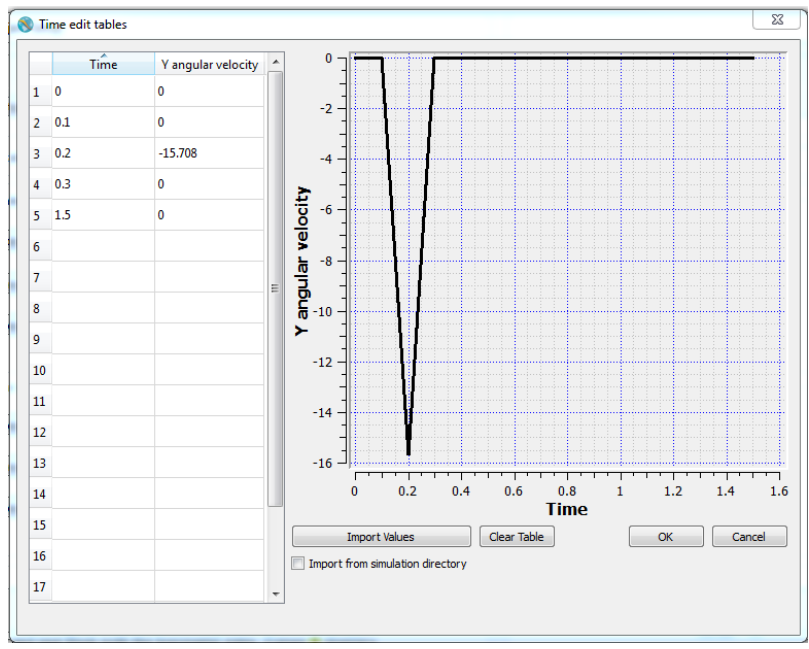


Figure 56. Design I: Gate Velocity Table

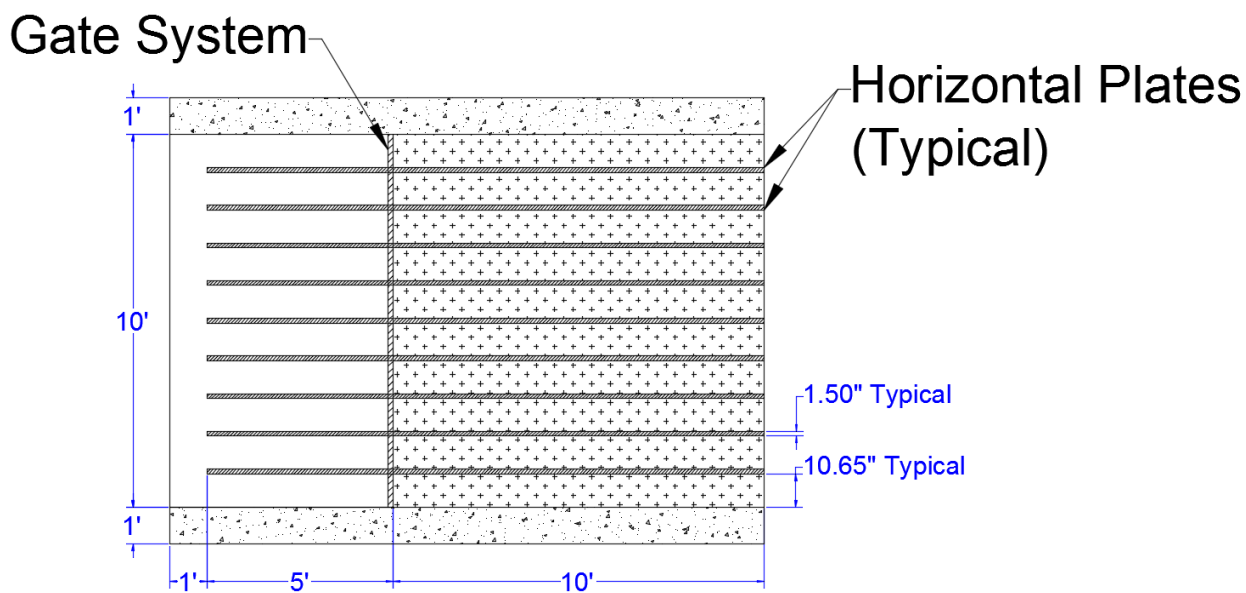


Figure 57. Design I Side Elevation (X-Z Plane)

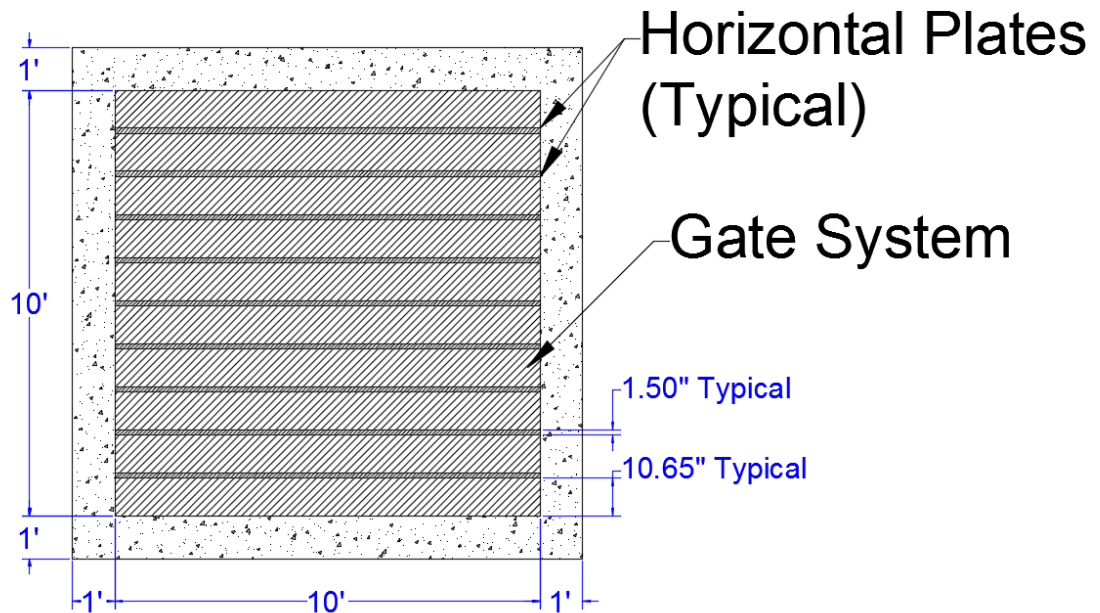


Figure 58. Design I Front Elevation (Y-Z Plane)

A variable pressure boundary with a peak of 4.34 psi was specified at the back of the conduit to act as the motive force. This value was calculated using the Bernoulli equation by solving for the pressure head equivalent to the velocity head associated with the target wave speed of 25.4 feet per second. Equation 7 displays the Bernoulli equation.

$$\frac{P_1}{\gamma} + Z_1 + \frac{V_1^2}{2g} = \frac{P_2}{\gamma} + Z_2 + \frac{V_2^2}{2g}$$

Equation 7: Bernoulli Equation

where P_i is a pressure, γ is the unit weight of water, z_i is a fluid elevation, V_i is a horizontal fluid velocity, and g is gravitational acceleration.

Equation 7 was simplified assuming elevation remains constant, and that the fluid velocity head was produced only by a pressure head. The simplified form of the Bernoulli equation used in the calculation is given by Equation 8. Appendix D provides the pressure calculations. Figure 59 displays the pressure boundary time table, and the pressure is displayed in pounds per square foot.

$$\frac{P_1}{\gamma} = \frac{V_2^2}{2g}$$

Equation 8: Simplified Bernoulli Equation

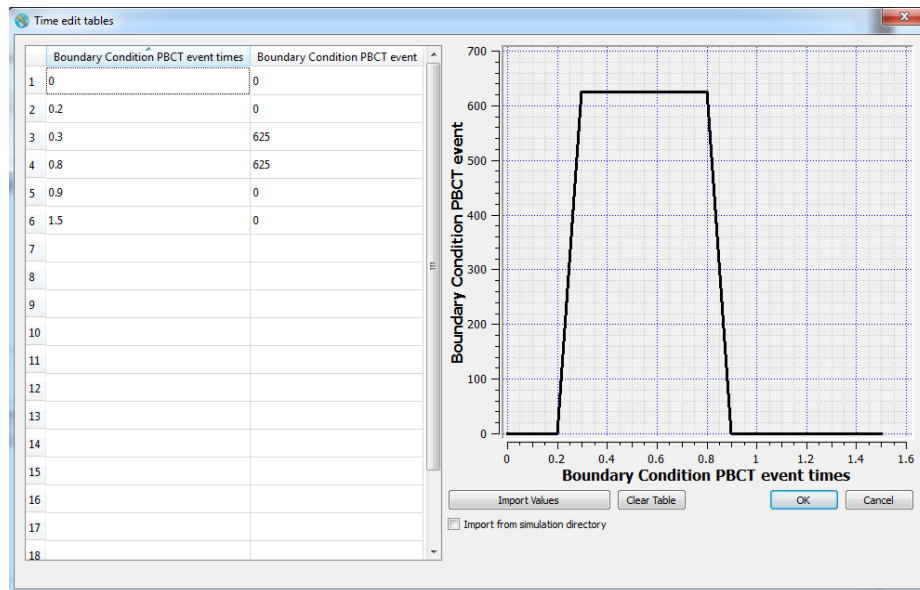


Figure 59. Design I: Pressure Boundary Table

In order to activate the time dependent pressure boundary, a simulation control event was specified. A fixed history probe was placed in the simulation domain at coordinates shown in Table 9. It was specified that once the history probe location was

identified to be at $z = 13.9$ feet at time zero, the time dependent pressure boundary table activates. The history probe location is shown by the green dot in Figure 60.

Table 9. History Probe Coordinates in Design I Simulation

	X-Axis	Y-Axis	Z-Axis
Location (ft)	20.0	1.5	13.9

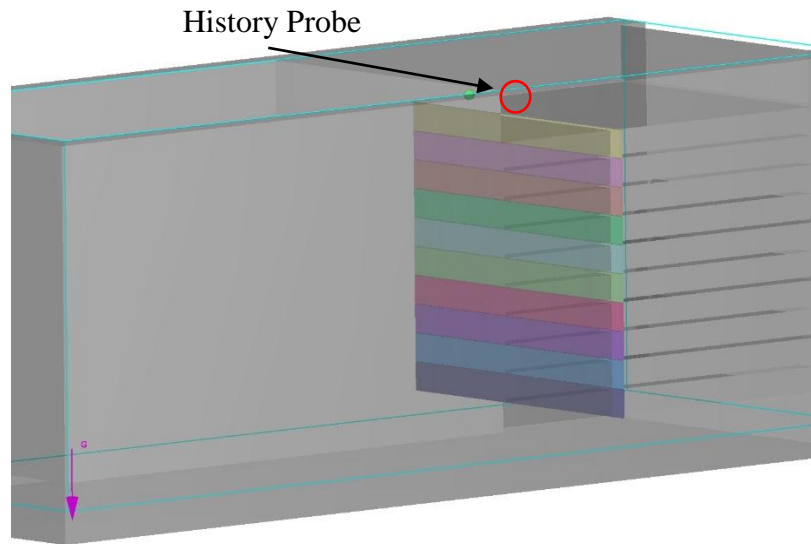


Figure 60. Design I: History Probe

Running the simulation, the horizontal gates rotated to rest flush with the horizontal plates. Then the pressure boundary accelerated the fluid, and the fluid entered the test pit, forming a near-vertical wave section. The wave section had a velocity profile near the target of 25.4 feet per second, and wave front moved forward with an atmospheric pressure. The simulation finish time was increased to 1.5 seconds to better observe the resulting wave section behavior.

Figure 61 displays Design J at time zero, Figure 62 shows the horizontal gates opening, and Figure 63 shows the resulting wave section velocity profile. The wave section was cohesive, vertical, and had a velocity profile very close to the target velocity of 25.4 feet per second.

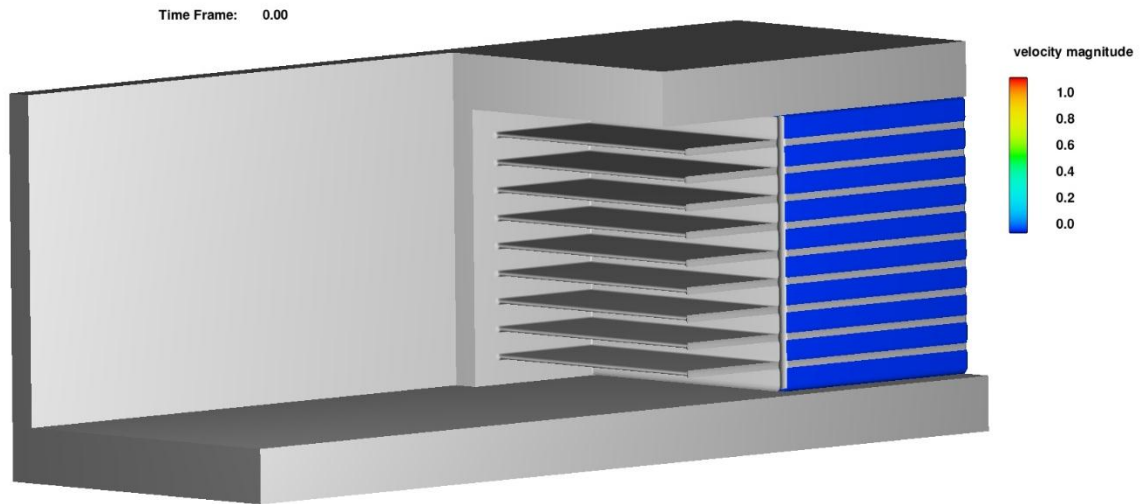


Figure 61. Design I Isometric View

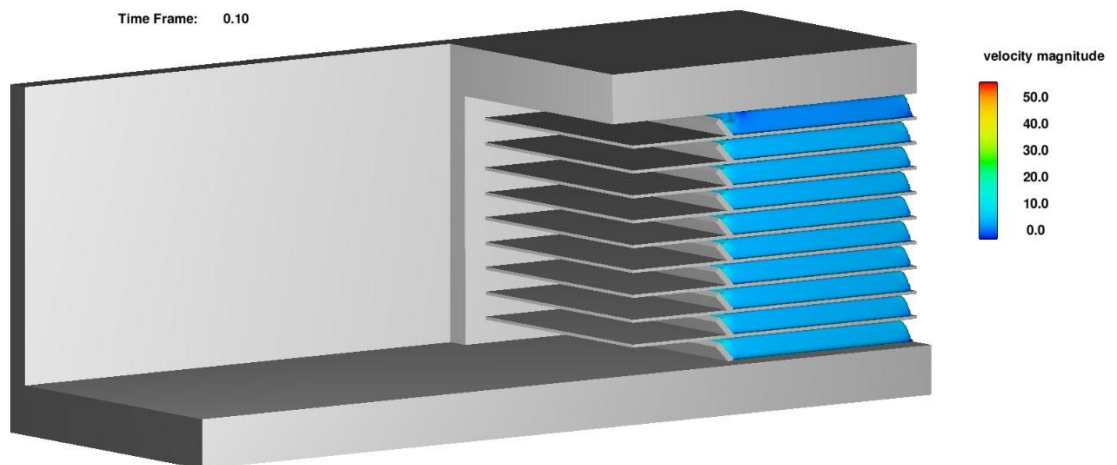


Figure 62. Design I Isometric View: Gates Opening

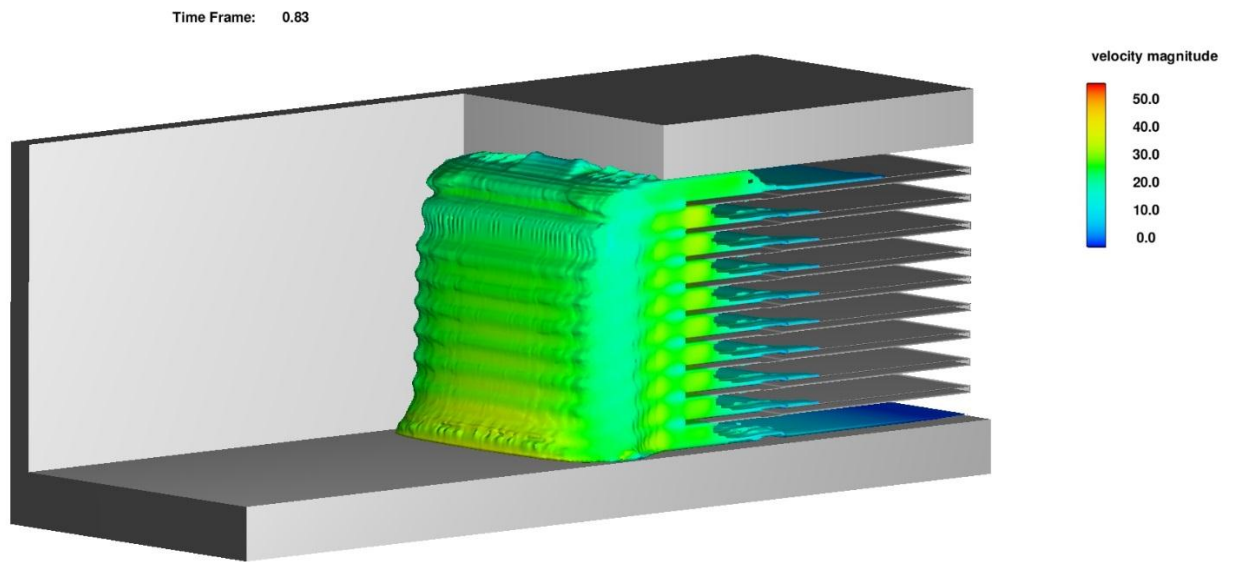


Figure 63. Design I isometric View: Wave Section Profile

Grid Convergence Test for Air Pressure WISD Design

A grid convergence test was run on a modified Design I to ensure the appropriate mesh size was being used in Flow-3D simulations. The modifications were the removal of the gates in the simulation and the use of a constant pressure boundary to displace the fluid in the channels. This was done to reduce computational time. A history probe was placed in the WISD simulation in the bottom fluid channel, and is indicated by the green sphere in Figure 64. The history probe recorded the fluid velocity at its location over time. The probe was located immediately behind the center of the removed horizontal gates. This location was chosen such that the maximum number data points possible were recorded as the fluid traveled through the bottom channel. The probe coordinates are listed in Table 10.

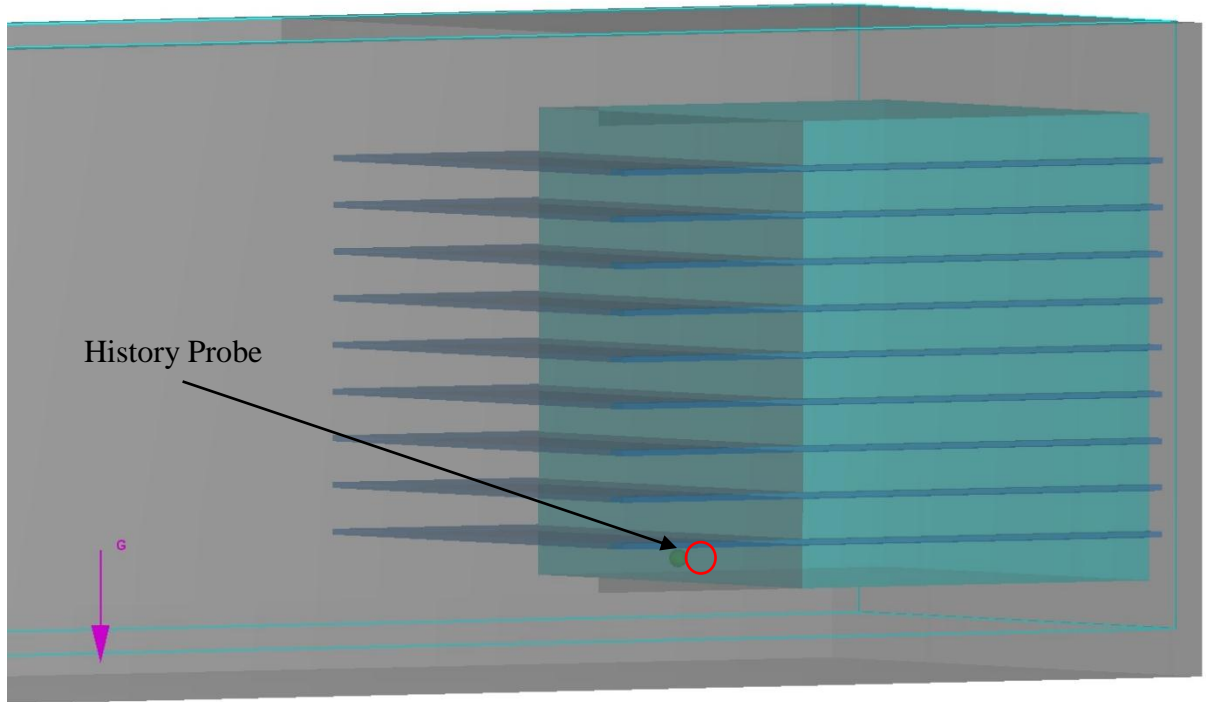


Figure 64. Modified Design I Grid Convergence: History Probe

Table 10. History Probe Coordinates in Modified Design I Simulation

	X-Axis	Y-Axis	Z-Axis
Location (ft)	27.2	7	2.5

The percent difference in the maximum velocity magnitudes recorded for each mesh size were used as the convergence criteria. The results of the simulation runs are presented in Tables 11 and 12. The simulation time of the peak velocity varied very little, and the oscillation of the maximum velocity value as the mesh was refined was attributed to the use of the law-of-the-wall velocity profile in Flow 3D boundary layer fluid velocity calculations (FLOW-3D user manual, 2017). It was concluded that the mesh size of eight cells per foot remained satisfactory.

Table 11. Modified Design I Grid Convergence: Maximum Velocity Values

Mesh	Maximum Velocity Magnitude (ft/s)	Simulation Time of Maximum Velocity (seconds)
4 cells/ft	24.8259	0.6424
6 cells/ft	25.2384	0.6360
8 cells/ft	25.0962	0.6394
10 cells/ft	24.4448	0.6380
12 cells/ft	24.3352	0.6041
14 cells/ft	25.4243	0.6209

Table 12. Modified Design I Grid Convergence: Fluid Velocity Percent Difference at Fluid Pointer

<u>Mesh</u>							
14 cells/ft	-2.41	-0.74	-1.31	-4.01	4.48	-	
12 cells/ft	1.98	3.58	3.03	0.45	-	4.28	
10 cells/ft	1.53	3.14	2.60	-	-0.45	3.85	
8 cells/ft	-1.09	0.56	-	-2.66	-3.13	1.29	
6 cells/ft	-0.17	-	-0.57	-3.25	-3.71	0.73	
4 cells/ft	-	1.63	1.08	-1.56	-2.02	2.35	
	4 cells/ft	6 cells/ft	8 cells/ft	10 cells/ft	12 cells/ft	14 cells/ft	<u>Mesh</u>

Design J

To improve upon Design I, plates angled at 45 degrees extended the channel, creating a void above each fluid channel at the pressure boundary. By doing this, the air pressure acted on the free surface of the fluid, circumventing the static pressure from fluid depth in the previous design. This concept was taken from Designs G and H. The

pressure boundary conditions were slightly modified to increase the peak pressure duration. The modified pressure boundary table for Design J is shown in Figure 65.

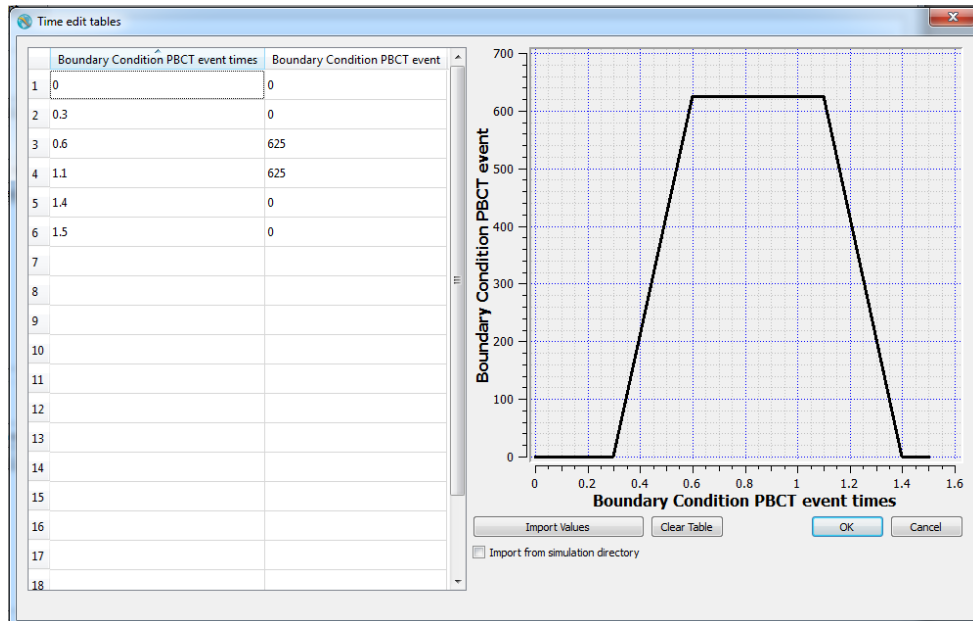


Figure 65. Design J: Pressure Boundary Table

Figure 66 illustrates the dimensions of Design J. The exit conduit, gate system, and test pit were unchanged from Design I, and the simulation finish time remained 1.5 seconds.

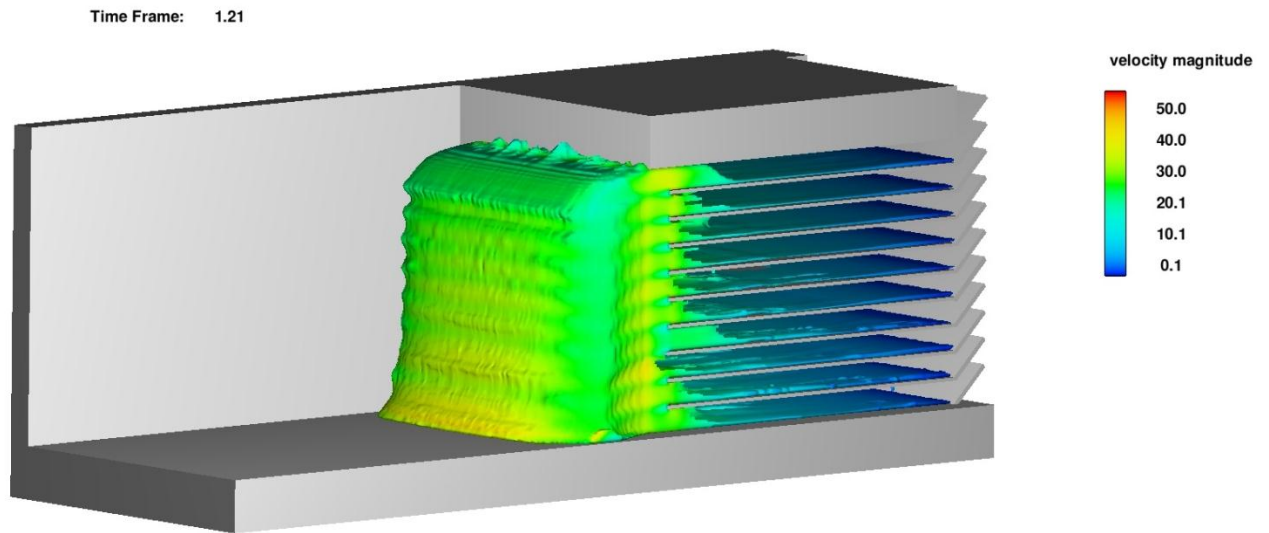


Figure 68. Design J Isometric View: Wave Section

WISD Results

To meet the CFEL testing goals of producing a near vertical wave section capable of simulating the impact of wave heights up to 20 feet, Designs F and J were the most promising for a plate driven and an air pressure driven option, respectively. Additional work is needed to evaluate the most effective design through prototype testing, and to determine the practical option to provide wave impact testing capability for CFEL.

An advantage of the air pressure design is the separation of the fluid depth into discrete channels. By doing this, various flow depths can easily be produced for impact tests. For flow depths less than ten feet, the appropriate channels can be filled and operated. For flow depths greater than ten feet, differences in air pressure in the discrete channels can be used to adjust the slope of the wave section and produce a desired flow

pattern. For this reason, Design J is proposed as the most viable option for validation and further study. Design J also produced the most cohesive, vertical wave section.

Conclusions and Future Work

In summary, WISD designs were developed to provide wave impact testing capability for CFEL. Flow 3D was used to model tsunami wave behavior using solitary wave assumptions. The variability of impact force values in the solitary wave simulations prompted the use of idealized wave equations to determine non-breaking tsunami wave velocities. To investigate breaking wave velocities and inundation flows, additional research is required. Scenario specific studies must be performed to identify fluid impact conditions of interest. The impact conditions, such as fluid velocity and depth, can then be replicated using the WISD.

Nonbreaking shallow water wave velocities were used to determine the fluid velocities to be produced by the WISD. Using this specification provides a wide range of testing capability for wave impact tests and for other fluid impacts with similar velocities. The maximum horizontal fluid velocity for a 20 foot tsunami wave, 25.4 feet per second, was the criteria used to meet CFEL testing requirements.

Design J is proposed as the most viable WISD option for validation and further study. The final dimensions of the WISD will depend on the final gate system design and the rate of fluid acceleration that can be achieved by the displacement mechanism. If the fluid is accelerated gradually, a longer exit conduit length will be required than those assumed in Flow 3D simulations. The assumed fluid reservoir dimensions may also be altered depending on the fluid volume required for CFEL tests.

Future work includes the testing necessary to ensure the validity of the WISD designs. Scaled testing of prototypes will help identify potential design flaws or unidentified design obstacles, and provide proof of design concepts. Once a WISD design is finalized, idealized wave impact tests can be performed using a full scale WISD. Flows other than those governed by idealized wave behavior can also be studied for WISD applications.

Impact tests performed with the WISD will be used to test components for the CFEL program and produce fragility data. The data collected will be used to develop probabilistic risk assessment models for nuclear power plant non-containment components and facilities.

References

Akan, A. Osman. "Open Channel Hydraulics." Burlington, MA: Elsevier; Butterworth-Heinemann, 2006.

Apelt, C.J. and Piorewicz, J. "Laboratory studies of breaking wave forces acting on vertical cylinders in shallow water." *Coastal Engineering*, Vol. 11(3), 1987.

Altomare, C., Crespo, A., Domínguez, J., Gómez-Gesteira, M., Suzuki, T., and Verwaest, T. "Applicability of Smoothed Particle Hydrodynamics for estimation of sea wave impact on coastal structures." *Coastal Engineering*, Vol. 96, 2015.

Baldock, T., Cox, D., Maddux, T., Killian, J., and Fayler, L. "Kinematics of Breaking Tsunami Wavefronts: A Data Set from Large Scale Laboratory Experiments," *Coastal Engineering*, Vol.56(5-6), 2009.

Bascom, W. "Waves and beaches: The dynamics of the ocean surface." Garden City, New York: Doubleday and Company, 1964.

Birknes, J. and Pedersen, G. "A particle finite element method applied to long wave run-up." *International Journal for Numerical Methods in Fluids*, Vol. 52(3), 2006.

Bullock G.N., Obhrai C., Peregrine, D.H., and Bredmose, H. "Violent breaking wave impacts. Part 1: Results from large-scale regular wave tests on vertical and sloping walls." *Coastal Engineering*, Vol. 54(8), 2007.

Chen, Q., Kirby, J., Dalrymple, R., Kennedy, A., and Chawla, A. "Boussinesq Modeling of Wave Transformation, Breaking, and Runup. II: 2D." *Journal of Waterway, Port, Coastal, and Ocean Engineering*, Vol. 126(1), 2000.

Choi, B.H., Kim, D.C., Pelinovsky, E., and Woo, S.B. "Three-dimensional simulation of tsunami run-up around conical island." *Coastal Engineering*, Vol. 54(8), 2007.

"Directional Wave Basin." Oregon State University, College of Engineering O. H.

Hinsdale Wave Research Laboratory, Facilities. (2017) [Online] Available:

http://wave.oregonstate.edu/sites/wave.oregonstate.edu/files/hwrl_data_sheet_dwb_2015_for_website.pdf

FLOW-3D user manual; excellence in flow modeling software, v 11.1. (2017). FLOW-3D. Flow Science, Inc., Santa FE, NM.

Goseberg, N., Wurpts, A., and Schlurmann, T. "Laboratory-scale generation of tsunami and long waves." *Coastal Engineering*, Vol. 79, 2013.

Johnson, M. and Savage, B. "Flow over Ogee Spillway: Physical and Numerical Model Case Study." *Journal of Hydraulic Engineering*, Vol. 127(8), 2001.

Ko, H., Cox, D., Riggs, H., and Naito, C. "Hydraulic Experiments on Impact Forces from Tsunami-Driven Debris." *Journal of Waterway, Port, Coastal, and Ocean Engineering*, Vol. 141(3), 2015.

"Large Wave Flume." Oregon State University, College of Engineering O. H. Hinsdale Wave Research Laboratory, Facilities. (2017) [Online]. Available:
http://wave.oregonstate.edu/sites/wave.oregonstate.edu/files/hwrl_data_sheet_lwf_2015_for_website.pdf

Leelawat, N., Suppasri, A., Charvet, I., Kimura, T., Sugawara, D., and Imamura, F. "A Study on Influential Factors on Building Damage in Kesenuma, Japan from the 2011 Great East Japan Tsunami." *Engineering Journal*, Volume 19 Issue 3, 2015.

Mayo, N. "Ocean Waves-Their Energy and Power." *Physics Teacher* 35, Sept. 1997.

Malek mohammadi, S., "Laboratory Generation and Physics of Propagation of Solitary Waves and Water Surface Depressions". All Dissertations. Paper 475. 2009.

Malek mohammadi, S. and Testik, F. "New Methodology for Laboratory Generation of Solitary Waves." *Journal of Waterway, Port, Coastal, and Ocean Engineering*, Vol. 136(5), 2010.

Matsutomi, H., Okamoto, K., and Harada, K. "Inundation Flow Velocity of Tsunami on Land and its Practical Use." Proceedings of 32nd Conference on Coastal Engineering, Vol. 32, 2010.

Park, H., Cox, D., Lynett, P., Wiebe, D., and Shin, S. "Tsunami inundation modeling in constructed environments: A physical and numerical comparison of free-surface elevation, velocity, and momentum flux." Coastal Engineering, Vol. 79, 2013.

Rossetto, T., Allsop, W. Charvet, I., and Robinson, D. "Physical modelling of tsunami using a new pneumatic wave generator." Coastal Engineering, Vol. 58(6), 2011.

"Shoaling." Science learning Hub, The University of Waikato. (2011, May 2) [Online]. Available: <https://www.sciencelearn.org.nz/resources/596-shoaling>

van Gent, M.R.A. "The New Delta Flume for Large Scale Testing." Deltares Facilities. (2015, July 3) [Online]. Available: <https://www.deltares.nl/app/uploads/2015/02/THE-NEW-DELTA-FLUME-FOR-large-scale-testing.pdf>

Wienkea, J. and Oumeracib, H. "Breaking wave impact force on a vertical and inclined slender pile - theoretical and large-scale model investigations." Coastal Engineering, Vol. 52(5), 2005.

Yeh, H. "Maximum Fluid Forces in the Tsunami Runup Zone." *Journal of Waterway, Port, Coastal, and Ocean Engineering*, Vol. 132(6), 2006.

Appendix A: Artificial Wave Generation References



O. H. HINSDALE

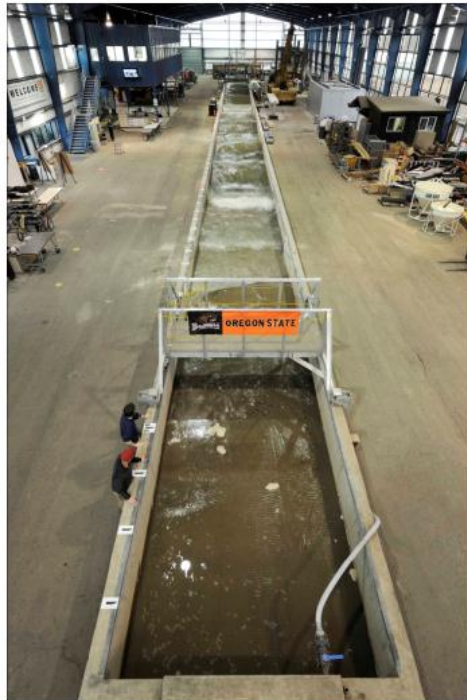
WAVE RESEARCH LABORATORY

OREGON STATE UNIVERSITY

Large Wave Flume

The Large Wave Flume is the largest of its kind in North America. Because of its size and ability to operate in high Reynolds regimes, the flume is ideally suited for:

- Scaled shallow water hurricane and storm wave conditions
- Long wave and tsunami generation
- Active wave absorption for large reflected waves
- Minimizing tank seiche for long duration studies



Wave Flume

- Length: 104 m 342 ft
- Width: 3.7 m 12 ft
- Depth: 4.6 m 15 ft

Wavemaker

- Type: Piston-type, Hydraulic Actuator Assembly
- Wave Types: Regular, Irregular, Tsunami, User Defined
- Period Range: 0.8 to 12 seconds
- Max Wave: 1.7 m (5.6 ft) @ 5 sec in max 2.7 m water
1.4 m (3.9ft) tsunami in max 2.0 m water
- Max Stroke: 4 m (13.1 ft) at 4 m/s (13.1 ft/s)

Instrumentation Carriage

- Powered carriage with full cross-shore traverse
- Carriage-mounted vertical instrument deployment frame
- Lightweight carriage for video and lighting applications





O. H. HINSDALE

WAVE RESEARCH LABORATORY

OREGON STATE UNIVERSITY

Directional Wave Basin

Previously known as the Tsunami Wave Basin, was designed to understand the fundamental nature of tsunami inundation, tsunami-structure impact, harbor resonance and to improve the numerical tools for tsunami mitigation.

In addition to tsunami research, the facility is particularly suited for general testing of coastal infrastructures, nearshore processes research, wave hydrodynamics, floating structures and renewable energy devices.

The wave machine is a unique powerful snake-type system made of 29 boards with up to 2.1 m long stroke. It has been designed to generate short- and long-period multidirectional high quality waves.

Wave Basin Dimensions

• Length:	48.8 m	160 ft
• Width:	26.5 m	87 ft
• Max depth:	1.37 m	4.5 ft
• Freeboard:	0.6 m	2.0 ft

Wavemaker

- Type: Piston-type, Electric motor
- Waveboards: 29 boards, 2.0 m (6.6 ft) high
- Wave types: Regular, Irregular, Tsunami, Multidirectional, User defined
- Period range: 0.5 to 10 seconds
- Max. Wave: 0.75 m (2.5 ft) in 1.37 m (4.5 ft) depth
- Max. Stroke: 2.1 m (6.9 ft)
- Max. Velocity: 2.0 m/s (6.6 ft/s)



Supporting infrastructure

- 7.5 T capacity bridge crane
- Instrumentation carriage, spans 26.5 m
- Unistrut installed in floor and sides to secure models
- Two access ramps, 14 ft width (4.2 m)
- Steady flow currents installed on project-by-project basis



THE NEW DELTA FLUME FOR LARGE-SCALE TESTING

BY MARCEL R.A. VAN GENT

The new Delta Flume in Delft was constructed to facilitate large-scale physical model testing. The new Delta Flume has a length of about 300m, a width of 5m and a height of 9.5m. The maximum significant wave height that can be generated is about $H_s = 2.2\text{m}$ and maximum individual wave heights in the range between $H_{\text{max}} = 4\text{m}$ and 4.5m . This unique facility enables physical modelling at prototype-scale or at close-to-prototype scale. Preventing or diminishing scale-effects is especially important for coastal structures in which sand, clay, grass or other natural construction material is being applied. Besides projects with dikes and dunes, structures such as breakwaters, bed protections, monopiles, offshore wind farms, and storm surge barriers are scheduled to be tested. Along with new facilities also new measurement techniques have been developed, both for the new Delta Flume and for the other wave facilities (e.g. wave basins). The new Delta Flume completes a set of wave facilities for physical model testing consisting of small and large-scale test facilities and 2D (wave flumes) and 3D (wave basins) facilities.

Introduction

To determine the response of coastal structures such as dikes, dunes, dune-revetments, breakwaters, cobble & gravel beaches, intake & outfall structures, offshore windfarms and bed protections, under loading of waves and/or currents physical model testing is an essential part of the design and evaluation process of such structures. Some aspects require modelling at a large scale since the materials and/or physical processes cannot be modelled properly on a small scale using Froude's scaling law.

Examples of materials that cannot be modelled properly at a small-scale are sand, clay, grass or natural construction material (e.g. brushwood). Physical processes that cannot be modelled properly at a small-scale are often related to flow characteristics that do not scale according to Froude's scaling law, e.g. for structures in which laminar (porous) flow plays an important role results may be affected by scale-effects. Nevertheless, tests at small-scale can provide valuable indicative results although for accurate quantitative results large scale models are still

Figure 1 - Examples of projects in the Delta Flume



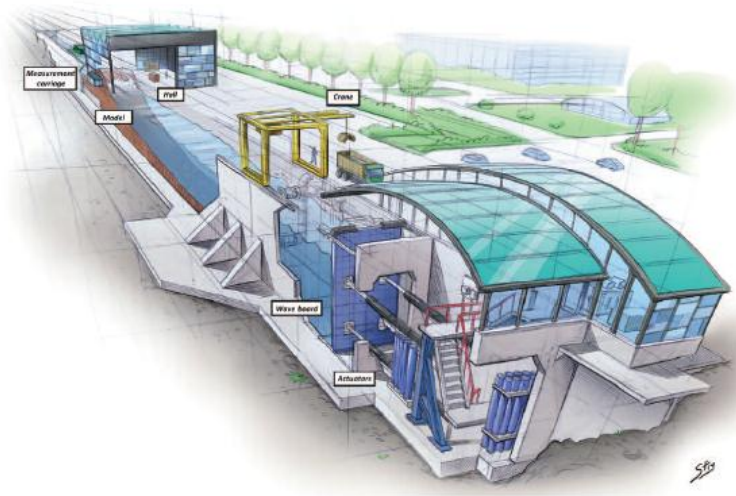


Figure 2 - Impression of the new Delta Flume (courtesy mr Stephan Timmers)

required. Many types of coastal structures can be modelled sufficiently accurate at small scales, e.g. most rubble mound breakwaters.

Besides the scale of models it is important to determine whether the structures can be modelled in a 2D model (wave flumes) or need to be modelled in a 3D model (wave basins). Often combinations of 2D and 3D models are applied, e.g. where cross-sections of structures are optimized in a wave flume, while 3D aspects are studied afterwards in a separate 3D model. Also the combination of small-scale tests and large-scale tests may be an efficient way to determine the performance of coastal structures for those structures in which some of the characteristics would be affected by scale-effects in smaller models. Therefore, it is essential to have a set of small-scale and large-scale facilities available, as well as 2D (wave flumes) and 3D facilities (wave basins). Not only the facilities are important, also the measurement equipment and experienced staff are key factors of the success of physical model tests. In Van Gent (2014) an overview of projects in the various physical model facilities is given.

Projects In The Old Delta Flume

In the old Delta Flume (240m*5m*7m) a large number of projects has been performed in the last 35 years. In these projects the choice for this facility has been based mainly on the need to limit or avoid scale-effects in physical model tests. The new Delta Flume in Delft (300m*5m*9.5m) has been constructed to facilitate measurements at an even larger scale. Figure 1 shows examples of projects performed in the old Delta Flume: Wave impacts on vertical walls, wave overtopping at dikes with grass, the dynamic behaviour of cobble beaches, the stability of placed-block revetments, the residual strength of clay-dikes, breakwater stability, dune erosion, and wave damping by brushwood mattresses. Other typical studies in the Delta Flume are related to for instance the validation of numerical models, testing and calibration of field measurement equipment, and the stability of pipeline covers.

Besides consultancy projects many research projects in the Delta Flume

have been performed and resulted in information on the performance of coastal structures, for instance:

- Placed-block revetments
- Grass slopes under wave attack
- Residual strength of dikes
- Dune erosion
- Gravel and cobble beaches
- Wave impacts on vertical walls
- Geotubes and gecontainers.

The New Delta Flume

The main characteristics of the new Delta Flume compared to the old Delta Flume are that the maximum wave height that can be generated is higher, the length is increased, tidal water level variations can be generated, and the new Delta Flume is close to the other wave facilities in Delft. One of the main advantages of the new Delta Flume over the old Delta Flume is that scale-effects are further reduced; a larger portion of the projects can be performed at (close-to) prototype scale. Figure 2 provides an impression of the new Delta Flume.

Flume dimensions The flume has a total length of about 300m. The size was determined based on tests that have been performed in the old Delta Flume. The modelling area has a total depth of 9.5m for a length of 183m, and an extra 75m section of 7m deep. The deep part has a length that is sufficient to model structures such as dikes while the combination with a shallower section allows for modelling of gentle foreshores over a length of about 250m in combination with for instance dunes. For the majority of the projects the water depth at the wave board will be between 2.5m and 8m. The flume is 5m wide.

Wave conditions The maximum wave heights that can be generated are about $H_{m0} = 2.2m$ and maximum individual wave heights in the range between $H_{max} = 4m$ and $4.5m$. The optimal water depth at the wave board for reaching the highest significant wave height for which also the wave height distribution is modelled accurately, is estimated at 6.9m. Spectral significant wave heights larger than $H_{m0} = 2.2m$ can be generated but these will cause some side wall overtopping. Irregular and regular waves, as well as some more special wave conditions can be generated (e.g. for

Tsunami modelling and focussed waves). It is expected that irregular wave conditions with standard spectral shapes (e.g. Jonswap) will be generated in the majority of experiments, so that during the design of the wave generator emphasis was put on precise specification of this type of wave conditions. Increasing wave height, wave period and water depth require more wave generating power, more wave board stroke and larger flume depths. In Holland et al (2013) the percentage of water defences in The Netherlands that can be modelled at full scale is discussed. It is estimated that the new Delta Flume is capable of generating sufficiently large wave heights to cover about 85% of the Dutch sea dikes at prototype scale under design conditions. This means an increase in number of Dutch dike sections that can be tested at full scale of about 50% compared to the old Delta Flume.

To generate the large wave heights (e.g. $H_{m0} = 2.2\text{m}$) with the corresponding wave periods (e.g. $T_p = 9.4\text{s}$), a certain wave board stroke is needed. However, waves will reflect from the structures in the wave flume. To absorb these reflected waves with our active reflection compensation system (ARC, see also Wenneker et al, 2010), also a part of the wave board stroke is needed. The stroke of the new wave board is 7m, allowing for the mentioned significant wave height in combination with space to absorb waves that are reflected by structures in the flume.

Wave generator To generate the waves that are required a piston-type wave board was selected because of its good performance for coastal applications. The wave board is of the dry-back type. A hydraulic system was opted for. Four actuators are applied to better distribute the forces that the board will experience. The wave generator utilizes Degree of Freedom (DOF) control on the four actuators to accurately control the linear motion of the board while zeroing out unwanted board deflections such as twisting or bending due to hydrodynamic forces and board compliance. The length of an actuator is 24.5m when fully extended. A novelty in the new Delta Flume is that a tidal variation in the water level is possible by filling and emptying the flume during an experiment. The maximum filling discharge is $1\text{ m}^3/\text{s}$.

Measurements Various measurement techniques are acquired and developed to extract data from the experiments in the flume (Holland et al,



Dr Marcel R.A. van Gent is a specialist in the field of coastal engineering, in particular coastal structures, wave modelling, dikes and dunes. He obtained his PhD at the Delft University of Technology in 1995 on the modelling of reshaping rubble mound coastal structures and gravel beaches. Dr Marcel van Gent is now head of the department 'Coastal Structures & Waves' at Deltares, Delft. His is leading a group that consists of about 35 scientists and assistants for performing physical model tests in wave flumes and wave basins, developing numerical wave models, and providing specialist consultancy services. Since 1991 Marcel van Gent participated in various research projects, including projects for the European Union, for the Dutch Government, and in co-operation with Universities, Consultancy firms, and Contractors. Dr Marcel van Gent published about 100 international scientific papers on coastal structures, wave modelling and dune erosion.

2012). Besides classic point measurements, also synoptic measurement techniques (i.e. high resolution measurements of time-varying spatial fields) have been developed. For the measurements of waves (at the wall) the proven resistance-type wave probes are used. Radars will be used to obtain wave height measurements at any location. In addition, the use of laser scanners and stereo matching of video images can be used to obtain spatially distributed information of waves and/or (deformed) structures. Also good visual observation of the tests is ensured using for instance a central video observation system and many (flush) cavities in the wall near the location of most models to install instruments.

REFERENCES

- Holland, B., R. Hoffmann and R. Lindenberg (2012), Wave measurement techniques for the new large-scale Delta Flume, Proc. Coastal2012, Gent.
- Holland, B., I. Wenneker and M. van Gent (2013), Description of the new Delta Flume, Proc. Coastal2013, Marine.
- Van Gent, M.R.A. (2014), Overview of physical modeling at Deltares including the new Delta Flume, Keynote, Proc. Coastal2014.
- Wenneker, I., J. Meesters, R. Hoffmann and D. Franciscan (2010), Active Wave Absorption System ARCH, Proc. Coastal2010, Barcelona.



(a) hydraulic power units for wave generator
 (b) crane above flume to construct structures to be tested
 (c) blue wave paddle

Appendix B: Design E Calculations

Equation 6: Flowrate Continuity Equation

$$V_1 A_1 = V_2 A_2$$

Where: V_1 = Displacement Plate Velocity

$$A_1 = \text{Plate Area} = 10 \text{ ft} \times 12 \text{ ft} = 120 \text{ ft}^2$$

$$V_2 = \text{Wave Section Velocity} = 25.4 \text{ ft/s}$$

$$A_2 = \text{Exit Conduit Area} = 10 \text{ ft} \times 10 \text{ ft} = 100 \text{ ft}^2$$

$$V_1(120 \text{ ft}^2) = 25.4 \text{ ft/s}(100 \text{ ft}^2)$$

$$V_1 = 21.167 \text{ ft/s} \cong 22 \text{ ft/s}$$

Appendix C: Design F Calculations

Equation 6: Flowrate Continuity Equation

$$V_1 A_1 = V_2 A_2$$

Where: V_1 = Displacement Plate Velocity

$$A_1 = \text{Plate Area} = 10 \text{ ft} \times 12 \text{ ft} = 120 \text{ ft}^2$$

$$V_2 = \text{Wave Section Velocity} = 25.4 \text{ ft/s}$$

$$A_2 = \text{Exit Conduit Area} = (10 \text{ ft} \times 10 \text{ ft}) - 9(10 \text{ ft} \times 0.125 \text{ ft})$$

$$A_2 = 88.75 \text{ ft}^2$$

$$V_1(120 \text{ ft}^2) = 25.4 \text{ ft/s}(88.75 \text{ ft}^2)$$

$$V_1 = 18.785 \text{ ft/s} \cong 20 \text{ ft/s}$$

Appendix D: Design I Calculations

Equation 8: Simplified Bernoulli Equation

$$\frac{P_1}{\gamma} = \frac{V_2^2}{2g}$$

Where: P_1 = Air Pressure

γ = Unit Weight of Water = 62.4 lb/ft^3

V_2 = Wave Section Velocity = 25.4 ft/s

g = Gravitational Acceleration = 32.2 ft/s^2

$$\frac{P_1}{62.4 \text{ lb/ft}^3} = \frac{(25.4 \text{ ft/s})^2}{2(32.2 \frac{\text{ft}}{\text{s}^2})}$$

$$P_1 = 625.124 \text{ psf} \cong 625.0 \text{ psf} = 4.34 \text{ psi}$$

Appendix E: Design F Flow-3D Input Text File

Title

This is a sample input file

&xput

```
remark='!! Remarks beginning with "!! " are automatically added and removed by FLOW-3D.',
remark='!! Do not begin any user added remarks with with "!! ". They will be removed',
twfin=1,
itb=1,
ifvisc=1,
ifvis=4,
imobs=1,
imphtc=0,
ifdynconv=1,
omega=0.5,
gz=-32.2,
idpth=1,
iorder=1,
tedit(1)=0,
tpltd(1)=0.0833,
thpltd(1)=0.001,
tapltd(1)=0.0166,
```

/

&limits

```
itmax=250,
itdtmx=20,
itflmx=50,
eps=0.005,
vfclean=0.001,
```

/

&props

```
units='eng',
tunits='f',
pcav=0,
mu1=2.0885434e-05,
cangle=-90,
fluid1='Water at 20 C',
muc1=0,
muctst=0.001,
mutmp2=32,
cv1=25008.1722282,
tl1=32.18,
ts1=32,
clht1=3.607240805e+06,
cvs1=12557.90571,
thcs1=0.2766994834,
rhofs=1.7792737151,
tsdrg=1,
fscr=1,
fsco=0,
rhof=1.9403203,
```

```

sigma=0.005002088918,
yieldt1=0,
mus=0,
thc1=0.07457769372,
yield1=-0.020885434,
/

&scalar
asqr=0,
pgasmp=0,
/

&PCAP
/

&BCDATA
remark='!! Boundary condition X Min',
ibct(1)=2,

remark='!! Boundary condition X Max',
ibct(2)=5,
pbct(1, 2)=100,
fbct(1, 2)=0,

remark='!! Boundary condition Y Min',
ibct(3)=2,

remark='!! Boundary condition Y Max',
ibct(4)=2,

remark='!! Boundary condition Z Min',
ibct(5)=2,

remark='!! Boundary condition Z Max',
ibct(6)=5,
pbct(1, 6)=0,
fbct(1, 6)=0,

remark='!! Boundary condition common parameters',
timbct(1)=0,
/

&MESH
nxcelt=296,
px(1)=1,
px(2)=38,

nycelt=96,
py(1)=1,
py(2)=13,

nzcelt=104,
pz(1)=1,
pz(2)=14,
/

```

```

&obs
nobs=13,

remark='!! Component 1',
obsid(1)='STL',

remark='!! Subcomponent 1',
iob(1)=1,
subcpid(1)='WT and Channel',
igen(1)=3,
fstl(1)='../...../Desktop/WT for CFEL fillet at top 10x10 5 ft conduit Fillet in 10x12x10 Tank.stl',

remark='!! Component 1 properties',
rough(1)=0.013,

remark='!! Component 2',
obsid(2)='Plate',

remark='!! Subcomponent 2',
iob(2)=2,
subcpid(2)='Plate',
xl(2)=37,
xh(2)=38,
yl(2)=1,
yh(2)=13,
zl(2)=1,
zh(2)=14,

remark='!! Component 2 properties',
imo(2)=3,
ifrc(2)=1,
rough(2)=0.013,
dxmcm(2)=-8,
dymcm(2)=0,
dzmcm(2)=0,
dxmcm(2)=0,
dymcm(2)=0,
dzmcm(2)=0,
rhomb(2)=2.5,
tjmb(2, 2, 1)=0,
tjmb(2, 3, 1)=0,
tjmb(2, 3, 2)=0,
iomxcal(2)=0,
iomycal(2)=0,
iomzcal(2)=0,
igf(2)=0,
omxtobs(1, 2)=0,
omxtobs(9, 2)=0,
omytobs(1, 2)=0,
omytobs(9, 2)=0,
omztobs(1, 2)=0,
omztobs(9, 2)=0,
utobs(1, 2)=0,
utobs(2, 2)=0,
utobs(3, 2)=-5,
utobs(4, 2)=-15,

```

utobs(5, 2)=-20,
utobs(6, 2)=-20,
vtobs(1, 2)=0,
wtobs(1, 2)=0,
fxtobs(1, 2)=-1.21e+05,
fxtobs(5, 2)=-1.21e+05,
fxtobs(7, 2)=0,
fxtobs(9, 2)=0,
ifobpq2(2)=1,

remark='!! Component 3',
obsid(3)='Gate',
ifCompEnabled(3)=1,

remark='!! Subcomponent 3',
iob(3)=3,
igen(3)=3,
fstl(3)='../../../../../Desktop/gate flap 3 in.stl',
trnx(3)=26.75,
trny(3)=11,
trnz(3)=1.5,

remark='!! Component 3 properties',
imo(3)=3,
rough(3)=0.013,
dxmcmmin(3)=0,
dymcmmin(3)=0,
dzmcmmin(3)=0,
dxmcmmax(3)=0,
dymcmmax(3)=0,
dzmcmmax(3)=0,
rhombv(3)=2.5,
tjmvb(3, 2, 1)=0,
tjmvb(3, 3, 1)=0,
tjmvb(3, 3, 2)=0,
iumcal(3)=0,
ivmcal(3)=0,
iwmcal(3)=0,
iomxcal(3)=0,
iomycal(3)=0,
iomzcal(3)=0,
xref0(3)=26.875,
yref0(3)=11.5,
zref0(3)=7,
omxtobs(1, 3)=0,
omytobs(1, 3)=0,
omztobs(1, 3)=-31.416,
omztobs(2, 3)=0,
omztobs(8, 3)=0,
utobs(1, 3)=0,
vtobs(1, 3)=0,
wtobs(1, 3)=0,

remark='!! Component 4',
obsid(4)='Gate 2',

remark='!! Subcomponent 4',
iob(4)=4,
igen(4)=3,
fstl(4)='../../../../Desktop/gate flap 3 in.stl',
trnx(4)=26.75,
trny(4)=10,
trnz(4)=1.5,

remark='!! Component 4 properties',
imo(4)=3,
rough(4)=0.013,
dxmcmmin(4)=0,
dymcmmin(4)=0,
dzmcmmin(4)=0,
dxmcmmax(4)=0,
dymcmmax(4)=0,
dzmcmmax(4)=0,
rhombv(4)=2.5,
tjmvb(4, 2, 1)=0,
tjmvb(4, 3, 1)=0,
tjmvb(4, 3, 2)=0,
xref0(4)=26.875,
yref0(4)=10.5,
zref0(4)=7,
omxtobs(1, 4)=0,
omytobs(1, 4)=0,
omztobs(1, 4)=-31.416,
omztobs(2, 4)=0,
omztobs(6, 4)=0,
utobs(1, 4)=0,
vtobs(1, 4)=0,
wtobs(1, 4)=0,

remark='!! Component 5',
obsid(5)='Gate 3',

remark='!! Subcomponent 5',
iob(5)=5,
igen(5)=3,
fstl(5)='../../../../Desktop/gate flap 3 in.stl',
trnx(5)=26.75,
trny(5)=9,
trnz(5)=1.5,

remark='!! Component 5 properties',
imo(5)=3,
rough(5)=0.013,
dxmcmmin(5)=0,
dymcmmin(5)=0,
dzmcmmin(5)=0,
dxmcmmax(5)=0,
dymcmmax(5)=0,
dzmcmmax(5)=0,
rhombv(5)=2.5,
tjmvb(5, 2, 1)=0,
tjmvb(5, 3, 1)=0,

tjmvb(5, 3, 2)=0,
xref0(5)=26.875,
yref0(5)=9.5,
zref0(5)=7,
omxtobs(1, 5)=0,
omytobs(1, 5)=0,
omztobs(1, 5)=-31.416,
omztobs(2, 5)=0,
omztobs(6, 5)=0,
utobs(1, 5)=0,
vtobs(1, 5)=0,
wtobs(1, 5)=0,

remark='!! Component 6',
obsid(6)='Gate 4',

remark='!! Subcomponent 6',
iob(6)=6,
igen(6)=3,
fstl(6)='../../../../Desktop/gate flap 3 in.stl',
trnx(6)=26.75,
trny(6)=8,
trnz(6)=1.5,

remark='!! Component 6 properties',
imo(6)=3,
rough(6)=0.013,
dxmcmmin(6)=0,
dymcmmin(6)=0,
dzmcmmin(6)=0,
dxmcmmax(6)=0,
dymcmmax(6)=0,
dzmcmmax(6)=0,
rhombv(6)=2.5,
tjmvb(6, 2, 1)=0,
tjmvb(6, 3, 1)=0,
tjmvb(6, 3, 2)=0,
xref0(6)=26.875,
yref0(6)=8.5,
zref0(6)=7,
omxtobs(1, 6)=0,
omytobs(1, 6)=0,
omztobs(1, 6)=-31.416,
omztobs(2, 6)=0,
omztobs(6, 6)=0,
utobs(1, 6)=0,
vtobs(1, 6)=0,
wtobs(1, 6)=0,

remark='!! Component 7',
obsid(7)='Gate 5',

remark='!! Subcomponent 7',
iob(7)=7,
igen(7)=3,
fstl(7)='../../../../Desktop/gate flap 3 in.stl',

trnx(7)=26.75,
trny(7)=7,
trnz(7)=1.5,

remark='!! Component 7 properties',

imo(7)=3,
rough(7)=0.013,
dxmcmmin(7)=0,
dymcmmin(7)=0,
dzmcmmin(7)=0,
dxmcmmax(7)=0,
dymcmmax(7)=0,
dzmcmmax(7)=0,
rhombv(7)=2.5,
tjmvb(7, 2, 1)=0,
tjmvb(7, 3, 1)=0,
tjmvb(7, 3, 2)=0,
xref0(7)=26.875,
yref0(7)=7.5,
zref0(7)=7,
omxtobs(1, 7)=0,
omytobs(1, 7)=0,
omztobs(1, 7)=-31.416,
omztobs(2, 7)=0,
omztobs(6, 7)=0,
utobs(1, 7)=0,
vtobs(1, 7)=0,
wtobs(1, 7)=0,

remark='!! Component 8',

obsid(8)='Gate 6',

remark='!! Subcomponent 8',

iob(8)=8,
igen(8)=3,
fstl(8)='../../../../Desktop/gate flap 3 in.stl',
trnx(8)=26.75,
trny(8)=6,
trnz(8)=1.5,

remark='!! Component 8 properties',

imo(8)=3,
rough(8)=0.013,
dxmcmmin(8)=0,
dymcmmin(8)=0,
dzmcmmin(8)=0,
dxmcmmax(8)=0,
dymcmmax(8)=0,
dzmcmmax(8)=0,
rhombv(8)=2.5,
tjmvb(8, 2, 1)=0,
tjmvb(8, 3, 1)=0,
tjmvb(8, 3, 2)=0,
xref0(8)=26.875,
yref0(8)=6.5,
zref0(8)=7,

omxtobs(1, 8)=0,
omytobs(1, 8)=0,
omztobs(1, 8)=31.416,
omztobs(2, 8)=0,
omztobs(6, 8)=0,
utobs(1, 8)=0,
vtobs(1, 8)=0,
wtobs(1, 8)=0,

remark='!! Component 9',
obsid(9)='Gate 7',

remark='!! Subcomponent 9',
iob(9)=9,
igen(9)=3,
fstl(9)='../../../../Desktop/gate flap 3 in.stl',
trnx(9)=26.75,
trny(9)=5,
trnz(9)=1.5,

remark='!! Component 9 properties',
imo(9)=3,
rough(9)=0.013,
dxmcmmin(9)=0,
dymcmmin(9)=0,
dzmcmmin(9)=0,
dxmcmmax(9)=0,
dymcmmax(9)=0,
dzmcmmax(9)=0,
rhombv(9)=2.5,
tjmvb(9, 2, 1)=0,
tjmvb(9, 3, 1)=0,
tjmvb(9, 3, 2)=0,
xref0(9)=26.875,
yref0(9)=5.5,
zref0(9)=7,
omxtobs(1, 9)=0,
omytobs(1, 9)=0,
omztobs(1, 9)=31.416,
omztobs(2, 9)=0,
omztobs(6, 9)=0,
utobs(1, 9)=0,
vtobs(1, 9)=0,
wtobs(1, 9)=0,

remark='!! Component 10',
obsid(10)='Gate 8',

remark='!! Subcomponent 10',
iob(10)=10,
igen(10)=3,
fstl(10)='../../../../Desktop/gate flap 3 in.stl',
trnx(10)=26.75,
trny(10)=4,
trnz(10)=1.5,

remark='!! Component 10 properties',
imo(10)=3,
rough(10)=0.013,
dxmcmmin(10)=0,
dymcmmin(10)=0,
dzmcmmin(10)=0,
dxmcmmax(10)=0,
dymcmmax(10)=0,
dzmcmmax(10)=0,
rhombv(10)=2.5,
tjmvb(10, 2, 1)=0,
tjmvb(10, 3, 1)=0,
tjmvb(10, 3, 2)=0,
xref0(10)=26.875,
yref0(10)=4.5,
zref0(10)=7,
omxtobs(1, 10)=0,
omytobs(1, 10)=0,
omztobs(1, 10)=31.416,
omztobs(2, 10)=0,
omztobs(6, 10)=0,
utobs(1, 10)=0,
vtobs(1, 10)=0,
wtobs(1, 10)=0,

remark='!! Component 11',
obsid(11)='Gate 9',

remark='!! Subcomponent 11',
iob(11)=11,
igen(11)=3,
fstl(11)='.././.././../Desktop/gate flap 3 in.stl',
trnx(11)=26.75,
trny(11)=3,
trnz(11)=1.5,

remark='!! Component 11 properties',
imo(11)=3,
rough(11)=0.013,
dxmcmmin(11)=0,
dymcmmin(11)=0,
dzmcmmin(11)=0,
dxmcmmax(11)=0,
dymcmmax(11)=0,
dzmcmmax(11)=0,
rhombv(11)=2.5,
tjmvb(11, 2, 1)=0,
tjmvb(11, 3, 1)=0,
tjmvb(11, 3, 2)=0,
xref0(11)=26.875,
yref0(11)=3.5,
zref0(11)=7,
omxtobs(1, 11)=0,
omytobs(1, 11)=0,
omztobs(1, 11)=31.416,
omztobs(2, 11)=0,

omztobs(6, 11)=0,
utobs(1, 11)=0,
vtobs(1, 11)=0,
wtobs(1, 11)=0,

remark='!! Component 12',
obsid(12)='Gate 10',

remark='!! Subcomponent 12',
iob(12)=12,
igen(12)=3,
fstl(12)='../.../Desktop/gate flap 3 in.stl',
trnx(12)=26.75,
trny(12)=2,
trnz(12)=1.5,

remark='!! Component 12 properties',
imo(12)=3,
rough(12)=0.013,
dxmcmmin(12)=0,
dymcmmin(12)=0,
dzmcmmin(12)=0,
dxmcmmax(12)=0,
dymcmmax(12)=0,
dzmcmmax(12)=0,
rhomvb(12)=2.5,
tjmvb(12, 2, 1)=0,
tjmvb(12, 3, 1)=0,
tjmvb(12, 3, 2)=0,
xref0(12)=26.875,
yref0(12)=2.5,
zref0(12)=7,
omxtobs(1, 12)=0,
omytobs(1, 12)=0,
omztobs(1, 12)=31.416,
omztobs(2, 12)=0,
omztobs(6, 12)=0,
utobs(1, 12)=0,
vtobs(1, 12)=0,
wtobs(1, 12)=0,

remark='!! Component 13',
obsid(13)='Conduit Plates',

remark='!! Subcomponent 13',
iob(13)=13,
subcmpid(13)='Plate 1',
igen(13)=3,
fstl(13)='../.../Desktop/1.5 in thick plate - 4 feet long.stl',
trnx(13)=22,
trny(13)=1.5,
trnz(13)=2.9375,

remark='!! Subcomponent 14',
iob(14)=13,
subcmpid(14)='Plate 2',

igen(14)=3,
fstl(14)='../../../../../Desktop/1.5 in thick plate - 4 feet long.stl',
trnx(14)=22,
trny(14)=1.5,
trnz(14)=3.9375,

remark='!! Subcomponent 15',
iob(15)=13,
subcmpid(15)='Plate 3',
igen(15)=3,
fstl(15)='../../../../../Desktop/1.5 in thick plate - 4 feet long.stl',
trnx(15)=22,
trny(15)=1.5,
trnz(15)=4.9375,

remark='!! Subcomponent 16',
iob(16)=13,
subcmpid(16)='Plate 4',
igen(16)=3,
fstl(16)='../../../../../Desktop/1.5 in thick plate - 4 feet long.stl',
trnx(16)=22,
trny(16)=1.5,
trnz(16)=5.9375,

remark='!! Subcomponent 17',
iob(17)=13,
subcmpid(17)='Plate 5',
igen(17)=3,
fstl(17)='../../../../../Desktop/1.5 in thick plate - 4 feet long.stl',
trnx(17)=22,
trny(17)=1.5,
trnz(17)=6.9375,

remark='!! Subcomponent 18',
iob(18)=13,
subcmpid(18)='Plate 6',
igen(18)=3,
fstl(18)='../../../../../Desktop/1.5 in thick plate - 4 feet long.stl',
trnx(18)=22,
trny(18)=1.5,
trnz(18)=7.9375,

remark='!! Subcomponent 19',
iob(19)=13,
subcmpid(19)='Plate 7',
igen(19)=3,
fstl(19)='../../../../../Desktop/1.5 in thick plate - 4 feet long.stl',
trnx(19)=22,
trny(19)=1.5,
trnz(19)=8.9375,

remark='!! Subcomponent 20',
iob(20)=13,
subcmpid(20)='Plate 8',
igen(20)=3,
fstl(20)='../../../../../Desktop/1.5 in thick plate - 4 feet long.stl',

trnx(20)=22,
trny(20)=1.5,
trnz(20)=9.9375,

remark='!! Subcomponent 21',
iob(21)=13,
subcmpid(21)='Plate 9',
igen(21)=3,
fstl(21)='../.../Desktop/1.5 in thick plate - 4 feet long.stl',
trnx(21)=22,
trny(21)=1.5,
trnz(21)=10.9375,

remark='!! Component 13 properties',
rough(13)=0.013,

remark='!! Component common parameters',
tobs(1)=0,
tobs(2)=0.1,
tobs(3)=0.2,
tobs(4)=0.3,
tobs(5)=0.4,
tobs(6)=0.5,
tobs(7)=0.6,
tobs(8)=1,
tobs(9)=5,
avrck=-3.1,

/

&fl
nfls=2,

remark='!! FluidRegion 1',
fxl(1)=27,
fxh(1)=37,
fyl(1)=2,
fyh(1)=12,
fzl(1)=2,
fzh(1)=14,

remark='!! FluidRegion 2',
fxl(2)=11,
fxh(2)=21,
fzl(2)=1,
fzh(2)=2,
if_flreg_enabled(2)=0,

remark='!! Region Pointer common parameters',
iflinittyp=0,

/

&bf
nbafs=10,

remark='!! Baffle 1',
if_baffle_enabled(1)=0,

ibaf(1)=1,
bz(1)=4,
bxl(1)=22,
bxh(1)=26,

remark='!! Baffle 2',
if_baffle_enabled(2)=0,
ibaf(2)=2,
bz(2)=6,
bxl(2)=22,
bxh(2)=26,

remark='!! Baffle 3',
if_baffle_enabled(3)=0,
ibaf(3)=3,
bz(3)=8,
bxl(3)=22,
bxh(3)=26,

remark='!! Baffle 4',
if_baffle_enabled(4)=0,
ibaf(4)=4,
bz(4)=10,
bxl(4)=22,
bxh(4)=26,

remark='!! Baffle 5',
if_baffle_enabled(5)=0,
ibaf(5)=5,
bz(5)=3,
bxl(5)=22,
bxh(5)=26,

remark='!! Baffle 6',
if_baffle_enabled(6)=0,
ibaf(6)=6,
bz(6)=5,
bxl(6)=22,
bxh(6)=26,

remark='!! Baffle 7',
if_baffle_enabled(7)=0,
ibaf(7)=7,
bz(7)=7,
bxl(7)=22,
bxh(7)=26,

remark='!! Baffle 8',
if_baffle_enabled(8)=0,
ibaf(8)=8,
bz(8)=9,
bxl(8)=22,
bxh(8)=26,

remark='!! Baffle 9',
if_baffle_enabled(9)=0,

```

ibaf(9)=9,
bz(9)=11,
bxl(9)=22,
bxh(9)=26,

remark='!! Baffle 10',
if_baffle_enabled(10)=0,
ibaf(10)=10,
bx(10)=18,
byl(10)=6.5,
byh(10)=7.5,
bzl(10)=2,
bzh(10)=4,
ifrcbf=1,
/

&motn
/

&grafic
  anmtyp(1)='p',
  anmtyp(2)='turb',
  anmtyp(3)='vel',
/

&RENDERSPACE
  iff3d(1)=1,
  iff3d(2)=1,
/

&HEADER
  project='fr Gates 10x12x10 WT 10x10x6 Conduit altered paddle speed Taper Tank w/ 1ft baffles',
  version='double',
  nprocs=0,
  runser=0,
  use_parallel_token=0,
/

&parts
/
Documentation: general comments, background, expectations, etc.

```

Appendix F: Design J Flow-3D Input Text File

Title

This is a sample input file

&xput

remark='!! Remarks beginning with "!! " are automatically added and removed by FLOW-3D.',
remark='!! Do not begin any user added remarks with with "!! ". They will be removed',

twfin=1.5,
itb=1,
ifenrg=2,
ifvisc=1,
ifvis=4,
imobs=1,
imphtc=0,
ifdynconv=1,
omega=0.5,
iphchg=3,
ifrho=0,
gz=-32.2,
idpth=1,
iorder=1,
tedit(1)=0,
tpltd(1)=0.0833,
thpltd(1)=0.001,
tapltd(1)=0.0166,

/

&limits

itmax=250,
itdtmx=20,
itflmx=50,
eps=0.005,
vfclean=0.001,

/

&props

units='eng',
tunits='f',
mu1=2.0885434e-05,
cangle=90,
fluid1='Water at 20 C',
fluid2='Air at 15 degrees C',
muc1=1,
muctst=0.001,
mutmp2=0,
cv1=25008.1722282,
cv2=4293.6077618,
t11=32.18,
ts1=32,
clht1=3.607240805e+06,
cvs1=12557.90571,

```

thcs1=0.2766994834,
rhofs=1.7792737151,
fscr=0.67,
rhof=1.9403203,
sigma=0.005002088918,
yieldt1=0,
mus=0,
mu2=3.7196957954e-07,
rhof2=0.0023768923675,
thc1=0.07457769372,
thc2=0.0029306410296,
yield1=-0.020885434,
/

&scalar
  asqr=0,
  pgasmp=0,
/

&PCAP
/

&BCDATA
  remark='!! Boundary condition X Min',
  ibct(1)=2,

  remark='!! Boundary condition X Max',
  ibct(2)=5,
  fbct(1, 2)=0,
  nevents_bc(2)=1,

  remark='!! BoundaryConditionProbeEvent 1',
  nprobes_bc(1, 2)=1,
  event_condition_logic_bc(1, 2)='ANY',
  nactions_bc(1, 2)=1,
  pbct_event(1, 1, 2)=0,
  pbct_event(2, 1, 2)=0,
  pbct_event(3, 1, 2)=625,
  pbct_event(4, 1, 2)=625,
  pbct_event(5, 1, 2)=0,
  pbct_event(6, 1, 2)=0,
  event_action_bc(1, 1, 2)='PBCT',

  remark='!! ProbeCondition 1',
  iprbd_bc(1, 1, 2)=1,
  prbvnam_bc(1, 1, 2)='z',
  ifprbvabs_bc(1, 1, 2)=1,
  prbvrop_bc(1, 1, 2)='EQ',
  prbval_critical_bc(1, 1, 2)=13.9,

  remark='!! Boundary condition Y Min',
  ibct(3)=2,

  remark='!! Boundary condition Y Max',
  ibct(4)=2,

```

```

remark='!! Boundary condition Z Min',
ibct(5)=2,

remark='!! Boundary condition Z Max',
ibct(6)=5,
pbct(1, 6)=0,
fbct(1, 6)=0,

remark='!! Boundary condition common parameters',
timbct(1)=0,
timbct(2)=0.3,
timbct(3)=0.6,
timbct(4)=1.1,
timbct(5)=1.4,
timbct(6)=1.5,
/

&MESH
  nxcelt=288,
  px(1)=1,
  px(2)=37,

  nycelt=96,
  py(1)=1,
  py(2)=13,

  nzcelt=104,
  pz(1)=1,
  pz(2)=14,
/

&obs
  nobs=14,

  remark='!! Component 1',
  obsid(1)='STL',

  remark='!! Subcomponent 1',
  iob(1)=1,
  subcmpid(1)='WT and Channel',
  igen(1)=3,
  fstl(1)='x 2.stl',

  remark='!! Component 1 properties',
  rough(1)=0.013,
  ifqsr(1)=2,

  remark='!! Component 2',
  obsid(2)='Plate',
  ifCompEnabled(2)=0,

  remark='!! Subcomponent 2',
  iob(2)=2,
  subcmpid(2)='Plate',
  xl(2)=36.001,
  xh(2)=37,

```

```

yl(2)=1,
yh(2)=13,
zl(2)=1,
zh(2)=13,

remark='!! Component 2 properties',
imo(2)=0,
ifrc(2)=1,
rough(2)=0.013,
dxmcm(2)=-8,
dymcm(2)=0,
dzmcm(2)=0,
dxmcm(2)=0,
dymcm(2)=0,
dzmcm(2)=0,
rhomb(2)=2.5,
tjmb(2, 2, 1)=0,
tjmb(2, 3, 1)=0,
tjmb(2, 3, 2)=0,
iomxcal(2)=0,
iomycal(2)=0,
iomzcal(2)=0,
igf(2)=0,
omxtobs(1, 2)=0,
omxtobs(9, 2)=0,
omytobs(1, 2)=0,
omytobs(9, 2)=0,
omztobs(1, 2)=0,
omztobs(9, 2)=0,
utobs(1, 2)=0,
utobs(2, 2)=0,
utobs(3, 2)=-5,
utobs(4, 2)=-15,
utobs(5, 2)=-20,
utobs(6, 2)=-20,
vtobs(1, 2)=0,
wtobs(1, 2)=0,
fxtobs(1, 2)=-1.21e+05,
fxtobs(5, 2)=-1.21e+05,
fxtobs(7, 2)=0,
fxtobs(9, 2)=0,
ifobpq2(2)=1,

remark='!! Component 3',
obsid(3)='Gate',
ifCompEnabled(3)=1,

remark='!! Subcomponent 3',
iob(3)=3,
igen(3)=3,
fstl(3)='./..././.../Desktop/1.5 in Gate .stl',
rotx(3)=90,
trnx(3)=26.75,
trny(3)=12.5,
trnz(3)=1.9375,

```

remark='!! Component 3 properties',
imo(3)=3,
rough(3)=0.013,
dxmcmmin(3)=0,
dymcmmin(3)=0,
dzmcmmin(3)=0,
dxmcmmax(3)=0,
dymcmmax(3)=0,
dzmcmmax(3)=0,
rhombv(3)=2.5,
tjmvb(3, 2, 1)=0,
tjmvb(3, 3, 1)=0,
tjmvb(3, 3, 2)=0,
iumcal(3)=0,
ivmcal(3)=0,
iwmcal(3)=0,
iomxcal(3)=0,
iomycal(3)=0,
iomzcal(3)=0,
xref0(3)=26.9375,
yref0(3)=6,
zref0(3)=1.9375,
omxtobs(1, 3)=0,
omytobs(1, 3)=0,
omytobs(2, 3)=0,
omytobs(3, 3)=-15.708,
omytobs(4, 3)=0,
omytobs(8, 3)=0,
omztobs(1, 3)=0,
utobs(1, 3)=0,
vtobs(1, 3)=0,
wtobs(1, 3)=0,

remark='!! Component 4',
obsid(4)='Gate 2',
ifCompEnabled(4)=1,

remark='!! Subcomponent 4',
iob(4)=4,
igen(4)=3,
fstl(4)='../../../../../Desktop/1.5 in Gate .stl',
rotx(4)=90,
trnx(4)=26.75,
trny(4)=12.5,
trnz(4)=2.95,

remark='!! Component 4 properties',
imo(4)=3,
rough(4)=0.013,
dxmcmmin(4)=0,
dymcmmin(4)=0,
dzmcmmin(4)=0,
dxmcmmax(4)=0,
dymcmmax(4)=0,
dzmcmmax(4)=0,
rhombv(4)=2.5,

```

tjmvb(4, 2, 1)=0,
tjmvb(4, 3, 1)=0,
tjmvb(4, 3, 2)=0,
iumcal(4)=0,
ivmcal(4)=0,
iwmcal(4)=0,
iomxcal(4)=0,
iomycal(4)=0,
iomzcal(4)=0,
xref0(4)=26.9375,
yref0(4)=6,
zref0(4)=2.95,
omxtobs(1, 4)=0,
omytobs(1, 4)=0,
omytobs(2, 4)=0,
omytobs(3, 4)=-15.708,
omytobs(4, 4)=0,
omytobs(8, 4)=0,
omztobs(1, 4)=0,
utobs(1, 4)=0,
vtobs(1, 4)=0,
wtobs(1, 4)=0,

remark='!! Component 5',
obsid(5)='Gate 3',
ifCompEnabled(5)=1,

remark='!! Subcomponent 5',
iob(5)=5,
igen(5)=3,
fstl(5)='../../../../Desktop/1.5 in Gate .stl',
rotx(5)=90,
trnx(5)=26.75,
trny(5)=12.5,
trnz(5)=3.9625,

remark='!! Component 5 properties',
imo(5)=3,
rough(5)=0.013,
dxmcmmin(5)=0,
dymcmmin(5)=0,
dzmcmmin(5)=0,
dxmcmmax(5)=0,
dymcmmax(5)=0,
dzmcmmax(5)=0,
rhomvb(5)=2.5,
tjmvb(5, 2, 1)=0,
tjmvb(5, 3, 1)=0,
tjmvb(5, 3, 2)=0,
iumcal(5)=0,
ivmcal(5)=0,
iwmcal(5)=0,
iomxcal(5)=0,
iomycal(5)=0,
iomzcal(5)=0,
xref0(5)=26.9375,

```

yref0(5)=6,
zref0(5)=3.9625,
omxtobs(1, 5)=0,
omytobs(1, 5)=0,
omytobs(2, 5)=0,
omytobs(3, 5)=-15.708,
omytobs(4, 5)=0,
omytobs(8, 5)=0,
omztobs(1, 5)=0,
utobs(1, 5)=0,
vtobs(1, 5)=0,
wtobs(1, 5)=0,

remark='!! Component 6',
obsid(6)='Gate 4',
ifCompEnabled(6)=1,

remark='!! Subcomponent 6',
iob(6)=6,
igen(6)=3,
fstl(6)='../../../../../Desktop/1.5 in Gate .stl',
rotx(6)=90,
trnx(6)=26.75,
trny(6)=12.5,
trnz(6)=4.975,

remark='!! Component 6 properties',
imo(6)=3,
rough(6)=0.013,
dxmcmmin(6)=0,
dymcmmin(6)=0,
dzmcmmin(6)=0,
dxmcmmax(6)=0,
dymcmmax(6)=0,
dzmcmmax(6)=0,
rhombv(6)=2.5,
tjmvb(6, 2, 1)=0,
tjmvb(6, 3, 1)=0,
tjmvb(6, 3, 2)=0,
iumcal(6)=0,
ivmcal(6)=0,
iwmcal(6)=0,
iomxcal(6)=0,
iomycal(6)=0,
iomzcal(6)=0,
xref0(6)=26.9375,
yref0(6)=6,
zref0(6)=4.975,
omxtobs(1, 6)=0,
omytobs(1, 6)=0,
omytobs(2, 6)=0,
omytobs(3, 6)=-15.708,
omytobs(4, 6)=0,
omytobs(8, 6)=0,
omztobs(1, 6)=0,
utobs(1, 6)=0,

vtobs(1, 6)=0,
wtobs(1, 6)=0,

remark='!! Component 7',
obsid(7)='Gate 5',
ifCompEnabled(7)=1,

remark='!! Subcomponent 7',
iob(7)=7,
igen(7)=3,
fstl(7)='.././.././../Desktop/1.5 in Gate .stl',
rotx(7)=90,
trnx(7)=26.75,
trny(7)=12.5,
trnz(7)=5.9875,

remark='!! Component 7 properties',
imo(7)=3,
rough(7)=0.013,
dxmcmmin(7)=0,
dymcmmin(7)=0,
dzmcmmin(7)=0,
dxmcmmax(7)=0,
dymcmmax(7)=0,
dzmcmmax(7)=0,
rhombv(7)=2.5,
tjmvb(7, 2, 1)=0,
tjmvb(7, 3, 1)=0,
tjmvb(7, 3, 2)=0,
iumcal(7)=0,
ivmcal(7)=0,
iwmcal(7)=0,
iomxcal(7)=0,
iomycal(7)=0,
iomzcal(7)=0,
xref0(7)=26.9375,
yref0(7)=6,
zref0(7)=5.9875,
omxtobs(1, 7)=0,
omytobs(1, 7)=0,
omytobs(2, 7)=0,
omytobs(3, 7)=-15.708,
omytobs(4, 7)=0,
omytobs(8, 7)=0,
omztobs(1, 7)=0,
utobs(1, 7)=0,
vtobs(1, 7)=0,
wtobs(1, 7)=0,

remark='!! Component 8',
obsid(8)='Gate 6',
ifCompEnabled(8)=1,

remark='!! Subcomponent 8',
iob(8)=8,
igen(8)=3,

fstl(8)='./.././.././../Desktop/1.5 in Gate .stl',
rotx(8)=90,
trnx(8)=26.75,
trny(8)=12.5,
trnz(8)=7,

remark='!! Component 8 properties',
imo(8)=3,
rough(8)=0.013,
dxmcmmin(8)=0,
dymcmmin(8)=0,
dzmcmmin(8)=0,
dxmcmmax(8)=0,
dymcmmax(8)=0,
dzmcmmax(8)=0,
rhombv(8)=2.5,
tjmvb(8, 2, 1)=0,
tjmvb(8, 3, 1)=0,
tjmvb(8, 3, 2)=0,
iumcal(8)=0,
ivmcal(8)=0,
iwmcal(8)=0,
iomxcal(8)=0,
iomycal(8)=0,
iomzcal(8)=0,
xref0(8)=26.9375,
yref0(8)=6,
zref0(8)=7,
omxtobs(1, 8)=0,
omytobs(1, 8)=0,
omytobs(2, 8)=0,
omytobs(3, 8)=-15.708,
omytobs(4, 8)=0,
omytobs(8, 8)=0,
omztobs(1, 8)=0,
utobs(1, 8)=0,
vtobs(1, 8)=0,
wtobs(1, 8)=0,

remark='!! Component 9',
obsid(9)='Gate 7',
ifCompEnabled(9)=1,

remark='!! Subcomponent 9',
iob(9)=9,
igen(9)=3,
fstl(9)='./.././.././../Desktop/1.5 in Gate .stl',
rotx(9)=90,
trnx(9)=26.75,
trny(9)=12.5,
trnz(9)=8.0125,

remark='!! Component 9 properties',
imo(9)=3,
rough(9)=0.013,
dxmcmmin(9)=0,

```

dymcmin(9)=0,
dzmcmin(9)=0,
dxmcmmax(9)=0,
dymcmmax(9)=0,
dzmcmmax(9)=0,
rhombv(9)=2.5,
tjmvb(9, 2, 1)=0,
tjmvb(9, 3, 1)=0,
tjmvb(9, 3, 2)=0,
iumcal(9)=0,
ivmcal(9)=0,
iwmcal(9)=0,
iomxcal(9)=0,
iomycal(9)=0,
iomzcal(9)=0,
xref0(9)=26.9375,
yref0(9)=6,
zref0(9)=8.0125,
omxtobs(1, 9)=0,
omytobs(1, 9)=0,
omytobs(2, 9)=0,
omytobs(3, 9)=-15.708,
omytobs(4, 9)=0,
omytobs(8, 9)=0,
omztobs(1, 9)=0,
utobs(1, 9)=0,
vtobs(1, 9)=0,
wtobs(1, 9)=0,

remark='!! Component 10',
obsid(10)='Gate 8',
ifCompEnabled(10)=1,

remark='!! Subcomponent 10',
iob(10)=10,
igen(10)=3,
fstl(10)='../...../Desktop/1.5 in Gate .stl',
rotx(10)=90,
trnx(10)=26.75,
trny(10)=12.5,
trnz(10)=9.025,

remark='!! Component 10 properties',
imo(10)=3,
rough(10)=0.013,
dxmcmmin(10)=0,
dymcmmin(10)=0,
dzmcmmin(10)=0,
dxmcmmax(10)=0,
dymcmmax(10)=0,
dzmcmmax(10)=0,
rhombv(10)=2.5,
tjmvb(10, 2, 1)=0,
tjmvb(10, 3, 1)=0,
tjmvb(10, 3, 2)=0,
iumcal(10)=0,

```

ivmcal(10)=0,
iwmcal(10)=0,
iomxcal(10)=0,
iomycal(10)=0,
iomzcal(10)=0,
xref0(10)=26.9375,
yref0(10)=6,
zref0(10)=9.025,
omxtobs(1, 10)=0,
omytobs(1, 10)=0,
omytobs(2, 10)=0,
omytobs(3, 10)=-15.708,
omytobs(4, 10)=0,
omytobs(8, 10)=0,
omztobs(1, 10)=0,
utobs(1, 10)=0,
vtobs(1, 10)=0,
wtobs(1, 10)=0,

remark='!! Component 11',
obsid(11)='Gate 9',
ifCompEnabled(11)=1,

remark='!! Subcomponent 11',
iob(11)=11,
igen(11)=3,
fstl(11)='../.../Desktop/1.5 in Gate .stl',
rotx(11)=90,
trnx(11)=26.75,
trny(11)=12.5,
trnz(11)=10.0375,

remark='!! Component 11 properties',
imo(11)=3,
rough(11)=0.013,
dxmcmmin(11)=0,
dymcmmin(11)=0,
dzmcmmin(11)=0,
dxmcmmax(11)=0,
dymcmmax(11)=0,
dzmcmmax(11)=0,
rhombv(11)=2.5,
tjmvb(11, 2, 1)=0,
tjmvb(11, 3, 1)=0,
tjmvb(11, 3, 2)=0,
iumcal(11)=0,
ivmcal(11)=0,
iwmcal(11)=0,
iomxcal(11)=0,
iomycal(11)=0,
iomzcal(11)=0,
xref0(11)=26.9375,
yref0(11)=6,
zref0(11)=10.0375,
omxtobs(1, 11)=0,
omytobs(1, 11)=0,

omytobs(2, 11)=0,
omytobs(3, 11)=-15.708,
omytobs(4, 11)=0,
omytobs(8, 11)=0,
omztobs(1, 11)=0,
utobs(1, 11)=0,
vtobs(1, 11)=0,
wtobs(1, 11)=0,

remark='!! Component 12',
obsid(12)='Gate 10',
ifCompEnabled(12)=1,

remark='!! Subcomponent 12',
iob(12)=12,
igen(12)=3,
fstl(12)='../../../../Desktop/1.5 in Gate .stl',
rotx(12)=90,
trnx(12)=26.75,
trny(12)=12.5,
trnz(12)=11.05,

remark='!! Component 12 properties',
imo(12)=3,
rough(12)=0.013,
dxmcmmin(12)=0,
dymcmmin(12)=0,
dzmcmmin(12)=0,
dxmcmmax(12)=0,
dymcmmax(12)=0,
dzmcmmax(12)=0,
rhombv(12)=2.5,
tjmvb(12, 2, 1)=0,
tjmvb(12, 3, 1)=0,
tjmvb(12, 3, 2)=0,
iumcal(12)=0,
ivmcal(12)=0,
iwmcal(12)=0,
iomxcal(12)=0,
iomycal(12)=0,
iomzcal(12)=0,
xref0(12)=26.9375,
yref0(12)=6,
zref0(12)=11.05,
omxtobs(1, 12)=0,
omytobs(1, 12)=0,
omytobs(2, 12)=0,
omytobs(3, 12)=-15.708,
omytobs(4, 12)=0,
omytobs(8, 12)=0,
omztobs(1, 12)=0,
utobs(1, 12)=0,
vtobs(1, 12)=0,
wtobs(1, 12)=0,

remark='!! Component 13',

```

obsid(13)='Conduit Plates',
ifCompEnabled(13)=0,

remark='!! Subcomponent 13',
iob(13)=13,
subcmpid(13)='Plate 1',
igen(13)=3,
fstl(13)='1.5in thick 14 ft horizontal plate.stl',
trnx(13)=22,
trny(13)=1.5,
trnz(13)=2.9375,

remark='!! Subcomponent 14',
iob(14)=13,
subcmpid(14)='Plate 2',
igen(14)=3,
fstl(14)='1.5in thick 14 ft horizontal plate.stl',
trnx(14)=22,
trny(14)=1.5,
trnz(14)=3.9375,

remark='!! Subcomponent 15',
iob(15)=13,
subcmpid(15)='Plate 3',
igen(15)=3,
fstl(15)='1.5in thick 14 ft horizontal plate.stl',
trnx(15)=22,
trny(15)=1.5,
trnz(15)=4.9375,

remark='!! Subcomponent 16',
iob(16)=13,
subcmpid(16)='Plate 4',
igen(16)=3,
fstl(16)='1.5in thick 14 ft horizontal plate.stl',
trnx(16)=22,
trny(16)=1.5,
trnz(16)=5.9375,

remark='!! Subcomponent 17',
iob(17)=13,
subcmpid(17)='Plate 5',
igen(17)=3,
fstl(17)='1.5in thick 14 ft horizontal plate.stl',
trnx(17)=22,
trny(17)=1.5,
trnz(17)=6.9375,

remark='!! Subcomponent 18',
iob(18)=13,
subcmpid(18)='Plate 6',
igen(18)=3,
fstl(18)='1.5in thick 14 ft horizontal plate.stl',
trnx(18)=22,
trny(18)=1.5,
trnz(18)=7.9375,

```

remark='!! Subcomponent 19',
iob(19)=13,
subcmpid(19)='Plate 7',
igen(19)=3,
fstl(19)='1.5in thick 14 ft horizontal plate.stl',
trnx(19)=22,
trny(19)=1.5,
trnz(19)=8.9375,

remark='!! Subcomponent 20',
iob(20)=13,
subcmpid(20)='Plate 8',
igen(20)=3,
fstl(20)='1.5in thick 14 ft horizontal plate.stl',
trnx(20)=22,
trny(20)=1.5,
trnz(20)=9.9375,

remark='!! Subcomponent 21',
iob(21)=13,
subcmpid(21)='Plate 9',
igen(21)=3,
fstl(21)='1.5in thick 14 ft horizontal plate.stl',
trnx(21)=22,
trny(21)=1.5,
trnz(21)=10.9375,

remark='!! Component 13 properties',
rough(13)=0.013,

remark='!! Component 14',
obsid(14)='Plug',
ifCompEnabled(14)=0,

remark='!! Subcomponent 22',
iob(22)=14,
subcmpid(22)='Plug',
xl(22)=35.5,
xh(22)=36.5,
yl(22)=1,
yh(22)=13,
zl(22)=1,
zh(22)=2,

remark='!! Component common parameters',
tobs(1)=0,
tobs(2)=0.1,
tobs(3)=0.2,
tobs(4)=0.3,
tobs(5)=0.4,
tobs(6)=0.5,
tobs(7)=0.6,
tobs(8)=1.5,
tobs(9)=5,
avrck=-3.1,

```

/

&fl
  nfls=1,

  remark='!! FluidRegion 1',
  ifdis(1)=-1,
  ffstl(1)='../.../.../Desktop/x 2 fluid.stl',

  remark='!! Valve 1',
  if_valve_enabled(1)=0,
  valx(1)=36.8,
  valy(1)=7,
  valz(1)=12.4,
  valp(1, 1)=0,
  valp(2, 1)=625,
  valp(3, 1)=625,
  valp(4, 1)=0,
  valarea(1)=0.196,
  if_2way(1)=2,
  timval(1)=0,
  timval(2)=0.3,
  timval(3)=0.8,
  timval(4)=1,
  iflinittyp=0,
/

&bf
  nbafs=10,

  remark='!! Baffle 1',
  if_baffle_enabled(1)=0,
  ibaf(1)=1,
  bz(1)=4,
  bxl(1)=22,
  bxh(1)=26,

  remark='!! Baffle 2',
  if_baffle_enabled(2)=0,
  ibaf(2)=2,
  bz(2)=6,
  bxl(2)=22,
  bxh(2)=26,

  remark='!! Baffle 3',
  if_baffle_enabled(3)=0,
  ibaf(3)=3,
  bz(3)=8,
  bxl(3)=22,
  bxh(3)=26,

  remark='!! Baffle 4',
  if_baffle_enabled(4)=0,
  ibaf(4)=4,
  bz(4)=10,
  bxl(4)=22,

```

```

bxh(4)=26,

remark='!! Baffle 5',
if_baffle_enabled(5)=0,
ibaf(5)=5,
bz(5)=3,
bxl(5)=22,
bxh(5)=26,

remark='!! Baffle 6',
if_baffle_enabled(6)=0,
ibaf(6)=6,
bz(6)=5,
bxl(6)=22,
bxh(6)=26,

remark='!! Baffle 7',
if_baffle_enabled(7)=0,
ibaf(7)=7,
bz(7)=7,
bxl(7)=22,
bxh(7)=26,

remark='!! Baffle 8',
if_baffle_enabled(8)=0,
ibaf(8)=8,
bz(8)=9,
bxl(8)=22,
bxh(8)=26,

remark='!! Baffle 9',
if_baffle_enabled(9)=0,
ibaf(9)=9,
bz(9)=11,
bxl(9)=22,
bxh(9)=26,

remark='!! Baffle 10',
if_baffle_enabled(10)=0,
ibaf(10)=10,
bx(10)=18,
byl(10)=6.5,
byh(10)=7.5,
bzl(10)=2,
bzh(10)=4,
ifrcbf=1,
/

&motn
/

&grafic
remark='!! HistoryProbe 1',
wintl(1)='Xmax event',
xloc(1)=20,
yloc(1)=1.5,

```

```
zloc(1)=13.9,  
anmtyp(1)='p',  
anmtyp(2)='turb',  
anmtyp(3)='vel',  
/  
  
&RENDERSPACE  
iff3d(1)=1,  
/  
  
&HEADER  
project='X2 Air w/gates 10x12x10 WT 10x10x6 Conduit w/ 1ft channels',  
version='double',  
nprocs=0,  
runser=0,  
use_parallel_token=0,  
/  
  
&parts  
/  
  
Documentation: general comments, background, expectations, etc.
```